

A Distribution-class Locational Marginal Price (DLMP) Index for Enhanced
Distribution Systems

by

Oluwaseyi Wemimo Akinbode

A Thesis Presented in Partial Fulfillment
of the Requirements for the Degree
Masters of Science

Approved July 2013 by the
Graduate Supervisory Committee:

Kory W. Hedman, Chair
Gerald T. Heydt
Muhong Zhang

ARIZONA STATE UNIVERSITY

August 2013

ABSTRACT

The smart grid initiative is the impetus behind changes that are expected to culminate into an enhanced distribution system with the communication and control infrastructure to support advanced distribution system applications and resources such as distributed generation, energy storage systems, and price responsive loads. This research proposes a distribution-class analog of the transmission LMP (DLMP) as an enabler of the advanced applications of the enhanced distribution system. The DLMP is envisioned as a control signal that can incentivize distribution system resources to behave optimally in a manner that benefits economic efficiency and system reliability and that can optimally couple the transmission and the distribution systems.

The DLMP is calculated from a two-stage optimization problem; a transmission system OPF and a distribution system OPF. An iterative framework that ensures accurate representation of the distribution system's price sensitive resources for the transmission system problem and vice versa is developed and its convergence problem is discussed. As part of the DLMP calculation framework, a DCOPF formulation that endogenously captures the effect of real power losses is discussed. The formulation uses piecewise linear functions to approximate losses. This thesis explores, with theoretical proofs, the breakdown of the loss approximation technique when non-positive DLMPs/LMPs occur and discusses a mixed integer linear programming formulation that corrects the breakdown.

The DLMP is numerically illustrated in traditional and enhanced distribution systems and its superiority to contemporary pricing mechanisms is demonstrated using price responsive loads. Results show that the impact of the inaccuracy of contemporary pricing schemes becomes significant as flexible resources increase. At high elasticity, aggregate load consumption deviated from the optimal consumption by up to about 45 percent when using a flat or time-of-use rate. Individual load consumption deviated by up to 25 percent when using a real-time price. The superiority of the DLMP is more pronounced when important distribution network conditions are not reflected by contemporary prices. The individual load consumption incentivized by the real-time price deviated by up to 90 percent from the optimal consumption in a congested distribution network. While the DLMP internalizes congestion management, the consumption incentivized by the real-time price caused overloads.

DEDICATIONS

This thesis is dedicated in part to my mother, Modupeola Abigail Akinbode, who sacrificed so much personally to provide me the best opportunities to succeed in life, and in part to my sisters, Seun, Tolu, and Tosin, who will continue to be a great source of motivation for me.

ACKNOWLEDGEMENTS

My gratitude goes to Dr. Kory W. Hedman, my thesis advisor, for his invaluable guidance, insights, advice, and encouragement and for constantly challenging me to be better. My gratitude also goes to Dr. Gerald T. Heydt and Dr. Muhong Zhang, members of my committee, for their time, comments and feedback. This thesis work is sponsored by the Power Systems Engineering Research Center (PSERC) under project M-25.

TABLE OF CONTENTS

LIST OF TABLES	ix
LIST OF FIGURES	xi
NOMENCLATURE	xvi
CHAPTER	Page
1. INTRODUCTION	1
1.1 Research Premise	1
1.2 Research Scope.....	2
1.3 Organization of this Thesis.....	5
2. BACKGROUND	8
2.1 Locational Marginal Pricing (LMP).....	8
2.2 Optimal Power-flow (OPF)	11
2.3 Cost-of-Service Regulation Ratemaking.....	18
Revenue Requirement.....	18
Rate Design.....	20
Deficiencies of the Cost-of-Service Regulation Construct...	22
2.4 Distribution System Rate Structures	24
2.5 Nodal Pricing in the Distribution System.....	29
2.6 Conclusion.....	33

CHAPTER	Page
3. THE DISTRIBUTION-CLASS LOCATIONAL MARGINAL PRICE (DLMP) INDEX	35
3.1 The Distribution-class Locational Marginal Price (DLMP) Index	35
3.2 Calculation Approach of the DLMP	39
3.3 Fairness of Nodal Prices in the Distribution System.....	44
3.4 Price Volatility with the use of the DLMP.....	45
3.5 Factors that will Affect Ultimate Usage.....	47
3.6 Conclusion.....	49
4. LOSSY DCOPF FOR DLMP CALCULATION.....	50
4.1 Lossy DCOPF Formulation.....	51
4.2 Conditions for Correct Solutions.....	56
4.3 Theoretical Proof of Lossy DCOPF Breakdown.....	64
4.4 Mixed-Integer Linear Programming (MILP) Formulation	71
4.5 Conclusion.....	75
5. ILLUSTRATIVE EXAMPLES OF THE DLMP.....	77
5.1 Roy Billinton Test System (RBTS).....	77
5.2 DLMP in a Traditional Distribution System	83

CHAPTER	Page
5.3 DLMP in an Enhanced Distribution System with Price Responsive Loads.....	87
5.4 DLMP in a Meshed Distribution System with Congestion.....	89
5.5 Optimal Coupling of the Transmission and the Distribution System.....	93
5.6 Conclusion.....	97
6. COMPARISON OF THE DLMP TO CONTEMPORARY PRICES IN THE DISTRIBUTION SYSTEM.....	98
6.1 Test System	98
6.2 Economic Modeling of Distribution Loads.....	101
6.3 Convergence Problems with Iterative Framework.....	106
6.4 Sampling Approach for Calculating Prices	112
6.5 Case Study 1: ϵ of -0.2 and No Congestion	116
6.6 Case Study 2: ϵ around -1.0 and No Congestion.....	118
6.7 Case Study 3: ϵ from around -2.0 to around -4.0 and No Congestion.....	122
6.8 Case Study 4: Congested Distribution Network.....	130
6.9 Conclusion.....	134
7. CONCLUSION AND FUTURE WORK	136

CHAPTER	Page
7.1 Conclusion.....	136
7.2 Future Work	138
APPENDIX	
A. SIMULATION DATA AND RESULTS DETAILS	148

LIST OF TABLES

Table	Page
2.1. Characteristics of a Smart Grid.....	30
4.1. Lossless and Lossy DCOPF LMPs, Losses, and Total Cost Results.....	62
4.2. Lossless and Lossy DCOPF Generation Dispatch Results	62
4.3. Piecewise Approximation Result for the Lossy DCOPF Study.....	63
4.4. Lossless and Lossy DCOPF Line Flow and Line Angle Difference Results	63
4.5. LMP, Losses, and Generation Cost Results.....	75
4.6. Generation Dispatch Results.....	75
4.7. Lossless and Lossy DCOPF Line Flow and Line Angle Difference Results	75
5.1. RBTS System Generator Details	79
5.2. Bus 3 Distribution System Load Details.....	80
5.3. Bus 3 Distribution System Feeder Summary.....	81
5.4. Bus 3 Distribution System Feeder Section Length	81
5.5. Summary of Distribution System at Bus 4 of RBTS System	83
5.6. Bus 4 Distribution System Load Type Details	83
5.7. Summary of Studies and Test Systems Used.....	83
5.8. Bid Value of Flexible Portion of Demand	87
5.9. Action Incentivized by DLMP and Flat Price.....	89
5.10. Action Incentivized by DLMP for Iterations 1 and 2	96

Table	Page
5.11. Comparison of Resulting Market Surplus for Iterative and Single-shot Approach	96
6.1. Summary of IEEE 30-Bus System.....	99
6.2. Generator Data for the Test Transmission System	100
A.1. RBTS Transmission System Branch Data	148
A.2. Flexible Load Data for RBTS Bus 3 Distribution System.....	149
A.3. RBTS Bus 4 Distribution System 11 kV Feeder Loading and Impedance Summary.....	150
A.4. RBTS Bus 4 Distribution System Feeder Section Summary	150
A.5. RBTS Bus 4 Distribution System 11 kV Network Feeders Impedance Summary.....	150
A.6. RBTS Bus 4 Distribution System 33 kV Feeders Impedance Summary	151
A.7. IEEE 30-Bus System Branch Data.....	152
A.8. 24 Hour Load Data for the Inelastic Loads in the Test Transmission System	154
A.9. RBTS Bus 4 Distribution System Bus and Load Details.....	157
A.10. Hourly Inelastic Loads in the RBTS Bus 4 Distribution System.....	158

LIST OF FIGURES

Figure	Page
3.1. Supply and Demand Curve	38
3.2. DLMP Calculation and Application Framework.....	41
4.1. Two-Bus System for Real Power Loss Expression Derivation	53
4.2. Plot of $1 - \cos(\theta_n - \theta_m)$ and its Piecewise Linear Approximation Curve ..	53
4.3. Three-Bus Network Example for Illustrating Lossy Formulation Breakdown	62
4.4. MILP Lossy DCOPF Implementation Triggered by Non-positive LMPs.....	74
5.1. RBTS Transmission System	78
5.2. Distribution System at Bus 3	80
5.3. Distribution System at Bus 4 with a Meshed Topology	82
5.4. DLMP Across Feeders in the Test Distribution System.....	85
5.5. Flexible Portion of Demand, DLMP, and Flat Price	89
5.6. Elastic Load Bids	90
5.7. DLMPs in Enhanced Distribution System with Congestion	92
5.8. DLMPs in Enhanced Distribution System without Congestion	92
5.9. Transmission LMP for 1st and 2nd Iterations.....	94
5.10. Comparison of the Iterative and Single-shot Solutions to the Solutions from a Single Model of the Transmission and the Distribution System.....	95
5.11. Flexible Portion of Demand and DLMP for Iterations 1 and 2	96

Figure	Page
6.1. One-line Diagram of IEEE 30-Bus System	99
6.2. 24 Hour Profile of the Total Inelastic Load in the Test Transmission System	100
6.3. 24 Hour Profile of the Total Perfectly Inelastic Load in the Test Dist. System	101
6.4. Type 2 Demand Curves with Different Coefficient of Elasticity	104
6.5. Type 3 Demand Curves with Different Coefficient of Elasticity	105
6.6. Type 4 Demand Curves with Different Coefficient of Elasticity	105
6.7. Type 5 Demand Curves with Different Coefficient of Elasticity	106
6.8. Generator sets Clearing Price.....	108
6.9. Load sets Clearing Price	108
6.10. Inelastic Distribution Load sets Clearing Price in Transmission OPF	109
6.11. Proxy LMP Changing from one Iteration to the other and the Optimal Proxy LMP.....	110
6.12. Infinite Generator Output Changing from one Iteration to the other and the Optimal Infinite Generator Output.....	110
6.13. Infinite Generator sets Clearing Price in Distribution OPF	111
6.14. Sampling Approach for Calculating DLMP	113
6.15. Sampling Approach for Calculating RTP	115
6.16. Prices at ϵ of -0.2.....	117

Figure	Page
6.17. 24 Hour Aggregate Load Consumption at ϵ of -0.2.....	117
6.18. Absolute Percentage Deviation from Optimal Aggregate Consumption at ϵ of -0.2	118
6.19. Prices at ϵ around -1.0.....	119
6.20. 24 Hour Aggregate Load Consumption at ϵ around -1.0.....	119
6.21. Absolute Percentage Deviation from Optimal Aggregate Consumption at ϵ around -1.0	120
6.22. Type 2 Loads Absolute Percentage Deviation from Optimal Consumption at ϵ around -1.0.....	121
6.23. Type 3 Loads Absolute Percentage Deviation from Optimal Consumption at ϵ around -1.0.....	121
6.24. Type 4 Loads Absolute Percentage Deviation from Optimal Consumption at ϵ around -1.0.....	121
6.25. Type 5 Loads Absolute Percentage Deviation from Optimal Consumption at ϵ around -1.0.....	122
6.26. FR Absolute Percentage Deviation from Optimal Consumption at Higher ϵ	123
6.27. TOU Absolute Percentage Deviation from Optimal Consumption at Higher ϵ	124

Figure	Page
6.28. RTP Absolute Percentage Deviation from Optimal Consumption at Higher ϵ	125
6.29. Type 2 Loads Absolute Percentage Deviation from Optimal Consumption at ϵ around -2.0.....	126
6.30. Type 2 Loads Absolute Percentage Deviation from Optimal Consumption at ϵ around -3.0.....	126
6.31. Type 2 Loads Absolute Percentage Deviation from Optimal Consumption at ϵ around -4.0.....	126
6.32. Type 3 Loads Absolute Percentage Deviation from Optimal Consumption at ϵ around -2.0.....	127
6.33. Type 3 Loads Absolute Percentage Deviation from Optimal Consumption at ϵ around -3.0.....	127
6.34. Type 3 Loads Absolute Percentage Deviation from Optimal Consumption at ϵ around -4.0.....	127
6.35. Type 4 Loads Absolute Percentage Deviation from Optimal Consumption at ϵ around -2.0.....	128
6.36. Type 4 Loads Absolute Percentage Deviation from Optimal Consumption at ϵ around -3.0.....	128
6.37. Type 4 Loads Absolute Percentage Deviation from Optimal Consumption at ϵ around -4.0.....	128

Figure	Page
6.38. Type 5 Loads Absolute Percentage Deviation from Optimal Consumption at ϵ around -2.0.....	129
6.39. Type 5 Loads Absolute Percentage Deviation from Optimal Consumption at ϵ around -3.0.....	129
6.40. Type 5 Loads Absolute Percentage Deviation from Optimal Consumption at ϵ around -4.0.....	129
6.41. DLMP at Node 25 and RTP in Congested Network.....	132
6.42. Real Power Consumption Incentivized by the DLMP and the RTP at Node 25 in the Congested Network.....	132
6.43. Absolute Percentage Deviation of the Consumption the RTP Incentivized at Node 25 from the Consumption Incentivized by the DLMP in the Congested Network.....	133
6.44. Power Flow on Branch 17 as a result of the Consumption Incentivized by the DLMP and RTP in the Congested Network.....	133
6.45. Comparison of the Absolute Percentage Deviation of the Consumption Incentivized by the RTP at Node 25 for Congested and Uncongested Network.....	134

NOMENCLATURE

AMI	Advanced Metering Infrastructure
b_d	Price associated with load bid d
B_k	Susceptance of line k
c_g	Linear operating cost of generator g
CBL	Customer baseline
COS	Cost-of-service regulation
CPP	Critical peak price
DCOPF	Direct current optimal power flow
DER	Distributed energy resources
DG	Distributed generation
DLMP	Distribution-class Locational Marginal Price
DMS	Distribution management system
D_n	Real power demand of inelastic load at bus n
$D_{n,d}$	Cleared real power demand quantity of bid d of price responsive load at bus n
DR	Demand response
DSM	Demand side management
EISA	Energy independence and security act
ESS	Energy storage system
F_k^+	Dual variable of line k 's upper line flow limit constraint (flowgate mar-

	ginal price)
F_k^-	Dual variable of line k 's lower line flow limit constraint (flowgate marginal price)
FR	Flat rate
G_k	Conductance of line k
G_n	Set of generators at bus n
IEEE	Institute of Electrical and Electronics Engineers
ISO	Independent system operator
KKT	Karush Kuhn Tucker
$k(n,;)$	Set of lines with bus n as the designated receiving end bus
$k(;,n)$	Set of lines with bus n as the designated sending end bus
LMP	Locational marginal price
LP	Load point
MILP	Mixed-integer linear programming
OPF	Optimal power flow
P_g	Real power output of generator g
P_g^{max}	Maximum real power capacity of generator g
P_g^{min}	Minimum real power capacity of generator g
P_k	Power flow on line k in the DCOPF model
P_k^{max}	Maximum power flow limit of line k
P_k^{min}	Minimum power flow limit of line k

P_k^{mn}	Alternating current power flow from bus n to bus m on line k
P_k^{nm}	Alternating current power flow from bus m to bus n on line k
P_n^L	Total losses on all lines connected to and delivering power to bus n
P_n^R	Real power injected at bus n and withdrawn at reference bus R
$P_n(w)$	Real power injection at bus n as a function of w
PRL	Price responsive load
$PTDF_{k,n}^R$	Power transfer distribution factor
Q_g	Reactive power output of generator g
Q_g^{max}	Maximum reactive power capacity of generator g
Q_g^{min}	Minimum reactive power capacity of generator g
Q_{L_n}	Reactive power load at bus n
$Q_n(w)$	Reactive power injected at bus n as a function of w
RBTS	A distribution system test bed, ‘Roy Billinton Test System’
RTO	Regional transmission organization
RTP	Real-time price
r/x	Ratio of conductor resistance to reactance
S_k	Apparent power flow on line k
S_k^{max}	Maximum apparent power flow capacity of line k
S_k^{min}	Minimum apparent power flow capacity of line k
t	Period index
TOU	Time-of-use rate
u_i^{k+}	Binary variable of positive orthant segment i

u_i^{k-}	Binary variable of negative orthant segment i
V_m	Voltage magnitude of designated sending end bus m
V_n	Voltage magnitude of designated receiving end bus n
V_n^{max}	Maximum voltage magnitude at bus n
V_n^{min}	Minimum voltage magnitude at bus n
w	Bus voltage magnitude and angle variables of the power flow equation
α_i	Slope of segment i
γ_n	Dual variable of piecewise linear loss equation constraint of bus n
δ_g^+	Dual variable of generator g 's power output upper limit constraint
δ_g^-	Dual variable of generator g 's power output lower limit constraint
ξ_k	Dual variable of line k 's line flow equation constraint (susceptance marginal price)
θ_i^{k+}	Length of positive orthant segment i
θ_i^{k-}	Length of negative orthant segment i
θ_i^{max}	Maximum length of segment i
θ_m	Voltage angle of designated sending end bus m
θ_n	Voltage angle of designated receiving end bus n
θ_{nm}	Voltage angle difference between bus n and bus m
θ_{nm}^{max}	Maximum voltage angle difference between bus n and bus m
θ_{nm}^{min}	Minimum voltage angle difference between bus n and bus m
λ_n	Dual variable of bus n 's node balance constraint, i.e., LMP at bus n

Λ^+	Set of lines connected to a bus with a positive LMP
Λ^-	Set of lines connected to a bus with a non-positive LMP
μ_k	Dual variable of line k 's angle difference approximation constraint
ρ_i^{k+}	Dual variable of positive orthant segment i 's upper limit constraint
ρ_i^{k-}	Dual variable of negative orthant segment i 's upper limit constraint

Chapter 1. Introduction

1.1 Research Premise

As competition became increasingly valued in the U.S. electric energy industry in the late 1990's and the early 2000's, spot pricing of electricity, proposed in [1], gained in popularity. Today, spot pricing in the form of locational marginal prices (LMP) has been implemented for transmission systems operated under the U.S. competitive bulk energy markets. As evidenced by its prevalence, the LMP index has been beneficial to both market and system operations. In market operation, the LMP index is an economically efficient price signal that can be used to incentivize market participant to behave optimally and in a manner that benefits social welfare [2]-[6]. In system operation, the LMP index is a valuable market-based tool for transparently managing congestion in the transmission network [3], [7]-[10].

Despite its benefit to the transmission system, LMPs are not used in the distribution system. The most prevalent distribution system prices, e.g., flat rates (FR) and time-of-use rates (TOU), are also independent of transmission system LMPs. This stems partly from the differences in the design and the operational paradigm of both systems. Unlike the transmission system, which is a highly meshed network and is routinely congested, most distributions systems are operated radially [46] (even though they may be designed as networks [32]) and have feeders and equipment that are overbuilt and oversized to avoid congestion [42], [43]. Similarly, while generators provide the transmission system a substantial amount of

price sensitive and controllable resources, the distribution system has very limited generation within it and loads are treated as highly or perfectly inelastic. Consequently, operation of the contemporary distribution system is not usually characterized by the active power flow management and control and short-term economic efficiency that are major parts of the operational paradigm in the transmission system. In certain municipalities, the transmission system LMP at the distribution proxy is used to price energy for some large industrial and commercial facilities as real-time prices (RTP) [66], [67]. Such prices, however, do not take into consideration the particulars of the distribution network.

With the smart grid initiative, the distribution system is evolving. The future distribution grid may look more like the transmission system with resources, such as price responsive loads (PRL), energy storage systems (ESSs), and distributed generators (DG) [43], [47], [53]. The smart grid initiative is expected to enhance the future distribution grid with the control and communications infrastructure to support such functions and applications [45], [47], [53]. The level of generation in the enhanced distribution system may be significant enough that future distribution grids that have a meshed network topology [43], [46] may be congested.

1.2 Research Scope

This research proposes the application of the LMP concept to the enhanced distribution system as a control signal to incentivize expected price sensitive and controllable distribution resources to behave optimally in a way that benefits economic efficiency and system operations both at the distribution and at the trans-

mission level. The aim of this thesis is to define the distribution-class LMP (DLMP), develop its calculation and application framework, and demonstrate its advantage over existing distribution pricing schemes. The work discusses the properties of the DLMP and its benefits to economic efficiency and systems operations both at the transmission and the distribution systems level. The work also discusses the framework for calculating the DLMP, which includes a two-staged optimization problem. Calculating the DLMP via a two-staged problem helps overcome the computational intractability that could possibly result from solving a unit commitment or an optimal power flow (OPF) problem for a single model of the transmission and the distribution systems. An iterative framework, between the stages of the optimization problem, is implemented to ensure accurate modeling of the price sensitive distribution system resources (DSR) and the distribution network conditions in one of the stages while the other stage captures the transmission system and its resources. While attractive, convergence of the iterative approach to a solution or to the optimal solution is not guaranteed. This convergence issue is included in the iterative framework discussions. A sampling approach is used in place of the iterative approach in some of the studies in this thesis to overcome the convergence problem of the iterative framework.

The two stages of the optimization process use a direct current optimal power flow (DCOPF) formulation that endogenously captures real power losses. The formulation overcomes the arbitrariness that results from using the slack or distributed slack bus method for approximating losses in a DCOPF formulation by using piecewise linear loss functions to approximate the non-linear real power

loss function. Under certain conditions, such as the occurrence of a non-positive DLMP or LMP, the loss approximation technique incorrectly creates non-physical artificial losses to improve the objective function. The lossy DCOPF formulation and its breakdown are explained in detail in this work.

As a way of setting up the illustration of the advantages of the DLMP, the work discusses cost-of-service (COS) regulation ratemaking and various rates structures that can be obtained in the contemporary distribution system. The contemporary rate structures are compared to the DLMP in terms of the DSR behavior incentivized and economic efficiency.

The DLMP is expected to benefit economic efficiency and reliability at both the distribution and the transmission system level by aligning the behavior of price sensitive DSRs with system operational objectives. The DLMP will incentivize optimal consumption from PRL, optimal generation from DGs and optimal operation of ESSs in the enhanced distribution grid. Optimally coupling the transmission and the distribution system, achieved by the iterative process, means the efficiency gains in the distribution system can also be translated into efficiency gains at the bulk energy system level. The optimal coupling could enable the utilization of DSR for ancillary services. Accurately representing price sensitive distribution load in the bulk energy market could also positively impact market efficiency: price sensitive demand is the greatest cure for the exercise of market power.

1.3 Organization of this Thesis

This thesis is organized into seven chapters. The goal in Chapter 2 is to provide readers with the knowledge of the concepts that are critical to understand the technical details in the later chapters and the background to understand the motivation behind this thesis. Chapter 2 provides information on LMPs and the OPF formulations used for calculating LMPs. Chapter 2 also provides information on COS regulation ratemaking and contemporary rate structures in the distribution system, the smart grid initiative, and a literature review of contemporary works on nodal pricing in the distribution system.

The focus in Chapter 3 is on the DLMP. The chapter defines the DLMP and discusses its properties and calculation and application framework. The chapter also discusses economic efficiency and the properties of the DLMP that provide the price signal the capability to improve economic efficiency as compared to contemporary distribution pricing schemes. The chapter argues strongly against perceived drawbacks, such as unfairness of locational prices in the distribution system and price volatility of the DLMP, and discusses the ultimate environment under which the DLMP is most applicable.

The mathematical optimization problem for calculating the DLMP is developed in Chapter 4. The DLMP is calculated based on a DCOPF formulation that uses piecewise linear functions to approximate real power losses. The piecewise linear approximation technique and the lossy DCOPF formulation are discussed. The breakdown of the loss approximation technique, under the condition of the

occurrence of non-positive DLMPs/LMPs, is discussed, proven theoretically using duality theory and the Karush Kuhn Tucker (K.K.T.) conditions, and illustrated numerically. A mixed integer linear programming (MILP) based formulation that can be used when the breakdown occurs is presented in the chapter.

The lossy DCOPF formulation developed in Chapter 4 is used to calculate and numerically illustrate the DLMP in Chapter 5. DLMPs are calculated for a traditional distribution system, an enhanced distribution system with PRLs and an enhanced distribution system with congestion. The results of the study on the enhanced distribution system with PRL are used to illustrate the superiority of the DLMP to average prices distorted by cross-subsidies. The results are also evaluated for social welfare and used to illustrate the importance of the iterative framework.

Chapter 6 presents a comparison of the DLMP to a RTP, a TOU and a FR. The price signals are compared based on PRL consumption in a meshed distribution system with and without congestion. The flexibility of the PRLs is varied to study the impact of the inaccuracy of the RTP, TOU and FR as demand becomes more flexible. A study is also conducted on a congested distribution system to demonstrate the superiority of the DLMP in terms of internalizing the distribution system network and generation conditions and efficiently aligning the behavior of controllable resources with system operational objectives.

Chapter 7 is a concluding chapter. It provides a summary of the work in this thesis and discusses future work. Tables of the data used in conducting the various simulations in the thesis are in Appendix A.

Chapter 2. Background

This chapter provides the background knowledge necessary to understand the technical details in the subsequent chapters. The information in this chapter also provides context for this research. The chapter describes the LMP concept in Section 2.1 and the optimal power flow problem used for calculating LMPs in Section 2.2. Cost-of-service ratemaking and contemporary rate structures in the distribution system are examined in Section 2.3 and Section 2.4. A discussion of the smart grid initiative is provided alongside a discussion and literature review of contemporary work on the subject of distribution system nodal prices in Section 2.5. Section 2.6 is a concluding paragraph.

2.1 Locational Marginal Pricing (LMP)

The concept of pricing electricity based on the location and time of injection and withdrawal was proposed in [1]. In this work, Schweppe *et al.* stated the main goals of proposing the concept as:

- i. economic efficiency
- ii. equity
- iii. utility control, operation, and planning
- iv. freedom of choice.

By economic efficiency, the authors envisaged using spot prices to incentivize a customer's electricity usage to match the marginal cost of its electric utility. By equity, a customer's price reflects what it costs a utility to serve the customer, i.e., no or reduced cross-subsidy between customers. By utility control, operation and

planning, the authors envisioned spot prices to reflect system conditions and the action motivated to be aligned with system control, operation, and planning objectives. By freedom of choice, the authors envisaged providing customers the freedom to choose how they use electricity, cost, and reliability. Owing to these benefits, particularly economic efficiency, equity, and control, operation and planning, and the deregulation of the utility industry, spot pricing of electricity in the form of LMP signals have become part of the design of competitive bulk energy markets in the U.S. [11]-[15].

A LMP is the cost to optimally deliver an increment of energy to a specific location on a grid while respecting the system's security and generation constraints. Although it is often thought of as the cost to supply an additional MW of load, the incremental energy that an LMP prices is not necessarily a MWh and it could be a negative increment, i.e., a decrement. A LMP is an economic signal used for system and market operations. It is calculated for a specific state of a power system and it reflects network conditions and supply and demand characteristics [3]. A LMP at a node on the grid captures the short-run marginal cost to generate an increment of energy and the effect on system congestion and system losses of delivering the increment of energy to a specific node on the grid.

Capturing the effect of the incremental consumption at a node, on system congestion and losses, provides the LMP its nodal property. That is, LMPs in the same system can vary from one node to another as a result of the contribution to losses and to congestion of the incremental consumption at different nodes. Congestion can occur in a system as a result of binding network security constraints,

such as branch thermal limits or transient stability limits. If congestion occurs in a system, the cheapest available generator(s) will be prevented from supplying the incremental energy to be delivered to a node. Instead, the incremental energy must come from a more expensive generator or a combination of generators. The LMP at a node, whose incremental consumption impacts congestion, will be different from the LMP of nodes whose incremental consumption can be supplied by the cheapest generator available. Hence, LMP separation as a result of a binding network constraint can be said to reflect the cost to re-dispatch a system while still satisfying all network constraints and reliability requirements. LMP separation as a result of losses reflects the cost to procure energy losses, as a result of the impedance of system components, incurred to deliver an increment of energy to a specific node. If a system has no congestion and losses are ignored, as is in a loss-less DCOPF, then the LMPs in the system will be the same at every node.

The nodal property of the LMP is very important because it provides the LMP its capability to reflect network conditions and its capability to price the individual contribution of consumption at a node to system conditions. As a result of the nodal property, the LMP can be used to incentivize price sensitive resources at a node to behave appropriately in a manner that benefits efficiency and system reliability. This is an important benefit of the LMP to short-term operations and it is why LMPs are sometimes referred to as a tool for managing system operations. As an illustration, congestion in a system can make the LMP at a node very high, to incentivize price sensitive loads at the node to reduce consumption and generators at the node to increase their output in order to respect the limit of a con-

strained branch. The nodal property also provides important, albeit limited, economic signal in terms of long term planning and investment. For example, the LMP separation in a system can be used to identify where upgrades are needed and it could be a signal for locating generation resources. A generator may make more money by locating at a node with perpetually high LMP and LMPs can signify the most effective node to locate a resource to relieve congestion. When scarcity occurs, high LMPs can also indicate the need for entry of new resources into a market.

2.2 Optimal Power-flow (OPF)

LMPs are obtained as the dual variables of the node balance constraints of an optimal power-flow (OPF) problem. An OPF problem is an economic dispatch problem that takes into consideration operational constraints such as branch thermal limits. The goal of an OPF problem is to optimally select some controllable or independent variables to optimize a benefit within the limits of reliable operation. For an electricity market framework, the controllable variables include generator outputs and the objective is usually to maximize social welfare. If demand is elastic, then load consumption is also a controllable variable. Social welfare, which will be discussed in Chapter 3, is a measure of the benefits to both consumers and producers for participating in a market [4]. In the OPF framework, social welfare, also known as market surplus, is often evaluated based on the bids and offers by loads and generators respectively.

Equation (2.1) represents the objective function of an OPF problem where loads submit monotonically non-increasing step-wise demand bids and generators submit monotonically non-decreasing step-wise offer curves. The first term of the equation is the total consumer bid value. It is the sum, for all load bids d , of the product of the price associated with a load bid (b_d) and the cleared demand of the load bid (D_d). The bid price for a load represents the maximum value the load places on consumption at a certain level. The second term is the total generation cost. It is the sum, for all generators g , of the product of the marginal cost (c_g) of a generator and the real power output (P_g) of the generator. An OPF problem with (2.1) as its objective is sometimes referred to as bid cost maximization problem, which is said to maximize the social welfare (when entities bid honestly) or the market surplus (when there is strategic bidding),

$$\text{Maximize: } \sum_d b_d D_d - \sum_g c_g P_g. \quad (2.1)$$

The representation in (2.1) assumes that demand is price responsive. Often times, electricity demand is viewed as perfectly inelastic with a fixed consumption regardless of price. In such a scenario, the first part of (2.1) is fixed as b_d for a perfectly inelastic load is also assumed fixed at a very high value of lost load (VoLL). For perfectly inelastic loads, the first part of (2.1) can be ignored or removed from the objective function. What is left is the maximization of a negative function, which is the same as minimizing the function. The objective function can, thus, be re-written as in (2.2) where generation cost is minimized. An OPF with (2.2) is referred to as a generation cost minimization problem,

$$\text{Minimize: } \sum_g c_g P_g. \quad (2.2)$$

The limits of reliable operation are defined in an OPF formulation by the constraints of the optimization problem. In general, these limits can be broadly categorized into three groups: power or node balance constraints, network constraints and generator constraints. Power balance constraints are equality constraints used to enforce conservation of energy. A power balance constraint requires the net power in a system to be zero, i.e., generation is equal to the sum of load and losses. Power balance constraints are usually enforced at each node in a system; hence, the name node balance constraint is frequently used. A node balance constraint enforces conservation of energy through Kirchhoff's Current Law (KCL). It forces the net power at a node to be zero. Network constraints are used to impose limits on network parameters, such as bus voltage magnitudes and angles, and line flows. By imposing limits on network parameters, network constraints define the reliability bounds of network elements and the network as a whole for operational purposes. For example, line flow limits are proxies for the thermal capacity of network elements and voltage angle limits are usually proxies for transient stability. Similar to network constraints, generator constraints define the reliable operating limits of the generators in a system.

OPF problems can be classified into two types: the alternating current OPF (ACOPF) and the DCOPF. While the objective function for both are the same and both OPF formulations have constraints that fall into the three categories of constraints discussed in the preceding paragraph, they use different power flow equa-

tions in the constraints. As the names imply, the ACOPF uses the AC power flow equations in (2.3) and (2.4). The DCOPF uses a linearized approximation of (2.3): shown in (2.15),

$$P_k^{nm} = |V_m^2|G_k - |V_m||V_n|(G_k \cos(\theta_m - \theta_n) + B_k \sin(\theta_m - \theta_n)) \quad (2.3)$$

$$Q_k^{nm} = -|V_m^2|B_k - |V_m||V_n|(G_k \sin(\theta_m - \theta_n) - B_k \cos(\theta_m - \theta_n)). \quad (2.4)$$

A generalized ACOPF formulation is shown in (2.5)-(2.12) [9]. Equation (2.5) is the objective function. Equation (2.6) and (2.7) are the node balance constraints. Equation (2.6) is the real power node balance constraint and (2.7) is the reactive power node balance constraint. Equations (2.8), (2.9) and (2.10) are the network constraints. Equation (2.8) is the proxy for the thermal limits of network branches. Equation (2.9) is the limit on bus voltage magnitudes and (2.10) is a proxy for transient stability limit. Equation (2.11) and (2.12) are the generator real and reactive power output limits. Note that w in the formulation represents the bus voltage magnitude and angle variables of the power flow equations,

$$\text{Minimize: } \sum_g c_g P_g \quad (2.5)$$

subject to:

$$P_n(w) + D_n - \sum_{g \in G_n} P_g = 0 \quad \forall n \quad (2.6)$$

$$Q_n(w) + Q_{L_n} - \sum_{g \in G_n} Q_g = 0 \quad \forall n \quad (2.7)$$

$$S_k^{min} \leq S_k \leq S_k^{max} \quad \forall k \quad (2.8)$$

$$V_n^{min} \leq V_n \leq V_n^{max} \quad \forall n \quad (2.9)$$

$$\theta_{nm}^{min} \leq \theta_{nm} \leq \theta_{nm}^{max} \quad \forall n \quad (2.10)$$

$$P_g^{min} \leq P_g \leq P_g^{max} \quad \forall g \quad (2.11)$$

$$Q_g^{min} \leq Q_g \leq Q_g^{max}. \quad \forall g \quad (2.12)$$

As stated earlier, the DCOPF is a linear approximation of the ACOPF problem. To obtain the DCOPF, the AC real power flow equation is linearized by recognizing the following about the transmission system:

- i. branch reactances are much larger than their resistances; therefore, the conductance term in the AC real power flow equations, (G_k), is approximately zero: this approximation essentially renders the DCOPF lossless
- ii. bus angle differences are small; therefore, $\cos \theta_{nm}$ is approximately 1 and $\sin \theta_{nm}$ is approximately θ_{nm}
- iii. bus voltage magnitudes ($|V_n|$ and $|V_m|$) are approximately 1 p.u.
- iv. reactive power is ignored in the DCOPF as a result of the first three assumptions: reactive power generation is scheduled by system operators as needed to maintain a stable operating system

The preceding assumptions are used to develop the DC approximation of the real power flow equation and the DCOPF. Note that reactive power load is also ignored in the DCOPF formulation. A DCOPF formulation is shown in (2.13)-(2.18). Equation (2.13) is the objective function. Equation (2.14) is the node balance constraint. The first and the second terms in (2.14) represent the power flowing into a bus and the power flowing out of a bus respectively. Equation (2.15) is the DC approximation of the line flow equation. P_k , in (2.15), is the DC approxima-

tion of the real power flow from a bus m to a bus n . Equation (2.16) is the real power branch flow limit and (2.17) is the transient stability limit proxy. Equation (2.18) is the generator real power output limit,

$$\text{Minimize: } \sum_g c_g P_g \quad (2.13)$$

subject to:

$$\sum_{\forall k(n,:)} P_k - \sum_{\forall k(:,n)} P_k - D_n + \sum_{g \in G_n} P_g = 0 \quad \forall n \quad (2.14)$$

$$B_k(\theta_n - \theta_m) - P_k = 0 \quad \forall k \quad (2.15)$$

$$P_k^{\min} \leq P_k \leq P_k^{\max} \quad \forall k \quad (2.16)$$

$$\theta_{nm}^{\min} \leq (\theta_n - \theta_m) \leq \theta_{nm}^{\max} \quad \forall n \quad (2.17)$$

$$P_g^{\min} \leq P_g \leq P_g^{\max}. \quad \forall g \quad (2.18)$$

The DCOPF formulation in (2.13)-(2.18) can be re-formulated as in (2.19)-(2.23). In (2.19)-(2.23), the DC approximation of the power flow equation is further approximated using power transfer distribution factors (PTDFs). A PTDF ($PTDF_{k,n}^R$) is the linear sensitivity of the power flow on a line k to the real power injected at a bus n and withdrawn at a reference bus R . Equation (2.21) is a power balance constraint,

$$\text{Minimize: } \sum_g c_g P_g \quad (2.19)$$

subject to:

$$P_n^R + D_n - \sum_{g \in G_n} P_g = 0 \quad \forall n \quad (2.20)$$

$$\sum_n P_n^R = 0 \quad (2.21)$$

$$P_k^{min} \leq \sum_n PTDF_{k,n}^R \cdot P_n^R \leq P_k^{max} \quad \forall k \quad (2.22)$$

$$P_g^{min} \leq P_g \leq P_g^{max}. \quad \forall g \quad (2.23)$$

The ACOPF, as a result of the AC power flow equation, is non-linear and non-convex and is as a non-linear programming problem. The DCOPF, with a linear objective function, is linear and convex, thereby making it a linear programming problem. The differences as a result of the power flow equation account for the advantages of the DCOPF over the ACOPF in terms of computation time and convergence. Non-linear programming problems are difficult to solve. According to [5], the computation time of an ACOPF problem could be 60 times greater than the computational time of a comparable DCOPF problem and the ACOPF often fails to converge to a solution or the global optimal solution. The ACOPF, however, is a full representation on the characteristics of the power system while the DCOPF is an approximate representation.

LMPs are the dual variables of the node balance constraint of either an ACOPF or a DCOPF problem. As such, LMPs represent the change to the objective function as an incremental change is made to the right hand side of the node balance constraint. With a bid surplus maximization objective, the LMP reflects the change in the market surplus as a change is made to the right hand side of the node balance constraint and the change in generation cost for a cost minimization problem. LMPs obtained from an ACOPF formulation will capture marginal cost of energy, congestion, and losses. LMPs obtained from the standard DCOPF will

not have a marginal loss component, since the standard DCOPF is a lossless model. Loss approximation for a DCOPF formulation is discussed in Chapter 4.

2.3 Cost-of-Service Regulation Ratemaking

Electric utility companies are operated in a regulated environment. Under the “regulatory compact”, utility companies, in exchange for being appointed as a franchised monopolies, are obligated to serve all customers in their service area, are subject to regulatory oversight that determines, amongst other things, distribution system rates and rate structures, and are allowed a fair rate-of-return on prudent investments [57], [60]. Ratemaking under this construct is termed the cost-of-service (COS) or rate-of-return regulation. COS regulation is governed by the notion that rates must be fair, reasonable, and non-discriminatory and utilities must be allowed a fair return on their investment [58] (see the classic work of J.C. Bonbright [56] for other objectives). Two issues are determined in a rate case under the COS regulation construct: the revenue requirement of a utility company and the rates and rate-structures to recover the revenue requirement [57].

Revenue Requirement

The revenue requirement of a utility represents the best estimate, in the regulator’s judgment, of the revenue that must be collected to recover the costs incurred by a utility to serve its customers and to provide a reasonable return on the utility’s capital investments. A utility’s revenue requirement includes the “prudent and necessary” operating costs required to service customers and a reasonable return on its rate base. The operating costs of a utility are expenses on labor,

maintenance, fuel, insurance, and other recurring costs directly related to providing service [60]. It also includes expenses, such as taxes, asset depreciation, and franchise fees, which are not directly related to providing service [59], [60]. A utility is only allowed to recover its operating expenses. It is not allowed to make a return on them. Instead, a utility receives a reasonable return on its rate base.

A rate base is the value of a utility's asset minus the depreciated value of such assets [59]. Establishment of the revenue requirements of a utility can be contentious especially in regards to the investments that can be included in the rate base. In general, capital assets, such as transmission and distribution lines, transformers, fleet vehicles and power plants, are included in a rate base. The assets must, however, be "used and useful". The "used and useful" concept requires an asset to be in use for providing services and for the asset to be a prudent and necessary investment such that disruption of service may occur without it [59], [60]. In some municipalities, utilities are allowed to include the carrying cost of capital during construction in their rate base once a facility meets the "used and useful" criterion. This concept is termed allowance for use during construction (AFUDC). For projects requiring huge capital burden, a utility could be allowed to include in its rate base, the carrying cost of capital while construction is still in progress. The concept is termed construction work in progress (CWIP). AFUDC and CWIP are controversial and may not be allowed in certain jurisdictions [60]. A rate base could also include the carrying capital a utility must borrow to meet its obligations before customers pay. A regulator determines the fair rate-of-return allowed on a rate base. The rate must take into cognizance a utility's capital structure, eq-

uity and debt, and the fact that the costs of both are different. The rate-of-return a utility is allowed must be such that it can continue to attract capital. According to [57], it is theoretically the rate that would be demanded for an investment of similar value and risk in a competitive market.

The product of allowed rate-of-return and the established rate base is added to a utility's operating expenses to obtain the utility's revenue requirement. It is established for a test year, which could be an actual year in the past (based on utility records) or a year in the future (based on an extensive budgeting process) [60]. In both cases, changes are made to reflect additional costs since the test year, if established based on a past year, or expected costs by the test year, if established based on a future year. The test year is used to determine if rates need to be increased or decreased. The rate case process under the COS regulation construct is lengthy and rates are established for long periods, e.g., a year to three years.

Rate Design

Once the revenue requirement of a utility has been established, rates are designed to recover the revenue. Rate design starts with the determination of customer classes. Customer classes vary from state to state and could include residential classes, general service classes, and agricultural classes. A rate class must be determined based on a rational set of commonalities between the rate class members. For example, the homogenous characteristic could include load characteristics, delivery voltage, and end use. The revenue requirement is allocated amongst the customer classes. Before allocation, the revenue requirement of a utility is functionalized. Functionalization is the division of the revenue require-

ment based on the functional areas of operations of the utility where a cost is incurred. For example, the revenue requirement can be functionalized into generation, transmission, distribution, and metering and services costs [62]. The functionalized revenue requirement may be further classified based on energy consumption, number of customers, and peak demand. There are several methods and approaches [62] for allocating the functionalized and classified revenue requirement between customer classes. Cost causation is usually kept in mind. Some costs are easy to allocate as only a certain class of consumers are responsible for them. For example, the cost of low voltage distribution lines and transformers that serve residential customers may not be allocated to large industrial users that are serviced at higher voltages. The challenging part of allocating a revenue requirement is the costs that multiple classes benefit from. Representatives of each rate class request for the method that favors their class. In general, residential and small commercial users greatly outnumber industrial users and both classes are responsible for a high percentage of peak demand. Hence, representatives of industrial users advocate for allocating more cost based on number of customers and peak demand [60]. On the other hand, cost allocation based on energy consumption fall equally of all users. Consequently, representatives of residential customers advocate for allocating more of the revenue requirement based on energy consumption.

The revenue allocated to each customer class is divided amongst the customers in the class. For the residential classes, the rates are usually divided into energy and customer charges with the demand related revenue requirement included

in the energy or the customer related charges. This is a two-part rate [61]. Demand related revenue requirements are included in either customer charges or in energy charges because residential customers may not have meters capable of measuring peak demand. For other classes, the rates could be broken into demand charges, energy charges, and customer related charges. This is a three-part rate [61].

Deficiencies of the Cost-of-Service Regulation Construct

The COS regulation construct provides protection for consumers and utilities alike. In theory, it offers price protection (regulation) for consumers and prevents utilities from making excessive profits that will unduly increase costs to consumers. It offers utilities the opportunity to make a fair rate on their investments and it focuses heavily on revenue recovery. Unlike in a competitive environment, however, the COS regulation construct offers only a weak incentive for efficiency. The construct offers little incentive to reduce cost. A utility, whose return is dependent of its rate base and whose cost of capital is less than the rate-of-return, has the incentive for a high rate base, i.e., to overinvest. This is termed the Averch-Johnson effect (see [65]). A regulator may not be in a position to always identify overinvestment. Similarly, there is little incentive for utilities to reduce operating expenses under COS regulation: expenses are passed on to the customers. For a utility that also has non-regulated businesses, expenses, such as cost of corporate liability insurance and headquarters facilities, could be shifted from the competitive side to the non-competitive side of the business [59], [60]. The COS regulation process is also very contentious. A commission has to balance compet-

ing interests and its decision may not always be purely technical. For example, there could be political considerations, such as keeping rates low for residential customers who vote.

Even if it were possible to do away with the deficiencies that arise with the implementation of the COS regulation, as discussed in the preceding paragraph, COS regulation cannot match the ability of competitive markets to keep prices at marginal cost and to minimize cost. In theory, COS regulation can be effective in keeping prices at marginal cost or at minimizing cost: it cannot do both well at the same time [2]. In order to keep prices at marginal cost, regulators have to ensure that the revenue recovered, including the cost of capital, is exactly the cost incurred. With such an objective, however, a utility has no incentive to reduce cost since such efficiency gains are given to the consumer. On the other hand, price caps can be imposed. The price cap incentivizes a utility to keep costs low. A utility keeps whatever efficiency saving it makes by keeping costs below the price cap. Price caps, however, have to be set higher than the marginal cost; otherwise, the regulator risks bankrupting the utility. What is obtained in practice is a mix of both. COS regulation is conducted with focus on keeping prices down [2]. Since the rate case process takes a very long time, prices are set for multiple years and must take into consideration the length of time the prices are in place. This result is a bit of price cap even when the regulator is attempting to keep prices close to marginal costs [2].

2.4 Distribution System Rate Structures

Several rate structures arise from the COS regulation construct. The most prevalent include the flat rate (FR), the block rate, and the time-of-use rate (TOU). The FR charges a uniform price per kWh regardless of the consumption level and the time of consumption. The block rate charge a different price as the consumption level of a customer passes a particular threshold. There are two major types of block rates: declining and inverted block rate. Rates reduce as consumption increases in a declining block rate structure, i.e., the rate for each block of consumption level decreases as consumption increases. Declining block rates were used in the early history of the electric utility industry to incentivize electricity applications, such as refrigeration [61]. They are still used today for a similar purpose. For example, a utility with summer-peaking load and excess capacity in the winter may use the declining block rate to incentivize electric heating [61]. The inverted block rate is the opposite of the declining block rate: rates increase as consumption increase. The inverted block rate is an attempt to incentivize efficient consumption.

The FR and block rates are simple rates that are easy to understand and are easy and cheap to implement. They are, however, determined with a heavy focus on revenue recovery. A rate can do more than recover costs, i.e., a rate can be used to incentivize other objectives. Prices in general are used to incentivize economic efficiency and prices in the distribution system should also be used for the same purpose, in addition to revenue recovery. A distribution system price should be able to incentivize consumption from the most willing consumer (efficient al-

location of scarce resources in an economy), reduce operation cost in the short-term (generation or fuel cost) and incentivize efficient investment in the long term (efficient mix of generators and optimal transmission and distribution investment).

In general, rates determined based on the COS construct are incapable of effectively achieving economic efficiency. Apart from the attendant problems discussed in the previous section, rates under the COS construct are average rates and are applied to all the customers in the same rate class. While a rate class is supposed to group customers with similarities together, customers in the same rate class could still have different consumption patterns, impact system operation differently, and have different individual preferences for electricity consumption [64]. Average prices that do not take into consideration the individual impact or cost of a load to the system result in cross-subsidies between customers [1], [64]. Some customers pay more than their cost to the system while others pay less. Cross-subsidies occur within the same rate class and it can also occur between rate classes. It distorts prices and sends improper signals to consumers. Average rates applied to all customers in the same class also do not provide customers the choice to determine the appropriate level of risk, in terms of price volatility and reliability, they would like to be exposed to [1], [64].

Rates under the COS construct are also in place for a long period of time and are mostly determined based on embedded costs. They do not reflect the true cost of consumption. Hence, they cannot be used to achieve allocative efficiency for short-term operation. The contemporary distribution system is a good illustration

of this point. Customers under a flat or block rate pay the same price regardless of time of consumption. The cost to the system during a peak period is highly unlikely to be the same cost during the off-peak period. The flat and block rates imply otherwise. Hence, customers, who may value consumption differently during both periods, have no incentive to consume differently during the periods. The inability of rates, such as the flat and block rates, to achieve allocative efficiency results in improper investments in the long run. For example, a utility may have to carry peak generation capacity, which may be needed for only a few periods in a year.

Incentivizing economic efficiency is more important with the advent of competitive bulk energy markets along with retail access or retail competition. The nature of the price of energy in the competitive markets is such that it could change significantly over time and between locations as a result of system state (network conditions, and demand and supply conditions). Consumers in the distribution system may not see the changes under the COS regulation construct, i.e., consumers are insulated from wholesale prices regardless of what happens in bulk energy market. This could negatively impact reliability and lead to inefficiencies, such as the exercise of market power and unnecessarily high levels of price volatility in the wholesale market. It also limits demand from being used for ancillary services and increases the reserve capacity that must be carried. In general, rates under the COS construct lead to higher operational costs. Other rate types have been proposed or implemented to shore up the perceived weaknesses of the tradi-

tional distribution system rates [64], [66], [67]. The prices include the TOU, critical peak price (CPP), and RTP.

The TOU rate is a time differentiated rate with two or three different rates for different time periods. The time periods are peak and off-peak for the two-period TOU rate and peak, partial or shoulder peak, and off-peak for the three-period TOU rate. Rates are fixed in each period. The TOU rate is a compromise between simplicity, cost of implementation, and price predictability and capture of the true nature of electricity prices. While it is time differentiated, the time periods in the TOU rate structure do not effectively capture the time dependence of electricity prices. TOU rates are also fixed for a season or longer and cannot properly reflect system conditions. The TOU rate is essentially an average rate and it is applied equally to all customers in the same rate class. While the TOU rate can be based on long-run marginal cost, a lot of utilities use embedded costs [64]. The CPP is similar to the TOU rate. For a limited number of hours in a year, a utility is allowed to charge a significantly higher rate during critical periods, such as during a contingency, to incentivize reduced consumption. Customers are notified in advance. While such a high rate can incentivize reduced consumption during a critical period, the incentivized consumption level may still be inaccurate since the high rate of a CPP could be independent of the true cost to consume at such periods. In addition, since the CPP is in place for a limited period of time in a year, a COS rate, such as the FR, will be in place for the periods the CPP is not used.

RTPs are generally hourly prices and are the most accurate prices for incentivizing economic efficiency in the contemporary distribution system. Several types

of RTPs exist and they expose customers to different levels of price risk. They include the basic RTP, the block and index RTP, the two-part RTP, and the unbundled RTP with self-selected baseline [64]. The basic RTP is simply the wholesale price at the distribution proxy. Customers are charged on an hourly basis at the rate of the proxy LMP. The basic RTP and the block and index RTP are operated in environments with retail competition or retail access. The two-part RTP and the unbundled RTP are operated under the traditional regulated environment. The basic RTP presents the highest level of risk to customers. The block and index RTP provides a hedge for customer. It allows a customer to enter into a forward contract, based on contract for differences, to hedge price risks. A premium is charged for the financial hedge. Consumption in excess of the contracted demand level is charged at real-time rates. Customers are credited at real-time rates for consumption under the fixed level. Under the two-part RTP structure, a utility establishes a customer's baseline consumption (CBL). The CBL consumption is charged at rates that could be based on the COS regulation. This is the first part of the rate structure. A customer's baseline is based on the historical consumption of the customer (usually the consumption level in the year before the RTP is in place) [64]. Consumption above the CBL is charged at real-time rates and consumption below the CBL are credited at real-time rates. This is the second part of the rate. The unbundled RTP separates the cost to generate or procure energy from the cost of other services. The energy cost is charged at real-time rates or based on the estimated system lambda (marginal cost of energy) of a utility [64]. A customer can enter into a contract for difference to hedge risks. Under the con-

tract, customers are allowed to select their own CBL. Consumption below the selected CBL are credited at real-time rates and consumption above the selected CBL are charged at real-time rates. RTPs have been implemented by different utilities, such as Georgia Power, Progress Energy, and Duke Power [63], [64]. RTP rates are mostly applied to large customers.

2.5 Nodal Pricing in the Distribution System

RTPs capture the nature of the cost in the wholesale market, i.e., the time variation and the reflection of generation availability and transmission system conditions. They do not capture or reflect conditions in the distribution system. While the traditional distribution system has limited price sensitive resources and has no need for active power management or for considering network conditions, the contemporary distribution system and the future distribution system will have such resources and such needs. Hence, improvement in operations and investment may be achieved with a distribution system nodal price that reflects not only the transmission system state but also the distribution system state.

The concept of nodal distribution prices has generated some interest as of late with [42]-[47] discussing or proposing the use of some sort of nodal price in the distribution system. While the applications and the approaches discussed in the papers vary, the motivation behind the proposals or the impetus behind nodal distribution prices is the same – the smart grid initiative. The smart grid initiative is an endeavor to modernize the U.S. electric grid for the 21st Century. It was formally accepted as a policy of the U.S. government by the passage of the Energy

Independence and Security Act of 2007 [48]. Title XIII of the bill calls for modernizing the U.S. transmission and distribution grid to provide a reliable and secure grid to meet future demand and to meet certain characteristics. The characteristics, listed in Table 2.1, are the envisioned functions of a modern grid.

Table 2.1. Characteristics of a Smart Grid [49]-[52]

Characteristic	Definition
Intelligent	Capable of autonomous control and operation
Efficient	Better utilization and optimization of system resources and grid operation
Accommodating	Integration of all fuel sources including wind and solar DGs and integration of new technologies, such as energy storage systems
Motivating	Enabling interaction between consumers and utilities such as real-time communication of prices for demand response
Opportunistic	Creating new markets and opportunities through its plug and play capability
Quality-focused	Delivering power-quality befitting of the digital economy
Resilient	Self-healing and resistant to attack and natural disaster

The smart grid is a confluence of information and communication technologies with power systems engineering [53]-[55]. It is the application of a layer of information and communication technologies such as, wide-area network and sensors, to the power systems infrastructure. The layer of information and communication technologies will enable fundamental communications and control applications, such as two way communication between utilities and customers, advanced metering infrastructure (AMI), distribution management system (DMS), and substation and other distribution system automation. The smart grid is expected to have a marked effect on the distribution system [47], [53]. The smart grid initiative is expected to result in a substantial presence of DGs, energy storage, and

demand response at the distribution level. Under such a scenario, the distribution system could become an active meshed network [42], [43], potentially congested, with an operational paradigm that includes economic efficiency, active management and control of power flow, volt/var optimization, and operation of distributed energy resources (DERs) [45]-[47], [54]. A properly determined nodal price that adequately reflects system conditions and optimally couples the distribution and the transmission system can be effectively utilized as a control signal to incentivize efficient behavior of DERs under the smart grid environment.

Distribution nodal prices are proposed in [42] to incentivize increased DG penetration and proper location of DGs in the distribution grid. Reference [42] develops a nodal price similar to the transmission system LMP. The nodal price, which has no congestion component, is calculated based on the energy price at the transmission proxy and the impact of a DG's generation on marginal losses. Reference [42] develops an equation for the nodal price by applying the KKT conditions to an economic dispatch problem that minimizes both real and reactive power costs subject to a node balance constraint. The equation essentially calculates the price at a node by adding to the proxy LMP, the marginal cost of losses that is determined by multiplying the proxy LMP by the sensitivity of losses to the injection at the corresponding node. The authors argue that paying DGs based on their location, rather than a uniform price (proxy price) will provide additional revenue for the DGs and incentivize increased penetration and proper DG location.

A distribution nodal price is proposed in [43] to increase DG benefits, reduce losses in the distribution system, and provide distribution companies a control

signal to align private DG operation with the goals of distribution system operation. The nodal price developed in [43] is not the same as the transmission system LMP. Rather, it is based on a loss reduction allocation mechanism. Under the mechanism, a base case is established and the deviation of losses from the base case as a result of a DG's production is used to calculate the nodal price at the DG's bus. Nodal prices are calculated for DG buses only. Load buses pay a uniform price. An iterative approach is employed to consider the possibility of DG output deviating from the output used to calculate a nodal price, i.e., an iterative approach is used to handle the fact that nodal prices are based on DG outputs, which are dependent on nodal prices. In the first iteration, a uniform price that is equal to the transmission proxy LMP is applied to all the buses in a distribution system. The resulting DG outputs are used to calculate distribution nodal prices. The distribution nodal prices are then used to calculate a new set of DG outputs. The iteration continues until convergence is achieved. Note that the iteration is not between the transmission and the distribution system; rather, it is within the distribution system for nodal prices in the distribution system. An artificial neural network (ANN) based mechanism to predict day-ahead distribution nodal prices to help distribution companies forecast DG generation for the next operating period is also developed in [43].

Distribution nodal pricing is proposed as a control signal for distribution system resources in [44] and [45]. The price in [44] is similar to the transmission LMP and it is calculated based off of a DCOPF formulated as a quadratic programming problem to include losses in the lossless DCOPF. The distribution nod-

al price scheme in [45] is proposed as a control signal around which multiple distribution operation objectives can be optimized. The work is motivated by the changing control possibilities in the distribution system. The nodal price is calculated based off of transmission proxy LMPs and a marginal loss and congestion cost calculated by a Jacobian based AC distribution factor. The work allows for multiple transmission connection to the distribution system by multiplying the proxy LMPs by a participation factor that represents the contribution of each transmission supply point to the consumption at a node. The distribution nodal price is applied, via a multi-objective programming formulation, for energy management control. The objectives include peak power, peak energy consumed, cost of energy, and the total energy loss in the power electronics of energy storage systems.

2.6 Conclusion

With discussions on the LMP concept, the OPF problem, COS regulation, distribution system rate structures and nodal pricing in the distribution system, this chapter provides the background and context necessary to understand the work in this thesis. The chapter defined the LMP as the cost to supply an increment of energy at a specific node in the grid and discussed the properties that provide the LMP the capability to incentivize economic efficiency. The chapter discussed the OPF problem, which is used to calculate LMPs. The chapter also discussed the COS regulation as a set-up to exploring the inability of rates, such as the flat rate, the TOU rate, and the CPP, to effectively incentivize economic efficiency. While the RTP represents the most accurate prices that can be obtained in the contempo-

rary distribution system, they may not suffice under an enhanced distribution system environment. Hence, nodal distribution prices have been proposed by several papers to incentivize appropriate behavior of price sensitive distribution system resources.

Chapter 3. The Distribution-Class Locational Marginal Price (DLMP)

Index

This chapter discusses the DLMP. It begins with the definition, properties, and benefits of the DLMP in Section 3.1. A two-stage optimization process for calculating the DLMP and for optimally coupling the transmission and the distribution system are discussed in Section 3.2. The chapter discusses the issues of fairness of nodal prices in the distribution system and the issue of customer exposure to price volatility in Section 3.3 and Section 3.4. It concludes with a discussion on the factors that may limit the ultimate usage of the DLMP in the distribution system in Section 3.5.

3.1 The Distribution-class Locational Marginal Price (DLMP) Index

The DLMP proposed in this thesis is a type of nodal distribution system price. It is the extension of the LMP concept to the distribution system. Apart from the system both are used in, the DLMP has the same definition as the LMP and it has similar properties to the LMP. It is the cost to optimally deliver an increment of energy to a specific node in a distribution system without violating any system security or operational constraints. It reflects the marginal cost of energy and it captures the effect, on congestion and system losses, of delivering incremental energy to a specific location in a distribution grid. Both the transmission system and the distribution system states are considered in calculating the DLMP. Hence, a DLMP reflects the network conditions and generation availability of both the transmission and the distribution systems. The DLMP is proposed for use as a

control signal to incentivize DSRs to behave optimally in way that benefits economic efficiency and system reliability, to optimally couple the transmission and the distribution system, and to incentivize DSRs to locate optimally.

The benefit of the DLMP to economic efficiency is similar to that of the LMP to economic efficiency. The DLMP, by being calculated by the interaction of the market supply and demand curves, is economically efficient. This is illustrated by the supply and demand curve in Figure 3.1. At the market clearing price (MCP), the price at which the supply and the demand curve intersects P^* , market surplus (MS) is maximized. MS or social surplus (SS) is a measure of economic efficiency. It is the benefit that accrues to both suppliers and consumers for trading in a market. The benefit that accrues to suppliers is the producer surplus (PS) and the benefit that accrues to consumers is the consumer surplus (CS). PS can be viewed as short-term producer profit and CS as consumer cost savings. MS or SS is the sum of PS and CS. In Figure 3.1, the PS is $D + E + F$, the CS is $A + B + C$, and the MS is $A + B + C + D + E + F$ if the price is P^* . At any price other than the MCP, there is a loss of efficiency, termed dead weight loss (DWL). In Figure 3.1, a DWL equal to G occurs if the price P_1 is imposed on the market. That is, the MS is equal to $A + B + C + D + E + F - G$. Wealth, equal to $D + E + H + I$, is transferred from producers to consumers. The PS is F . If the price P_2 is imposed, a DWL equal to $C + E$ occurs. The MS is equal to $A + B + D + F$. Wealth, $B + D$, is transferred from consumers to producers. The CS is A . Only the MCP supports equilibrium between the desire to consume versus the desire to produce. Imposing a lower price will result in a shortage as the quantity available for con-

sumption will be less than the quantity desired for consumption. Imposing a higher price will result in over-production as the quantity available for consumption will be greater than the quantity desired for consumption. In a power system, a price lower than the MCP will result in over-consumption and a price higher than the MCP will result in under-consumption.

The DLMP is determined based on the interaction of the supply bids of generators and the demand bids of loads. Hence, the DLMP is a MCP and the consumption it will incentivize will, theoretically, maximize bid surplus for a convex market. For a power system, this translates to optimal energy production and consumption. Energy production will be optimal if the cost to generate energy to reliably serve distribution loads is the cheapest possible. That is, subject to reliability, the cheapest DGs and ESSs are dispatched and an optimal mix of production from distribution resources and the transmission system is achieved. Consumption will be optimal, if consumption is from the PRLs that value consumption the most and consumption is matched to generator marginal costs.

In addition to its determination by the interaction of supply offers and demand bids, the DLMP is nodal. The nodal property allows the DLMP to reflect the individual contribution of consumption at a node to system condition and costs. Consequently, the DLMP can capture the individual cost of loads at a node to system conditions and, as such, it is not distorted by and reduces cross-subsidy between customers. Cross-subsidies occur when a consumer does not pay the “true cost to the system” of its consumption. Some customers pay more than their true costs

while others pay less. Cross-subsidies distort prices and incentivize suboptimal behavior. Hence, cross-subsidies degrade economic efficiency.

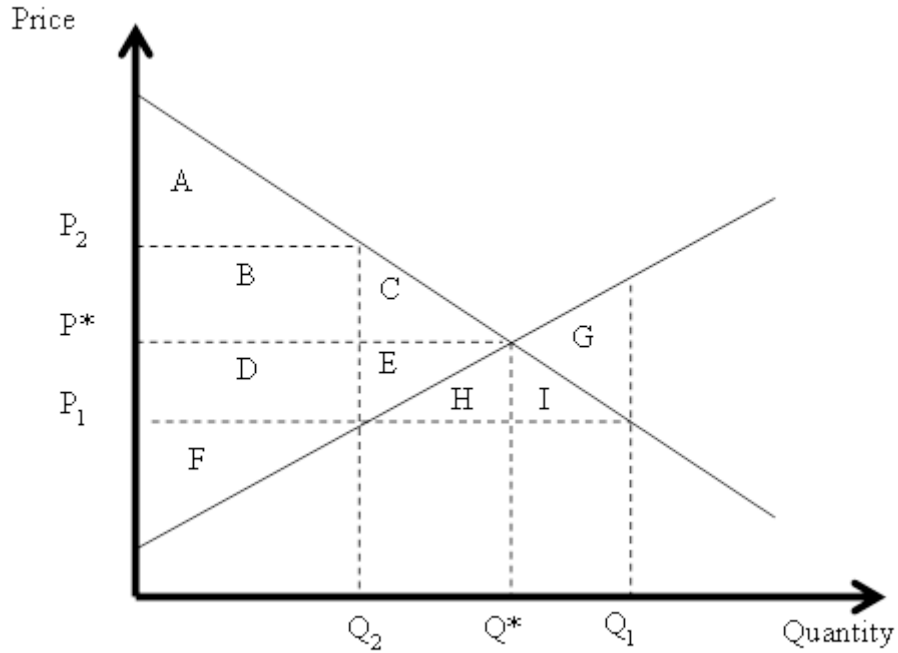


Figure 3.1. Supply and Demand Curve

The benefit of the DLMP to system reliability is also similar to the benefit of the LMP to system reliability. The DLMP, by its nodal property and by reflecting the impact of marginal consumption on network conditions (rather than reflecting embedded costs), can align a DSR's behavior with the system operational objective. If a network is stressed or generation is scarce, the DLMP appropriately incentivizes DSRs to act in a way to help maintain reliability; this is accomplished by matching consumption to generation based on the value loads place on consumption and the marginal cost of generation and reliability.

Incentivizing optimal DSR behavior or improving economic efficiency could lead to reduced operational cost, not only in the distribution system but for the

power system as a whole. The benefit of the DLMP to reliability could also be to the power system as a whole. For example, DSRs controlled by the DLMP could potentially be used for demand response (DR) and for ancillary services. In order to realize the benefit of the DLMP at the transmission system level, the transmission and the distribution systems must be optimally coupled. Optimal coupling of both systems can be achieved by the DLMP correctly reflecting both the transmission and the distribution system states.

In the long term, the DLMP is efficient because it can signal where upgrades are most needed and it can be used to guide investment decisions. Information about where upgrades are needed and where resources should be located in a system could be gleaned from the nodal separation of DLMPs. Information about the optimal technology to investment in could be gleaned from the DLMP. The DLMP could also incentivize reduced peak consumption, which could help defer expensive upgrades and help utilize existing resources more efficiently.

3.2 Calculation Approach of the DLMP

Similar to the LMP, the DLMP will be calculated as the dual variable of a node balance constraint in an OPF problem. Ideally, the OPF problem should be solved for a single transmission and distribution system model. Such an approach provides the opportunity to consider the resources and the network condition of the entire power system. The approach may, however, be computationally intractable as a result of size. Consequently, a two-stage optimization approach, illustrated in Figure 3.2, is proposed for calculating DLMPs. The first stage of the op-

timization process is the transmission system OPF. The details of the distribution network are not modeled in the transmission system OPF. Rather, the distribution system is represented by its aggregate demand. The second stage is the distribution system OPF. The details of the transmission system are not modeled in the distribution system OPF. Rather, the transmission system is modeled as an infinite generator with its marginal cost equal to the distribution proxy LMP in the transmission system OPF. The two-stage decomposition approach is similar to current practices where the transmission and the distribution model are separated to improve computational efficiency. It is also the approach in the other papers [42]-[45] proposing nodal distribution system prices.

The separation of both systems poses a problem regarding accurate modeling of one system in the other. Usually, the distribution system aggregate demand is forecasted and used in the transmission system model. For a distribution system lacking in price sensitive resources and lacking in important network characteristics, such as congestion, it is sufficient to simply use the distribution proxy LMP to calculate DLMPs, which can be described as a single-shot approach. For an enhanced distribution system with price sensitive resources and important network characteristics, it may be more difficult to accurately forecast the distribution system's aggregate demand. Without properly representing the distribution system's network and price sensitive resources in developing forecasts for the distribution system, it is possible that distribution system resources will deviate from the model used in the transmission system OPF. The deviation could result in a

sub-optimal solution for both the transmission and the distribution systems OPF and resources may be improperly incentivized.

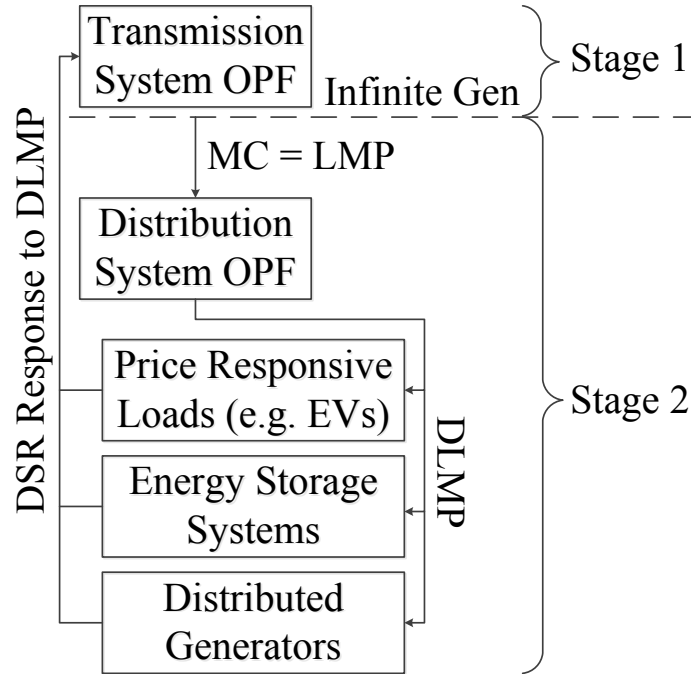


Figure 3.2. DLMP Calculation and Application Framework

In order to ensure an accurate representation of the distribution system for the transmission system OPF and vice versa, the DLMP calculation framework can iterate between the first and the second stages of the optimization process until the problems converge to a solution where further iterations neither leads to changes in LMPs or changes in the distribution system aggregate load. At each iteration, the latest results from the other process will be an input to the optimization problem that is been solved. For example, in the first iteration, the forecasted aggregate load of a distribution system will be used to model the distribution system for the transmission system OPF. The resulting LMPs at the distribution proxies in the transmission system OPF will be the marginal cost of the infinite generators in

the distribution system OPF. In the second iteration, the new aggregate load that results from the first distribution OPF is used to model the distribution system in the new transmission system problem and the new LMPs that results from the second transmission system OPF will be used to calculate new DLMPs.

The iterative framework essentially couples the transmission and the distribution system in an optimal manner. The iterative approach allows the price sensitivity of distribution system resources and the distribution system network condition to be accurately modeled for the transmission system OPF and the impact of network conditions and generation availability in the transmission system to be optimally translated into a control signal for distribution system resources. The transmission system state, which will affect transmission LMPs, will be reflected in DLMPs and the benefits of having distribution system resources will be reflected in the distribution system's aggregate demand from iteration to iteration. Optimally coupling the transmission and the distribution systems provides ample opportunities for demand response and for utilizing distribution resources for ancillary services. Demand response can have a marked impact on market efficiency. It is the most effective cure for exercise of market power, which results in price volatility. It is also an effective tool for reliability especially with variable generation. Demand response can be faster than generator ramp rates and demand response could be cheaper than carrying more reserves or building new facilities to provide reserves. Demand response can also help with peak shaving and deferring expensive system upgrades. While [42]-[45] separate the transmission and the distribu-

tion system OPF problems, the calculation approaches in the papers do not iterate between both problems.

Both OPFs in the two-stage optimization process can be based on either the DCOPF or the ACOPF. In this research, the DCOPF formulation is used for both the transmission system problem and the distribution system problem. The assumptions used to obtain the DCOPF (discussed in Section 2.2) are, however, based on the characteristics of the transmission system and may not hold for the distribution system. Particularly, the percentage of energy losses in the distribution system is higher than in the transmission system as a result of higher r/x ratios and as a result of lower voltage level of operation [32], [46]. To correct for this assumption, a lossy DCOPF model is used for the distribution system OPF. The lossy DCOPF model is also used for the transmission system OPF as it improves on the current practice of marginal loss modeling. The marginal loss modeling technique, which uses a slack or distributed slack bus method to approximate losses, can result in inaccurate dispatch solutions and LMPs. Furthermore, the slack or distributed slack bus method can produce varying LMP results for the same dispatch solution based on the approximation method used to distribute losses [68]. The lossy DCOPF formulation is discussed extensively in Chapter 4. The DCOPF also assumes that voltages are kept within a tight range around 1 p.u. for transmission system operation. Hence, voltages are assumed to be approximately 1 p.u. in the DCOPF. Voltages in the distribution system can deviate significantly from 1 p.u. ANSI C84.1 recommends maintaining service voltage between $\pm 5\%$ of nominal voltage [71]. For the studies in this research, DLMPs are

calculated only on the primary distribution system feeders or at the secondary terminals of a distribution transformer. The DCOPF and the ACOPF assume balanced 3-phase operation. The distribution system is unbalanced. This DCOPF assumption is not corrected for the distribution system. Taking into consideration distribution system unbalance requires a 3-phase unbalanced power flow with prices potentially differing between the different phases. The assumption will not impact the studies conducted in this research, which are focused on economic efficiency. Future research can consider expanding the iterative framework to incorporate an unbalanced OPF formulation for the distribution system.

The calculation of the DLMP is assumed, in this work, to be done by the system operator. The system operator will individually optimize the distribution system and centrally optimize the transmission system. The iterative process is conducted for the system as a whole: the transmission system and the distribution systems. The communications and the control infrastructure to support the functions of the DLMP will be available as a result of the smart grid initiative. The DLMP will be suitable for both day-ahead and real-time purposes.

3.3 Fairness of Nodal Prices in the Distribution System

Fairness is a major objective in rate making and in utility regulation [69]. It is a topic that has been discussed in regards to ratemaking for many decades. The question of fairness, for the DLMP, goes to the appropriateness of rate discrimination based on customer location. That is, is it fair to have consumers in the same distribution system pay different prices because they are located at different nodes

on the grid? Fairness is difficult to judge as it is dependent on the observer. For example, a load at the end of a feeder may feel unfairly treated if it has to pay more than the load at the beginning of the feeder. At the same time, the load at the beginning of a feeder may feel unfairly treated if it has to subsidize the losses for the consumer at the end of the feeder. Regardless of the price signal or the rate structure, there are always winners and losers. It is not the goal of this research or the responsibility of an Independent System Operator (ISO) to decide who the winners and the losers are. Rather, the primary objective of the ISO is to maximize social welfare and this is partially achieved by ensuring that the prices are proper economic signals in order to optimally incentivize economically efficient behavior. For a convex market, the DLMP is the optimal pricing mechanism to incentivize efficient and reliable behavior from the market participants.

3.4 Price Volatility with the use of the DLMP

Concerns about customer exposure to price volatility may arise with the implementation of the DLMP. Unlike a flat rate or a TOU rate, which are established and fixed over long time periods, the DLMP can change as frequently as it is calculated and it can theoretically be as high as infinity. Factors that may affect the volatility of the DLMP include the transmission LMP, congestion, scarcity in the distribution system, and bid practices of distribution system resources. The volatility of the LMP represents a major source of volatility for the DLMP. The LMP could be volatile as a result of bid practices in the transmission system and as a result of congestion and scarcity in the transmission system. As an input into the DLMP calculation, the volatility of the LMP at the transmission proxy of a distri-

bution system may translate into volatility for the DLMP. DLMP volatility could also result from system conditions, such as congestion and scarcity. During the times when the distribution system is stressed, the system conditions will be reflected through the DLMP. DLMP volatility could also occur, theoretically, as a result of strategic bidding from distribution system resources.

While price volatility may be regarded as undesirable, DLMP volatility as a result of system conditions provides information about the state of the system. For example, a high DLMP as a result of congestion shows there may be need for an upgrade at a location and it incentivizes system resources to behave in a manner to achieve economic efficiency and reliability subject to the congestion. Hedging mechanisms can be developed and offered alongside the DLMP. The mechanism can offer different degree of protection against price volatility for risk-averse consumers. The mechanism can be based on a contract for differences similar to that described in Section 2.4 for contemporary RTPs. Prices for the contracts will be determined by market forces. Unlike contemporary rates, such as the flat, block, or TOU rates, which protects against volatility but are determined based on COS regulation, a market-based hedging mechanism allows for price discovery.

Price volatility as a result of bid practices negatively impacts market efficiency. Strategic behavior can be expected to be insignificant in the distribution system as the option to purchase from the transmission system is always available. A resource can only exercise market power or behave strategically up to the point that the option of purchasing from the transmission system becomes a viable option. The use of the DLMP can help reduce price volatility in bulk energy markets

by optimally representing price responsive demands in the bulk energy market. One of the major reasons generators have the opportunity to bid strategically or exercise market power in the transmission system is because loads are assumed to be largely inelastic. Price elasticity of demand can curb strategic behavior because there is always the threat that a generator bidding strategically or exercising market power can miss out on an opportunity to produce. If a generator does not bid its true marginal cost, the generator's bid in the market may not be cleared if loads view the cost as too high. Hence, the environment surrounding the use of the DLMP can reduce price volatility in the LMP, which can in turn reduce the DLMP volatility. The extent to which demand flexibility can curb strategic behavior will be dependent of the flexibility of demand resources and the amount of flexible resources available.

3.5 Factors that will Affect Ultimate Usage

There are differences between the contemporary distribution system design and the transmission system that can limit the ultimate usage and benefit of the LMP concept in the distribution system. The transmission system is a highly meshed network with multiple generators. There could be multiple congested interfaces in the transmission system and as such, there is a need for the LMP to help manage congestion. The contemporary distribution system often has the transmission system as the major, and sometimes the only, source of energy into the distribution system. The contemporary distribution system is operated predominantly in a radial configuration with power flowing from the distribution substation to loads. As a result of radial power flow, distribution circuits and

equipment are overbuilt to avoid congestion. Consequently, the DLMP in a radial distribution system may have no congestion component. Only losses will cause separation between DLMPs at different nodes. As a result, the improvement that may be obtained for such a system, over the FR, the TOU, or a contemporary RTP, may not justify the complexities of administering a DLMP, especially if loads are treated as inelastic and there are limited generation resources. Also, while the transmission system has multiple generators that are price sensitive and, to a lesser extent, price responsive loads and agents, such as virtual bidders and market makers, the distribution system has limited price responsive resources: load is viewed as perfectly or highly inelastic.

The benefits of the DLMP to the contemporary distribution system may be limited but the DLMP is developed for the enhanced distribution grid expected as a result of the smart grid initiative. The enhanced distribution system is expected to have a substantial amount of price responsive resources such as PRLs, ESSs, and DGs. These resources are already materializing in the distribution system. For example, DR is implemented in various forms in electricity markets and rates such as the TOU, CPP, and RTP are an admission that loads do respond to prices. Also, with DGs, there can be multidirectional flows in the future distribution system. For such a grid, the benefit of the DLMP to the distribution system will be impacted by network topology, distribution system losses, and congestion. There will also be a major benefit to the whole power system as the coupling between the transmission and the distribution system will affect economic efficiency and reliability for the whole system.

3.6 Conclusion

The DLMP is defined and its properties and benefits are discussed in this chapter. The objective of introducing the DLMP in enhanced distribution systems is also discussed. The DLMP is envisioned as an efficient control signal for incentivizing optimal DSR behavior such that DSR behavior is aligned with system operation objectives and economic efficiency is improved. The DLMP is also envisioned to optimally couple the transmission and the distribution system. The coupling is proposed to be effected through an iterative approach to calculating DLMPs. The coupling will allow the gains realized from the use of the DLMP to be translated to economic and reliability gains for the transmission system. Issues, such as fairness and price volatility, surrounding the DLMP usage are also discussed. The DLMP is proposed for use in an enhanced distribution system.

Chapter 4. Lossy DCOPF for DLMP Calculation

As discussed in Section 2.2, the traditional DCOPF is a lossless formulation. Nodal prices and dispatch solutions obtained from a lossless DCOPF do not reflect the effects of real power losses. Real power losses are of particular importance in distribution system applications: distribution system circuits have high resistances and the voltage level is low. Real power losses will also be the only factor that results in nodal price separation in a distribution system that is not congested. As a result, a lossy DCOPF formulation is developed in this chapter for calculating DLMPs. The same formulation can be applied in the transmission system to calculate LMPs. The lossy DCOPF formulation is particularly attractive because loss approximation does not require an iterative process [16] and loss approximation, rather than being conducted ex-post [16], is endogenous to the formulation. The formulation is also attractive because it does not require the definition or existence of a slack bus. Hence, the formulation is not arbitrary as solutions do not change with a changing slack bus definition [7], [17]-[19], which is what occurs with an iterative technique that places losses at the slack or distributed slack bus.

The lossy DCOPF formulation is developed and some issues surrounding its use are presented in this chapter. In Section 4.1, a discussion on the loss approximation technique, the derivation of the linear expressions that approximates the AC loss equation and the lossy DCOPF, formulated as a linear programming problem, is presented. Under the scenario that non-positive DLMPs or LMPs occur in a problem with the lossy DCOPF formulation, artificial losses could be in-

correctly created and resulting solutions could be wrong. The scenario and an adjacency and an exclusivity condition, which when satisfied guarantee correct loss approximation and solutions, are discussed in Section 4.2. The occurrence of artificial or non-physical losses is theoretical proven in Section 4.3 using duality theory and the Karush Kunh Tucker (K.K.T.) conditions. The presented theoretical proof is one of the major contributions of this work to the existing body of knowledge in this field. Several publications, e.g., [20]-[22], have used the loss approximation technique without discussing its breakdown. The presented proof goes beyond the scope of the work in [23]-[27]. If the lossy DCOPF formulation breaks down, integer constraints can be applied to enforce the adjacency and the exclusivity conditions. The constraints and a mixed-integer linear programming (MILP)-based lossy DCOPF formulation is presented in Section 4.4. The MILP-based formulation is only used in place of the linear programming-based formulation when the lossy formulation breaks down.

4.1 Lossy DCOPF Formulation

The lossy DCOPF formulation is developed by simply adding linearized real-power loss equations to the standard DCOPF problem. By including the linearized loss equations, the DCOPF formulation endogenously approximates real power losses and endogenously captures the effect of losses on dispatch solutions and prices. By linearizing losses, the linear properties of the DCOPF, discussed in Section 2.1, are retained for the lossy formulation. For example, the lossy DCOPF does not suffer from the convergence issues of the ACOPF and it converges to a

solution relatively quickly. The approach employed to develop the linearized equations is the piecewise linear technique discussed in [21] and [22].

The first step in developing the lossy DCOPF formulation is to linearly approximate real power losses. Equation (4.1) is the AC expression for real power losses that is to be linearized. Equation (4.1) is obtained for any line k by subtracting the AC power flow expression for the power delivered to the receiving end bus of k from the AC power flow expression for the power injected at the sending end of k and applying the approximation that bus voltages are approximately 1 p.u. This can be illustrated with the two bus system in Figure 4.1. Equation (4.2), the full AC equation of real power losses on k as a result of k 's resistance and the current it carries, is obtained by subtracting the AC power flow expression of P_k^{nm} from the AC power flow expression of $-P_k^{mn}$. Note that P_k^{mn} is the power injected from bus n onto line k and its negative is the power delivered to bus n . Also note that the AC power flow expression for P_k^{nm} and $-P_k^{mn}$ follow the power flow expression in (2.3). The approximation that bus voltages V_m and V_n are 1 p.u is applied to (4.2) to derive (4.1). The approximation, which is one of the approximations used to develop the DC approximation of the line flow equation, allows for (4.1) to be linearized over $(\theta_n - \theta_m)$, the bus angle difference across k .

The non-linear part of (4.1), i.e., $1 - \cos(\theta_n - \theta_m)$, along with a piecewise linear curve approximation is shown in Figure 4.2. The product of the expression that describes the piecewise linear approximation curve and $2G_k$, the conductance term in (4.1), is the linearized loss expression. An expression for the piecewise curve is developed by using the length of the segments of the curve to approxi-

mate $(\theta_n - \theta_m)$ as in (4.3) - (4.5). The length and the slope of the segments used in the angle difference approximation are then used to represent the piecewise linear curve as in (4.6). Equation (4.6) is multiplied by $2G_k$ to linearly approximate real power losses as in (4.7),

$$P_n^L = 2G_k(1 - \cos(\theta_n - \theta_m)) \quad (4.1)$$

$$Loss = |V_m|^2 G_k + |V_n|^2 G_k - 2|V_m||V_n|(G_k \cos(\theta_n - \theta_m)) \quad (4.2)$$

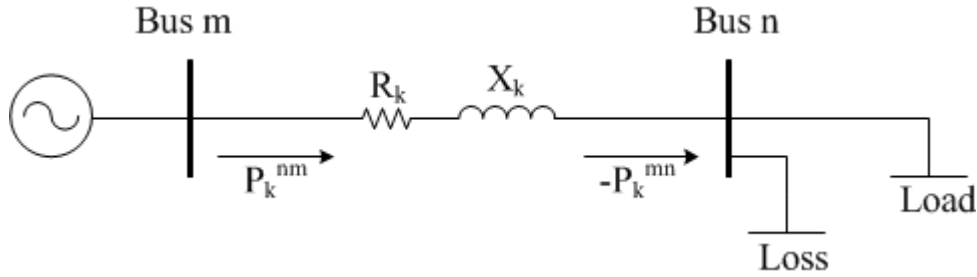


Figure 4.1. Two-Bus System for Real Power Loss Expression Derivation

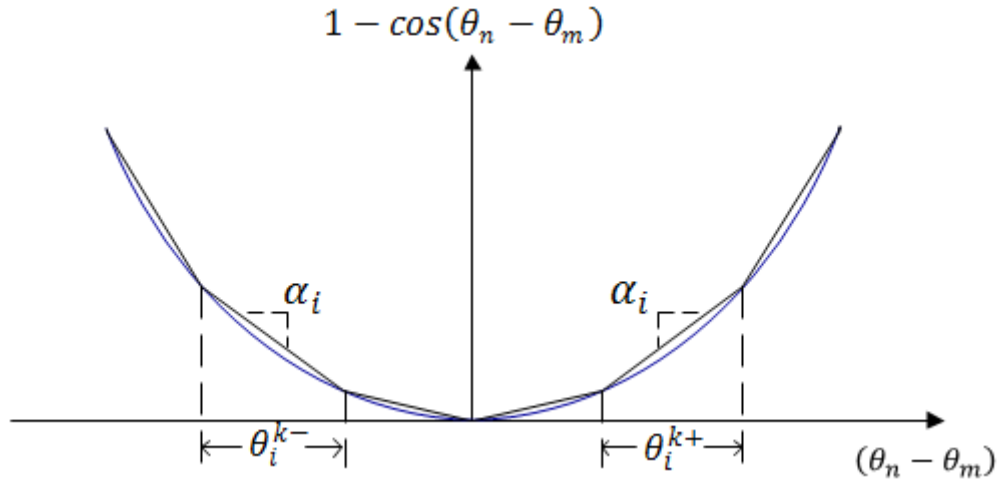


Figure 4.2. Plot of $1 - \cos(\theta_n - \theta_m)$ and its Piecewise Linear Approximation Curve

$$(\theta_n - \theta_m) = \left(\sum_{\forall i} \theta_i^{k+} - \sum_{\forall i} \theta_i^{k-} \right) \quad (4.3)$$

$$0 \leq \theta_i^{k+} \leq \theta_i^{\max} \quad \forall i \quad (4.4)$$

$$0 \leq \theta_i^{k-} \leq \theta_i^{\max} \quad \forall i \quad (4.5)$$

$$1 - \cos(\theta_n - \theta_m) = \left(\sum_{\forall i} \alpha_i \theta_i^{k-} \right) + \left(\sum_{\forall i} \alpha_i \theta_i^{k+} \right) \quad (4.6)$$

$$P_n^L = \left[\sum_{\forall k(n,:)} 2G_k \left(\sum_{\forall i} \alpha_i \theta_i^{k-} \right) \right] + \left[\sum_{\forall k(:,n)} 2G_k \left(\sum_{\forall i} \alpha_i \theta_i^{k+} \right) \right]. \quad (4.7)$$

The first term on the RHS of (4.7) is the expression for the loss contribution of lines that have a bus n as their receiving end bus and the second term is the expression for the loss contribution for lines that have the bus as their sending end bus. Distinction is made between the two because the real power losses associated with a line is placed as a fictitious demand (FD) at the bus that is receiving a positive injection of real power from the line. Determination of loss placement is done endogenously by the lossy DCOPF formulation based on the sign of the bus angle difference across a line. For the DC approximation of the line flow equation in this research, a negative angle difference indicates that power flow is in the pre-defined direction. Consequently, losses are placed at the designated receiving end of a line if a negative angle difference occurs across the line. A positive angle difference indicates that power flow is in the opposite of the pre-defined direction. Consequently, losses are placed at the designated sending end bus of a line if a positive angle difference occurs across the line. In Figure 4.1, the losses on k will be placed at bus n because the angle difference across k will be negative, i.e., power flow will be to bus n . As will be discussed in Section 4.2, the loss approximation technique uses the two terms on the RHS of (4.3), to determine loss or FD placement. The terms correspond to the sum of the lengths of positive and nega-

tive orthant segments used to approximate the angle difference across a line respectively.

The lossy DCOPF is formulated as a linear programming problem in (4.8) - (4.20). The formulation is developed by adding (4.3) - (4.5) and (4.7) to the standard DCOPF formulation. Equation (4.8), the objective function of the lossy formulation, represents market surplus (MS) or bid surplus. Constraint (4.9) is the DC approximation of the line flow equation. Constraint (4.10) is the node balance equation. The loss term in the constraint is a variable load and its value is determined using constraint (4.11), the linearized loss equation. The other terms in (4.10) are the sum of the generator injections at a bus, the sum of the power flowing into the bus and the sum of the power flowing out of the bus. Constraint (4.12) is the angle difference approximation from (4.3). Constraints (4.13) - (4.16) are the restrictions in (4.4) and (4.5) that define the minimum and maximum length of the segments in the piecewise linear approximation. Constraint (4.17) and (4.18) are the constraints for line capacity limits and (4.19) and (4.20) are the constraints for generator output limits. A DCOPF can include an angle difference constraint as a proxy for transient stability limit. Rather than include an explicit angle difference constraint, the limit is enforced by the maximum possible sum of the length of the piecewise linear curve used for loss approximation. For example, if the angle difference limit is to be set at 30 degrees, then the maximum possible sum of the length of segments in the same orthant will be 30 degrees,

$$\text{Maximize: } \sum_t \sum_d b_{d,t} D_{n,d,t} - \sum_t \sum_g c_{g,t} P_{g,t} \quad (4.8)$$

subject to:

$$B_k(\theta_{n,t} - \theta_{m,t}) - P_{k,t} = 0 \quad \forall k, t \quad (4.9)$$

$$\sum_{g \in G_n} P_{g,t} + \sum_{\forall k(n,:)} P_{k,t} - \sum_{\forall k(:,n)} P_{k,t} - P_{n,t}^L - \sum_d D_{n,d,t} = 0 \quad \forall n, t \quad (4.10)$$

$$P_{n,t}^L - \left[\sum_{\forall k(n,:)} 2G_k \left(\sum_{\forall i} \alpha_i \theta_{i,t}^{k-} \right) \right] - \left[\sum_{\forall k(:,n)} 2G_k \left(\sum_{\forall i} \alpha_i \theta_{i,t}^{k+} \right) \right] = 0 \quad \forall n, t \quad (4.11)$$

$$(\theta_{n,t} - \theta_{m,t}) - \left(\sum_{\forall i} \theta_{i,t}^{k+} - \sum_{\forall i} \theta_{i,t}^{k-} \right) = 0 \quad \forall k, t \quad (4.12)$$

$$\theta_{i,t}^{k+} \geq 0 \quad \forall i, k, t \quad (4.13)$$

$$\theta_{i,t}^{k-} \geq 0 \quad \forall i, k, t \quad (4.14)$$

$$-\theta_{i,t}^{k+} \geq -\theta_i^{\max} \quad \forall i, k, t \quad (4.15)$$

$$-\theta_{i,t}^{k-} \geq -\theta_i^{\max} \quad \forall i, k, t \quad (4.16)$$

$$P_{k,t} \geq -P_k^{\max} \quad \forall k, t \quad (4.17)$$

$$-P_{k,t} \geq -P_k^{\max} \quad \forall k, t \quad (4.18)$$

$$P_{g,t} \geq P_g^{\min} \quad \forall g, t \quad (4.19)$$

$$-P_{g,t} \geq -P_g^{\max} \quad \forall g, t \quad (4.20)$$

$$P_{g,t}, P_{k,t}, \theta_{n,t}, P_{n,t}^L \text{ free.}$$

4.2 Conditions for Correct Solutions

Equation (4.12) in the lossy DCOPF formulation is the link between the piecewise linear approximation of losses and the DC approximation of the line flow equation. By coupling (4.9) and (4.11), (4.12) enforces a proportional relationship between the magnitude of the real power losses and the magnitude of the real power flow on a line. Equation (4.12) also pegs the placement of approximat-

ed losses to the direction of actual power flow. If the order in which segments are selected in (4.12), to approximate $(\theta_n - \theta_m)$, satisfies an adjacency and an exclusivity condition, the lossy DCOPF formulation will correctly approximate and place losses.

The adjacency condition requires the length of all lower positioned segments to be fully utilized if there is a higher positioned segment in the same orthant that is used to approximate a bus angle difference. Mathematically, this can be written for segments in the positive orthant as:

$$\theta_j^{k+} = 0 \text{ if for any } i < j \exists \theta_i^{k+} < \theta_i^{max}$$

Since there is no explicit constraint in the linear programming-based lossy DCOPF formulation that defines segments selection order, each θ_i^{k-} and each θ_i^{k+} is treated independently of every other θ_i^{k-} and θ_i^{k+} in the selection process. As a result, segments, regardless of position, can be selected to approximate $(\theta_n - \theta_m)$ in any order. An indirect selection order exists in the form of the slope of the piecewise segments. For segments in the same orthant, segment slopes increase with distance from the origin and each segment has a slope that is different from the slope of every other segment in the same orthant. If the linear programming-based lossy formulation works correctly, artificial losses are not created and the losses associated with a problem are correctly approximated. The increasing slopes of segments in the same orthant forces the formulation to respect the adjacency condition in order to properly reflect power losses. Respecting the adjacency condition ensures correct approximation of losses because (4.11) is a sum of

the product of the lengths and the slopes of the segments selected to approximate $(\theta_n - \theta_m)$ in (4.12). Using a higher segment with a higher slope in place of a lower segment with a lower slope to approximate the same angle difference will result in over-estimation of losses, i.e., artificial losses created. If the linear programming-based lossy DCOPF formulation breaks down in such a way that artificial losses are created, the adjacency condition will be violated and losses will be incorrectly approximated by selecting segments with higher slopes in place of segments with lower slopes.

The exclusivity condition requires that all the segments used to approximate an angle difference lie in the same orthant. Segments in the positive orthant must be exclusively used to approximate positive angle differences and segments in the negative orthant must be exclusively used to approximate negative angle differences. Mathematically this can be written as:

$$\theta_i^{k+} = 0 \text{ when } (\theta_n - \theta_m) < 0 \forall i \text{ and } \theta_i^{k-} = 0 \text{ when } (\theta_n - \theta_m) > 0$$

As discussed in Section 4.1, loss placement is determined endogenously based on the sign of $(\theta_n - \theta_m)$. Loss placement is effected by the selection of θ_i^{k+} and θ_i^{k-} . The exclusivity condition is necessary because θ_i^{k+} and θ_i^{k-} for a line k appear in different FD equations. That is, θ_i^{k+} and θ_i^{k-} appear in (4.11) for different buses. θ_i^{k+} for a line k appear in the FD equation for the designated sending end bus and θ_i^{k-} appear in the FD equation for the designated receiving end bus. If the angle difference across a line is positive and θ_i^{k+} s are selected to approximate the angle difference while the θ_i^{k-} s are zero, losses will be correctly placed at the

sending end bus of the line. If the angle difference across a line is negative and θ_i^{k-} s are selected to approximate the angle difference while the θ_i^{k+} s are zero, losses will be correctly placed at the receiving end bus of the line. If in either case, both terms in (4.12) are non-zeros, that is the exclusivity condition does not hold, losses will be placed at both ends of a line in a proportion determined by the split of the angle difference and the slope of the segments selected in each orthant. The split is possible because (4.12) only requires the magnitude of the angle difference across a line to be equal to the sum of the lengths of the segment approximating it. Since each θ_i^{k-} and each θ_i^{k+} is treated independently of every other θ_i^{k-} and θ_i^{k+} and since there is no explicit constraint on selection order, the lossy formulation can select segments in both orthants to approximate an angle difference.

In addition to the incorrect placement of losses, violation of the exclusivity condition also results in the magnitude of the approximated loss being artificially increased. This results from the two terms in (4.12) having opposite signs. If the exclusivity condition is violated, the absolute value of the magnitude of the sum of the lengths of the segments in one orthant must be greater than the absolute value of the angle difference approximated and the sum of the lengths of the segments in the other orthant must be non-zero in order for (4.12) to hold. Since (4.11) is a sum of products of the lengths and slopes of all selected segments in (4.12), losses will be over-estimated. The lossy formulation behaves in such a manner when it breaks down in order to artificially increase the losses at a bus without violating a constraint manifested as a binding angle difference limit.

For a problem with strictly positive DLMPs/LMPs, the lossy formulation appropriately estimates losses. A positive DLMP/LMP indicates that additional consumption at a bus will increase total cost. If a load is a parameter, the optimization problem has to secure generation to meet the load regardless of the effect of the consumption on the objective function. In the case of a variable load, such as the approximated loss term in the node balance constraint of the lossy formulation, the optimization problem will prevent additional consumption if such consumption degrades the objective function. Hence, in a problem with strictly positive DLMPs/LMPs, extra losses (artificial losses) beyond the correct approximation of losses will not be created to prevent degrading the objective function (in a bid maximization problem, artificial losses degrade the objective function since there is no bid value assigned to them). On the contrary, if non-positive DLMPs/LMPs occur, additional consumption at a bus may benefit an objective function. If a DLMP/LMP is zero, the optimization problem is indifferent between creating and not creating artificial losses: more consumption neither benefits nor degrades the objective function. If a negative DLMP/LMP occurs at a bus, any additional consumption at the bus will improve the objective function. If additional consumption improves an objective function, the lossy formulation has the opportunity, through the loss approximation technique, to create artificial losses to improve the objective function. The lossy formulation will violate the adjacency condition to create artificial losses at the bus until additional consumption either does not improve the objective function any longer or until a constraint in the problem prevents additional consumption solely at the bus. That is, if there is no reason why addition-

al losses cannot be created, fictitious losses will be created until the negative DLMP/LMP is zero. If a constraint limits the fictitious losses that can be created solely at a bus with a negative DLMP/LMP, then if beneficial, the formulation will violate the exclusivity condition to create losses at an adjacent bus so as to create more losses at the bus with the negative DLMP/LMP.

The breakdown of the lossy DCOPF formulation is illustrated with the 3-bus network in Figure 4.3. The network has an inelastic load; hence, the DCOPF formulations used to study the network have generation cost minimization as their objective. Results of a lossless DCOPF study, Table 4.1, establish the occurrence of a negative LMP at bus 2 of the network. The negative LMP occurs as a result of congestion on the line between bus 2 and bus 3. To supply an additional MW at bus 2, the output of generator 2 (an expensive generator) has to be decreased by 2 MW and the output of generator 1 (a cheaper generator) increased by 3 MW. The re-dispatch will cause a reduction of \$50 in total generation cost. In the lossless DCOPF formulation, fixed loads prevent the formulation from taking advantage of the opportunity to further improve the objective function. The lossy DCOPF formulation, however, could take advantage of the opportunity because the FDs that represent the losses on a line are variable loads. The total generation cost in Table 4.1 shows that the objective of the lossy formulation is indeed better than the objective of the lossless formulation. Artificial losses in the lossy formulation caused the system to re-dispatch away from the expensive generator as shown in Table 4.2.

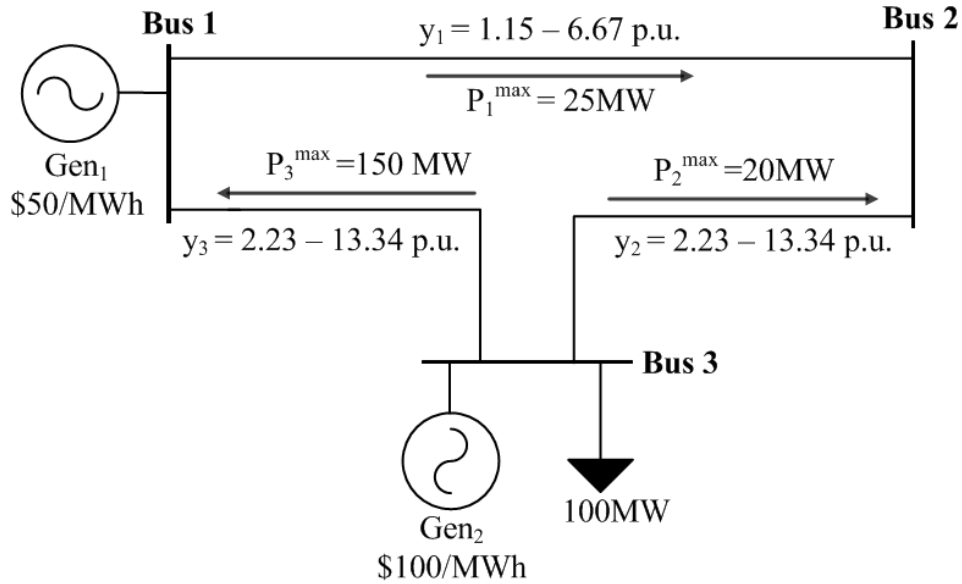


Figure 4.3. Three-Bus Network Example for Illustrating Lossy Formulation Breakdown

Table 4.1. Lossless and Lossy DCOPF LMPs, Losses, and Total Cost Results

Bus No.	Lossless DCOPF	Lossy DCOPF	
	LMP (\$/MWh)	LMP (\$/MWh)	Losses (MW)
1	50.00	50.00	0.11
2	-50.00	-5.71	5.00
3	100.00	100.00	0.75
Total Losses (MW)	0	5.86	
Total Cost (\$)	6000.00	5830.32	

Table 4.2. Lossless and Lossy DCOPF Generation Dispatch Results

Gen No.	Lossless DCOPF	Lossy DCOPF
	Output (MW)	Output (MW)
1	80.00	95.11
2	20.00	10.75

Examining the piecewise approximation results of the lossy DCOPF study, Table 4.3, indicates that artificial losses were created by violating the adjacency and the exclusivity conditions. Both conditions were violated in approximating the angle difference across the lines connected to bus 2: lines 1 and 2. In the case of line 1, negative orthant segments 10 and 11 were selected to approximate $(\theta_2 - \theta_1)$ while lower segments, 1 through 9, were not selected. Segments 1

through 4 in the positive orthant were also selected to approximate $(\theta_2 - \theta_1)$. Since the power flow on line 1 is to bus 2 and since the flow on line 1 is correctly designated, $(\theta_2 - \theta_1)$ is a negative angle. Consequently, only negative orthant segments should have been selected to approximate the angle difference. In the case of line 2, a negative orthant segment, 11, was one of the segments selected to approximate $(\theta_2 - \theta_3)$, a positive angle difference.

Table 4.3. Piecewise Approximation Result for the Lossy DCOPF Study

Line No. (k)	$\sum_{\forall i} \theta_i^{k+}$	$\sum_{\forall i} \theta_i^{k-}$	i for θ_i^{k+} Used	i for θ_i^{k-} Used
1	0.03076	0.06824	1, 2, 3, 4	10, 11
2	0.01745	0.00246	1, 2	11
3	0.05300	0.00000	1 thru 6	—

The artificial losses created by incorrectly approximating $(\theta_2 - \theta_1)$ are placed at bus 2 and bus 1. For bus 1, this is easily verified by the fact that the FD at bus 1 is not equal to zero, Table 4.1. As shown in Table 4.4, the power flow on line 1 is to bus 2, the power-flow on line 2 is to bus 3 and the power-flow on line 3 is to bus 3. There is no flow into bus 1. As a result, losses should not have been placed at the bus. The artificial losses created by incorrectly approximating $(\theta_2 - \theta_3)$ are placed at bus 2 and bus 3.

Table 4.4. Lossless and Lossy DCOPF Line Flow and Line Angle Difference Results

Line No. (k)	Lossless DCOPF		Lossy DCOPF	
	Line Flow (MW)	$\theta_n - \theta_m$ (rad)	Line Flow (MW)	$\theta_n - \theta_m$ (rad)
1	20	-0.0300	25	-0.037
2	-20	0.0150	-20	0.015
3	-60	0.4498	-70	0.053

4.3 Theoretical Proof of Lossy DCOPF Breakdown

It can be shown that the linear programming-based lossy formulation breaks down with the occurrence of negative DLMPs/LMPs by proving theoretically that negative DLMPs/LMPs cannot result from the lossy formulation if consumption at a bus that is supposed to have a negative DLMP/LMP is not limited by any constraints. That is, if a constraint, e.g., active line, stability or generator output limit, does not limit the amount of energy that could be consumed at all buses that are supposed to have negative DLMPs/LMPs, the lossy formulation will artificially increase the amount of losses at such buses until all the negative DLMPs/LMPs are equal to zero, i.e., until creating artificial losses no longer benefits the objective. Since it is known that a DLMP/LMP can indeed be negative (due to negative bidding and also due to Kirchhoff's laws, i.e., negative DLMPs/LMPs can exist even when all generators submit positive bids), having a formulation that cannot result in negative DLMPs/LMPs shows the lossy formulation improperly create artificial losses to improve the objective function. In the case where additional consumption at a negative DLMP/LMP bus is limited by a constraint, losses are artificially created by violating the adjacency condition, i.e., artificial losses are created through the slope of the segments approximating an angle difference. The mathematical proof for the claims is developed by examining the dual and the K.K.T. conditions of the lossy formulation.

The dual of the lossy formulation, for a single period, is shown in (4.21) - (4.28). For the ease of the reader, the primal formulation for the lossy DCOPF formulation, for a single period, is also shown in (4.29) - (4.41). Perfectly inelas-

tic loads are assumed in the primal formulation for ease of the dual derivation. The variables in braces in the dual formulation are the primal variables for the dual constraint they appear next to and the variables in braces in the primal formulation are the dual variables for the primal constraint they appear next to. The proof holds for the case of elastic loads.

Dual Formulation

$$\begin{aligned} \text{Maximize: } & \sum_n \lambda_n D_n - \sum_{\forall k} (F_k^- + F_k^+) P_k^{\max} - \sum_{\forall i,k} (\rho_i^{k-} + \rho_i^{k+}) \theta_i^{\max} \\ & + \sum_g \delta_g^- P_g^{\min} - \sum_g \delta_g^+ P_g^{\max} \end{aligned} \quad (4.21)$$

subject to :

$$\lambda_n + \delta_g^- - \delta_g^+ = c_g \quad \forall g \quad \{P_g\} \quad (4.22)$$

$$\lambda_n - \lambda_m - \xi_k + F_k^- - F_k^+ = 0 \quad \forall k \quad \{P_k\} \quad (4.23)$$

$$\gamma_n - \lambda_n = 0 \quad \forall n \quad \{P_n^L\} \quad (4.24)$$

$$\sum_{\forall k(n,:)} B_k \xi_k - \sum_{\forall k(:,n)} B_k \xi_k + \sum_{\forall k(n,:)} \mu_k - \sum_{\forall k(:,n)} \mu_k = 0 \quad \forall n \quad \{\theta_n\} \quad (4.25)$$

$$-2G_k \alpha_i \gamma_m - \mu_k - \rho_i^{k+} \leq 0 \quad \forall i,k \quad \{\theta_i^{k+}\} \quad (4.26)$$

$$-2G_k \alpha_i \gamma_n + \mu_k - \rho_i^{k-} \leq 0 \quad \forall i,k \quad \{\theta_i^{k-}\} \quad (4.27)$$

$$F_k^-, F_k^+, \delta_g^-, \delta_g^+, \rho_i^{k-}, \rho_i^{k+} \geq 0 \quad (4.28)$$

$$\lambda_n, \mu_k, \xi_k, \gamma_n \text{ free}$$

Primal Formulation

$$\text{Minimize: } \sum_g c_g P_g \quad (4.29)$$

subject to :

$$B_k(\theta_n - \theta_m) - P_k = 0 \quad \forall k \quad \{\xi_k\} \quad (4.30)$$

$$\sum_{g \in \widehat{G}_n} P_g + \sum_{\forall k(n,:)} P_k - \sum_{\forall k(:,n)} P_k - P_n^L = D_n \quad \forall n \quad \{\lambda_n\} \quad (4.31)$$

$$P_n^L - \left[\sum_{\forall k(n,:)} 2G_k \left(\sum_{\forall i} \alpha_i \theta_i^{k-} \right) \right] - \left[\sum_{\forall k(:,n)} 2G_k \left(\sum_{\forall i} \alpha_i \theta_i^{k+} \right) \right] = 0 \quad \forall n \quad \{\gamma_n\} \quad (4.32)$$

$$(\theta_n - \theta_m) - \left(\sum_{\forall i} \theta_i^{k+} - \sum_{\forall i} \theta_i^{k-} \right) = 0 \quad \forall k \quad \{\mu_k\} \quad (4.33)$$

$$\theta_i^{k+} \geq 0 \quad \forall i, k \quad (4.34)$$

$$\theta_i^{k-} \geq 0 \quad \forall i, k \quad (4.35)$$

$$-\theta_i^{k+} \geq -\theta_i^{\max} \quad \forall i, k \quad \{\rho_i^{k+}\} \quad (4.36)$$

$$-\theta_i^{k-} \geq -\theta_i^{\max} \quad \forall i, k \quad \{\rho_i^{k-}\} \quad (4.37)$$

$$P_k \geq -P_k^{\max} \quad \forall k \quad \{F_k^-\} \quad (4.38)$$

$$-P_k \geq -P_k^{\max} \quad \forall k \quad \{F_k^+\} \quad (4.39)$$

$$P_g \geq P_g^{\min} \quad \forall g \quad \{\delta_g^-\} \quad (4.40)$$

$$-P_g \geq -P_g^{\max} \quad \forall g \quad \{\delta_g^+\} \quad (4.41)$$

$$P_{g,t}, P_{k,t}, \theta_{n,t}, P_{n,t}^L \text{ free}$$

If the lossy formulation artificially increase the amount of losses at a bus with a negative DLMP/LMP by violating the adjacency condition, for such a scenario, there exists at minimum a prior segment i and a later segment j such that (4.42) and (4.43) hold. Note that while the discussions here are restricted to the negative

orthant, the same arguments are true for the positive orthant. From complementary slackness, (4.27) for segment i and j are equal to zero since the lengths of i and j are greater than zero. Also from complementary slackness, the dual variable of (4.37) for i is equal to zero since the maximum length of i is not used in the angle approximation, i.e., (4.37) is not active. Consequently, constraint (4.27) for i and j can be written as in (4.44) and (4.45). When (4.37) for j is also inactive, its dual variable is also equal to zero and (4.45) for j is further re-written as in (4.46). It is reasonable to assume constraint (4.37) for j is inactive since one of the arguments for this proof is that no constraint limits the creation of artificial losses at the bus with the negative DLMP/LMP. With (4.44) and (4.46) equaling zero, (4.47) must be true since, as shown in (4.48), the slopes of segments i and j are not equal. If (4.47) is true, then from (4.24), the DLMP/LMP at bus n , which is supposed to be negative, is equal to zero. The proof shows that a lossy DCOPT problem that is supposed to have negative DLMPs/LMPs will have none if additional consumption at all the negative DLMP/LMP busses is not prevented by a constraint,

$$0 < \theta_i^{k-} < \theta_i^{\max} \quad (4.42)$$

$$0 < \theta_j^{k-} \quad (4.43)$$

$$-2G_k \alpha_i \gamma_n + \mu_k = 0 \quad (4.44)$$

$$-2G_k \alpha_j \gamma_n + \mu_k - \rho_j^{k-} = 0 \quad (4.45)$$

$$-2G_k \alpha_j \gamma_n + \mu_k = 0 \quad (4.46)$$

$$\gamma_n = 0 \quad (4.47)$$

$$\alpha_i \neq \alpha_j. \tag{4.48}$$

If a constraint limits the angle difference across a line connected to a bus with a negative DLMP/LMP, such that more power cannot flow across the line to artificially increase the amount of losses at the bus, the lossy formulation may create artificial losses at an adjacent bus. Creating artificial losses at the adjacent bus will allow more artificial losses to be created at the bus with the negative DLMP/LMP and it will further improve the objective function and drive the negative DLMP/LMP closer to zero. This occurs in the 3-bus example in Section 4.2. The artificial losses at bus 2 of the network cause congestion on line 1, seen by comparing the power flow on line 1 for the lossless and the lossy DCOPF studies in Table 4.4, which limits the amount of artificial losses that can be further created solely at bus 2. The congestion on line 1, which is also manifested in the maximum value $(\theta_2 - \theta_1)$ can be, is respected and at the same time while more losses are created at bus 2 to improve the solution, by violating the exclusivity condition. The same occurs for line 2 where artificial losses are created at bus 3 as a result of the congestion on line 2 to create more losses at bus 2. The limit placed on artificial loss creation by congestion on both lines 1 and 2 prevent the LMP at bus 2 from being zero.

As described in Section 4.2, violating the exclusivity condition allows artificial losses to be created without changing the angle difference across a line. If a limiting constraint manifested as a restriction on angle difference limits the flow across a line, the lossy formulation can respect the limit and create artificial losses by selecting segments in both orthants to approximate the angle difference. That

is artificial losses are created through the lengths of the segments used to approximate the angle difference. If this occurs, there exists, at minimum, a positive orthant segment i and a negative orthant segment j such that (4.49) and (4.50) hold. From complementary slackness, (4.26) for segment i and (4.27) for j are equal to zero and can be written as in (4.51) and (4.52). Equation (4.53) can then be obtained by summing (4.51) and (4.52) together. From (4.28) it is known that the dual variables corresponding to the constraint that defines the maximum length of each segment, (4.36) and (4.37), are both non-negative. Consequently (4.54) can be deduced. When (4.55) and (4.56) holds, that is the angle limitation is not as a result of all the piecewise segments being completely used up, then the dual variables of (4.36) and (4.37) are equal to zero and (4.54) can be written as in (4.57). From (4.24), (4.57) can be re-written as in (4.58).

$$\theta_i^{k+} > 0 \quad (4.49)$$

$$\theta_j^{k-} > 0 \quad (4.50)$$

$$-2G_k \alpha_i \gamma_m - \mu_k - \rho_i^{k+} = 0 \quad (4.51)$$

$$-2G_k \alpha_j \gamma_n + \mu_k - \rho_j^{k-} = 0 \quad (4.52)$$

$$\alpha_i \gamma_m + \alpha_j \gamma_n = \frac{\rho_i^{k+} + \rho_j^{k-}}{-2G_k} \quad (4.53)$$

$$\alpha_i \gamma_m + \alpha_j \gamma_n \leq 0 \quad (4.54)$$

$$\theta_i^{k+} < \theta_i^{\max} \quad (4.55)$$

$$\theta_j^{k-} < \theta_j^{\max} \quad (4.56)$$

$$\alpha_i \gamma_m + \alpha_j \gamma_n = 0 \quad (4.57)$$

$$\alpha_i \lambda_m + \alpha_j \lambda_n = 0 \quad (4.58)$$

The proof in (4.49) to (4.58) show that if enough artificial losses cannot be created at a bus because a constraint prevents power flow into the bus or the losses may force the formulation to select a different solution that may be worse off and, if all the lengths of the segments in the piecewise approximation has not been used up, the formulation will create additional artificial losses at an adjacent bus until the weighted sum of the DLMPs/LMPs at both buses is equal to zero, (4.58). This can be explained easily using the simple case where i is equal to j . For such a case, artificial losses will be created until the sum of the DLMPs/LMPs at both buses is equal to zero. That is, the formulation will create more consumption until the net change in the cost to consume, i.e., the objective function, is zero. This means the formulation will create artificial losses until it cost more to create artificial invalid losses at the adjacent bus than the cost saved by creating artificial invalid losses at the bus with the negative DLMP/LMP. Equation (4.54) can only hold for a combination of a non-positive LMP and a positive LMP and for a combination of non-positive LMPs. Artificial losses can be created at an adjacent bus with either negative, positive or zero DLMP/LMP. A combination of non-positive DLMPs/LMPs can theoretically result in an unbounded situation where the resulting DLMPs/LMPs are as negative as possible. Note that when artificial losses are created at an adjacent bus, the DLMP/LMP at the negative DLMP/LMP bus will not be completely reduced to zero. This can also be seen in the 3-bus example in Section 4.2.

The dual of a standard DCOPF formulation does not have (4.26) or (4.27). These additional constraints are responsible for the lossy formulation approximating bus angle differences in such a way that fictitious losses are created to improve the solution of a problem when negative DLMPs/LMPs occur. It is important to recognize this inadequacy of the lossy DCOPF formulation because the resulting solutions (DLMPs/LMPs, losses, dispatches and line flows), when a negative DLMP/LMP occurs, may be wrong. It is also important to understand how the inadequacy is manifested in the DLMPs/LMPs so that the breakdown of the formulation can be readily identified.

4.4 Mixed-Integer Linear Programming (MILP) Formulation

The possibility of loss approximation errors require that the lossy DCOPF solutions be inspected for compliance with the adjacency and the exclusivity conditions. If loss approximation errors occur with the linear programming-based formulation, the lossy DCOPF problem must be converted to a MILP formulation as it is not possible to generate a set of linear constraints to enforce the adjacency and the exclusivity conditions (except by defining the convex hull). In the MILP formulation, (4.59) - (4.66) are added to the original linear programming-based lossy formulation for lines whose angle difference approximation violates the adjacency or the exclusivity conditions. Similar to [27], constraints (4.59), (4.60), (4.65), and (4.66) restrict the formulation to selecting the maximum length of lower segments if higher segments are also used to approximate a bus angle difference. By combining (4.61) with (4.59), (4.60), (4.65), and (4.66), the formulation is restricted from using segments in both orthants to approximate the same

angle difference. Note that the mixed-integer linear constraints are applied only to lines whose angle difference approximations have violated the adjacency and exclusivity conditions. This reduces the computational complexity by not requiring these constraints for all lines but simply those corresponding to fictitious loss approximations. The resulting solution from such a decomposition approach must, however, also be checked for loss approximation errors. An algorithm for implementing the MILP formulation is shown in Figure 4.4. While non-positive LMPs are the trigger in the figure, non-positive DLMPs will be the trigger in a distribution system OPF,

$$\theta_{i,t}^{k+} \geq u_{i+1,t}^{k+} \theta_i^{\max} \quad \forall i, k, t \mid k \in \Lambda^- \quad (4.59)$$

$$\theta_{i,t}^{k-} \geq u_{i+1,t}^{k-} \theta_i^{\max} \quad \forall i, k, t \mid k \in \Lambda^- \quad (4.60)$$

$$u_{1,t}^{k+} + u_{1,t}^{k-} \leq 1 \quad \forall k, t \mid k \in \Lambda^- \quad (4.61)$$

$$u_{i,t}^{k+}, u_{i,t}^{k-} \in \{0,1\} \quad \forall i, k, t \mid k \in \Lambda^- \quad (4.62)$$

$$-\theta_{i,t}^{k+} \geq -\theta_i^{\max} \quad \forall i, k, t \mid k \in \Lambda^+ \quad (4.63)$$

$$-\theta_{i,t}^{k-} \geq -\theta_i^{\max} \quad \forall i, k, t \mid k \in \Lambda^+ \quad (4.64)$$

$$-\theta_{i,t}^{k+} \geq -u_{i,t}^{k+} \theta_i^{\max} \quad \forall i, k, t \mid k \in \Lambda^- \quad (4.65)$$

$$-\theta_{i,t}^{k-} \geq -u_{i,t}^{k-} \theta_i^{\max}. \quad \forall i, k, t \mid k \in \Lambda^- \quad (4.66)$$

The MILP formulation is used to conduct a study on the 3-bus network in Section 4.2. Its results and the results of the lossless and the linear programming-based lossy formulations are compared in Table 4.5 to Table 4.7. Comparison of the loss results of the linear programming-based lossy DCOPF study to the loss

results of the MILP lossy study in Table 4.5 confirms that fictitious losses are created at the 3 buses in the network in the linear programming-based lossy study. Fictitious losses are created at bus 1 and bus 3 in addition to the fictitious losses at bus 2 because of the congestion on lines 1 and 2 respectively, Table 4.7. It is cheaper and more effective to create fictitious losses at the bus with the negative LMP than it is to also create fictitious losses at an adjacent bus with a positive LMP. Consequently, the fictitious losses at bus 2 are approximately 45 times the fictitious losses at bus 1 and approximately 21 times the fictitious losses at bus 3. The total losses in the linear programming-based study are approximately 9.5 times the total losses in the MILP lossy study. Bus 2's LMP in the linear programming-based lossy study is not completely reduced to zero because the congestion on lines 1 and 2 limit the creation of artificial losses. Table 4.7 shows that the congestion on line 1 is purely as a result of the flow of fictitious losses to bus 2. Table 4.6 shows that the dispatch solutions of the linear programming-based lossy study and the MILP study are significantly different. Table 4.5 shows that bus 2's LMP in the linear programming-based lossy study and the MILP study are also significantly different and the total cost in the linear programming study is about \$216 less than the total cost in the MILP study.

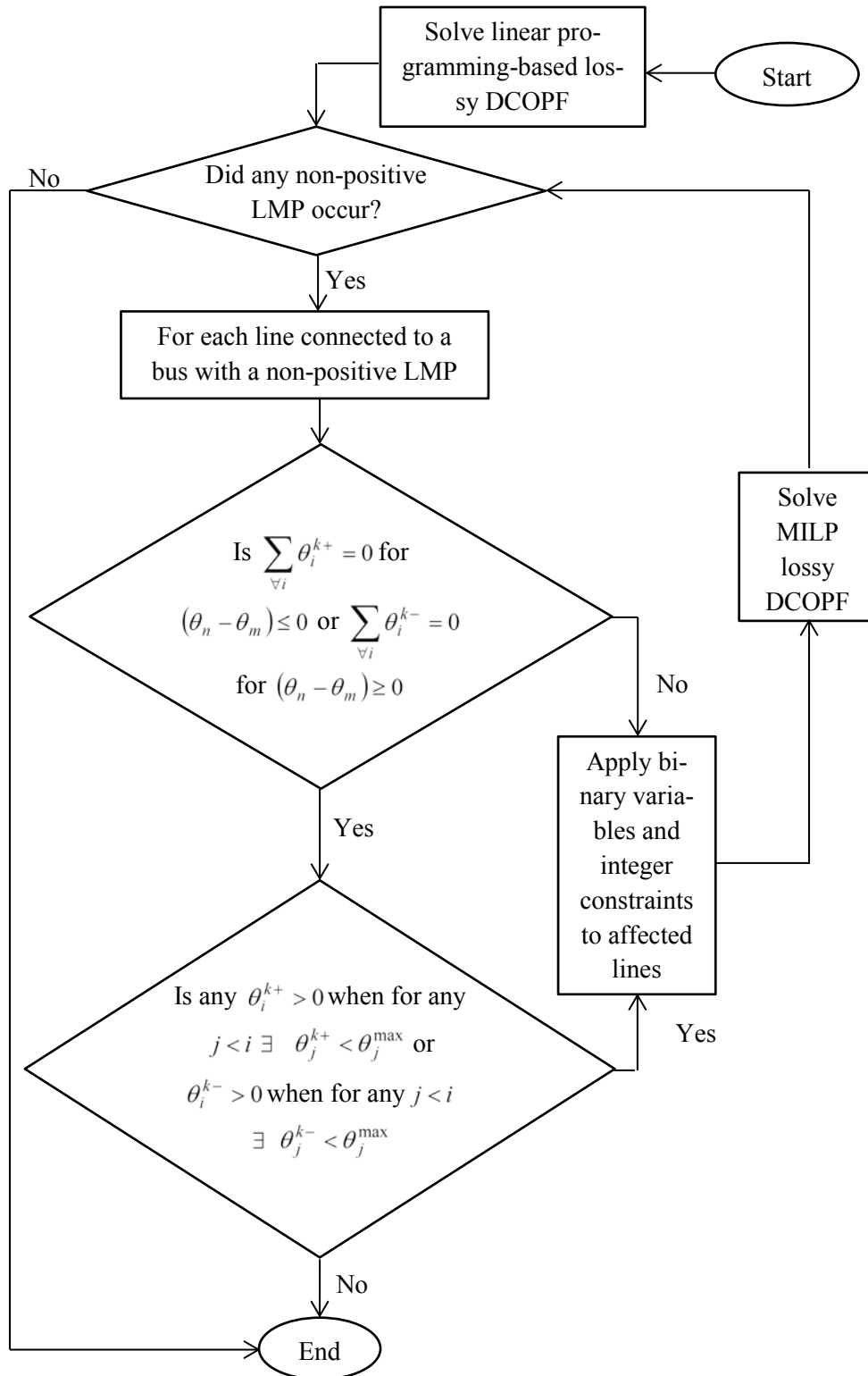


Figure 4.4. MILP Lossy DCOPF Implementation Triggered by Non-positive LMPs

Table 4.5. LMP, Losses, and Generation Cost Results

Bus No.	Lossless DCOPF	Linear Programming Lossy DCOPF		MILP Lossy DCOPF	
	LMP (\$/MWh)	LMP (\$/MWh)	Losses (MW)	LMP (\$/MWh)	Losses (MW)
1	50.00	50.00	0.11	50.00	0
2	-50.00	-5.71	5.00	-46.10	0.10
3	100.00	100.00	0.75	100.00	0.52
Total Losses	0 MW	5.86 MW		0.62 MW	
Total Cost	\$6000.00	\$5830.32		\$6046.95	

Table 4.6. Generation Dispatch Results

Gen No.	Lossless DCOPF	Linear Programming Lossy DCOPF	MILP Lossy DCOPF
	Output (MW)	Output (MW)	Output (MW)
1	80.00	95.11	80.31
2	20.00	10.75	20.31

Table 4.7. Lossless and Lossy DCOPF Line Flow and Line Angle Difference Results

Line No. (k)	Lossless DCOPF		Linear Programming Lossy DCOPF		MILP Lossy DCOPF	
	Line Flow (MW)	$\theta_n - \theta_m$ (rad)	Line Flow (MW)	$\theta_n - \theta_m$ (rad)	Line Flow (MW)	$\theta_n - \theta_m$ (rad)
1	20	-0.0300	25	-0.037	20.1	-0.0301
2	-20	0.0150	-20	0.015	-20.0	0.0150
3	-60	0.4498	-70	0.053	-60.2	0.0451

4.5 Conclusion

The lossy OPF for calculating DLMPs is developed in this chapter. The OPF formulation uses a piecewise linear approximation technique to approximate real power losses. The lossy DCOPF formulation can be used both for LMPs in the transmission system and the DLMPs in the distribution system. The loss approximation technique places additional constraints on the lossy formulation that may

cause the formulation to create fictitious losses. Fictitious losses are created as long as the objective decreases due to fictitious losses, which generally drives negative DLMPs/LMPs to zero or as close to zero as possible depending on binding constraints in the problem. When loss approximation errors occur, the lossy formulation has to be solved as a MILP formulation with binary variables and constraints applied to lines whose angle difference approximations violates an adjacency or an exclusivity condition. It is important to be aware of the loss approximation error and to correct for it because the artificial losses created could be substantial and could lead to a wrong dispatch and wrong DLMPs/LMPs.

Chapter 5. Illustrative Examples of the DLMP

The lossy DCOPF formulation in Chapter 4 is used to calculate DLMPs for different test distribution systems in this chapter. The calculations are conducted for: (1) a traditional distribution system with inelastic loads, radial topology and no congestion, (2) an enhanced distribution system with price responsive loads, radial topology and no congestion, and (3) an enhanced distribution system with price responsive loads, meshed topology and congestion. The iterative framework described in Section 3.2 is also illustrated numerically with an enhanced distribution system with price responsive loads.

5.1 Roy Billinton Test System (RBTS)

The RBTS system is used in all of the studies in this chapter. It consists of a transmission system and five load busses that represent the distribution systems connected to the transmission system. The system was developed in [28] - [31]. Figure 5.1 shows the one-line diagram of the transmission system, which is operated at 230 kV and has a peak load of 185 MW. The transmission system also has 11 generators. Six of the generators are located at bus 1 and the remaining five are located at bus 2. For the purpose of the studies in this chapter, the maximum generation capacity of the transmission system is modified from 240 MW to 222.5 MW. Details of the generators and the marginal costs used in the simulations are shown in Table 5.1. The marginal costs in the table have also been modified from the original RBTS data. Details of the transmission system's branch data are listed in Table A.1 in Appendix A.

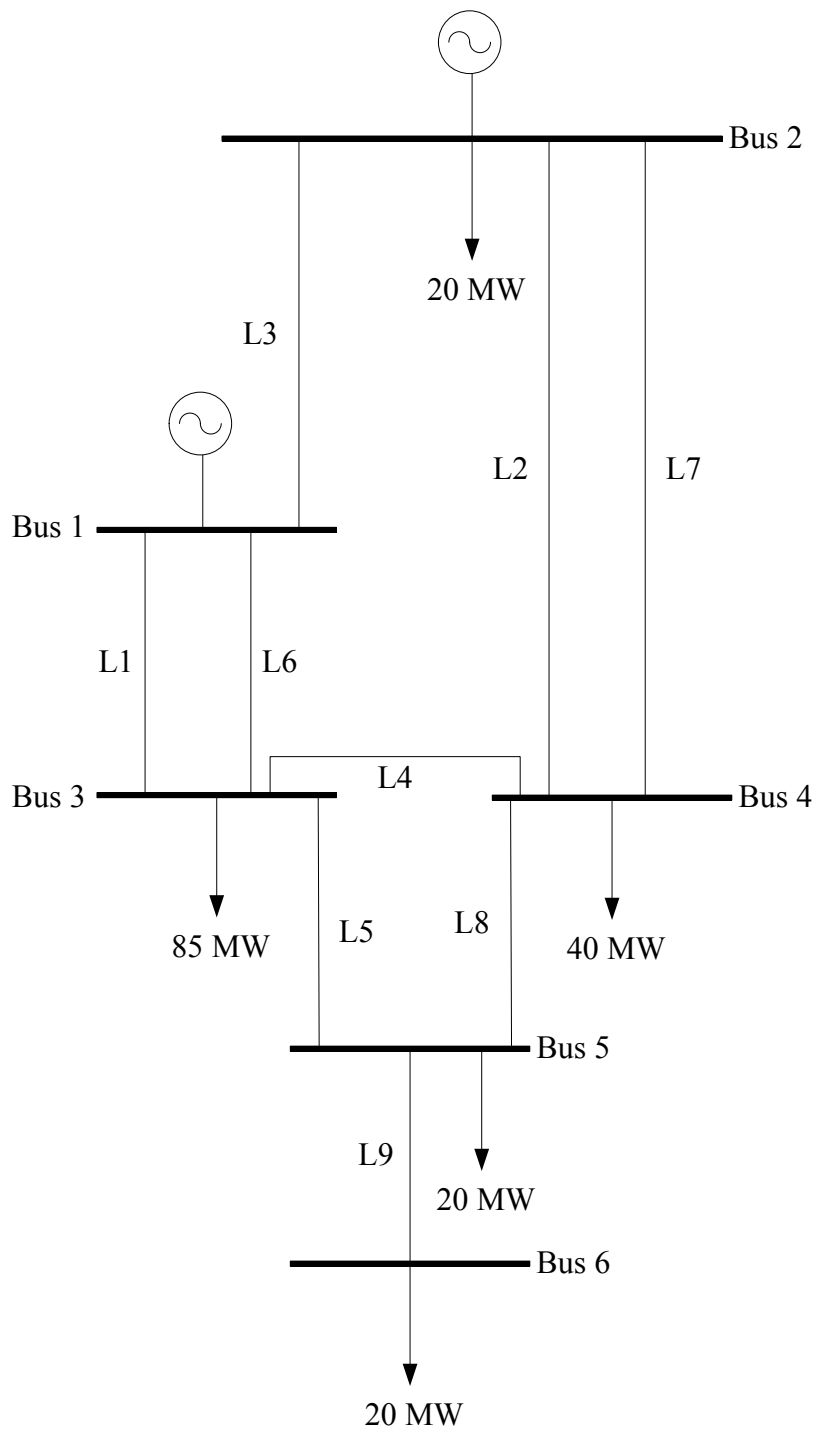


Figure 5.1. RBTS Transmission System

Table 5.1. RBTS System Generator Details

Unit No.	Bus	Marginal Cost (\$/MWh)	Min. Output (MW)	Max. Output (MW)
1	1	53	0	22.5
2	1	50	0	40
3	1	80	0	10
4	1	55	0	20
5-6	2	20	0	5
7	2	20	0	40
8-11	2	20	0	20
Maximum Capacity				222.5

The distribution systems at bus 3 and at bus 4 of the transmission system are the test distribution systems. The bus 3 system has a peak load of 85 MW distributed along 8 primary feeders between 44 load points (LP). As shown in Table 5.2, the LPs are aggregates of multiple customers with similar service requirements: residential users, large industrial users, small industrial users, commercial users, and office buildings. The one-line diagram of the system is shown in Figure 5.2. The main substation is energized at 138 kV and the main substation is the only source of energy to the system. The main substation is connected to two other substations by 33 kV lines. Feeders 1 (F1) to F6 are operated at 11 kV and F7 and F8 at 138 kV. The 8 primary feeders in the distribution system have section types listed in Table 5.4. The impedance and the peak loading data for each feeder are listed in Table 5.3. For the simulations in this chapter, two 230/138 kV sub-transmission transformers that connect the transmission system to the substation of the bus 3 distribution system are added between bus 3 and a new bus (bus 7) in the transmission system and the load at bus 3 is moved to the new bus. This was

done so that the sub-transmission system transformers could be included in the transmission system network model.

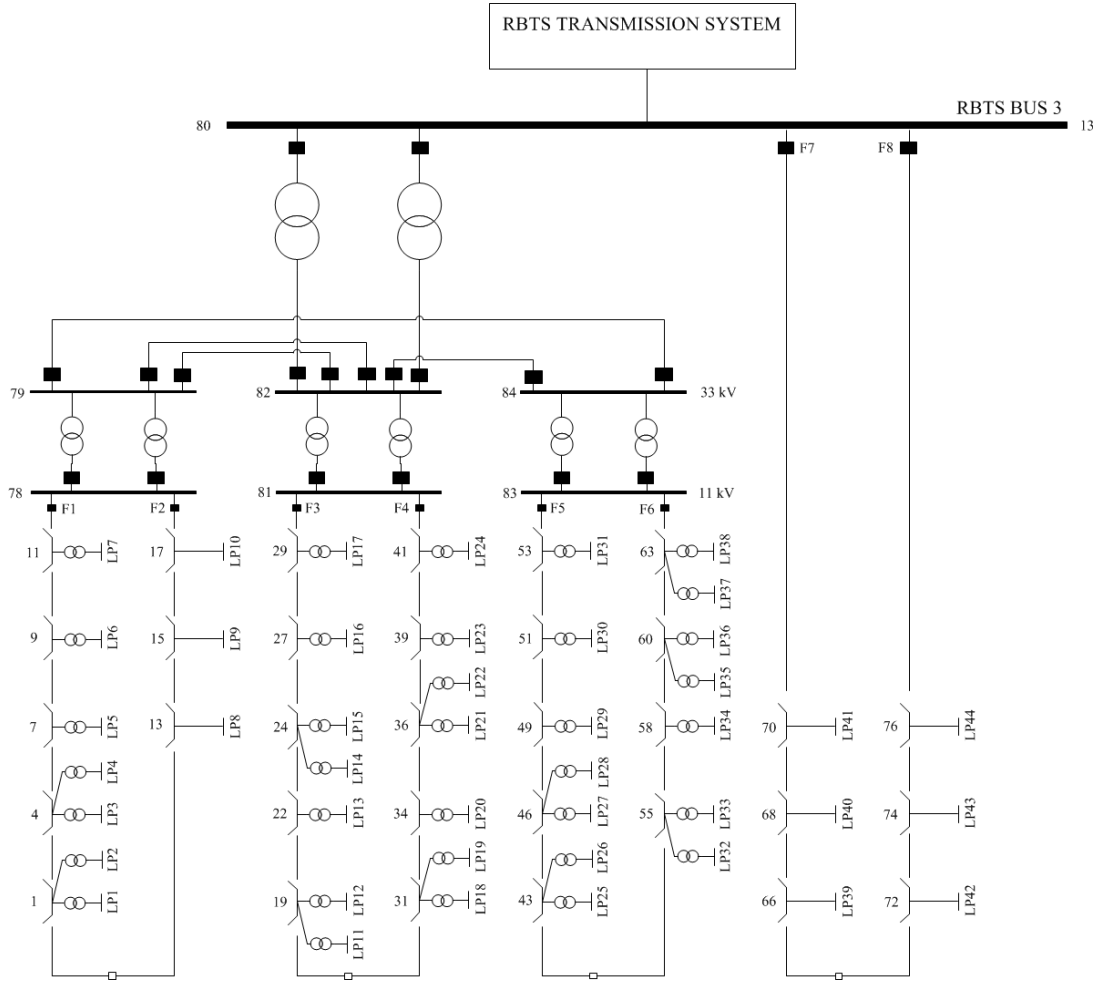


Figure 5.2. Distribution System at Bus 3

Table 5.2. Bus 3 Distribution System Load Details

Customer type	Peak Load (MW)	Load Points
Residential	0.8367	1, 4-7, 20, 24, 32, 36
	0.85	11, 12, 13, 18, 25
	0.775	2, 15, 26, 30
Large users	6.9167	39, 40, 44
	11.5833	41-43
Small Industrial	1.0167	8, 9, 10
Commercial	0.5222	3, 16, 17, 19, 28, 29, 31, 37, 38
Office Buildings	0.925	14, 27

Table 5.3. Bus 3 Distribution System Feeder Summary

Feeder	kV Level	Total MW Load	Total Length (mi)	R (Ω /mi)	X (Ω /mi)		
1	11	5.4807	5.4057	0.307088	0.62958		
2		3.0501	3.0446				
3		5.2944	5.7164	0.187726	0.60014		
4		5.5557					
5		4.8916					
6		5.2279	5.1572				
7	138	25.4167	2.8582			0.592606	0.76279
8		30.0833					
Total		85.0004	30.0833				

Table 5.4. Bus 3 Distribution System Feeder Section Length

Section Type	Length (mi)	Section Number
1	0.3728	1, 2, 3, 7, 11, 12, 15, 21, 22, 29, 30, 31, 36, 40, 42, 43, 48, 49, 50, 56, 58, 61, 64, 67, 70, 72, 76
2	0.4971	4, 8, 9, 13, 16, 19, 20, 25, 26, 32, 35, 37, 41, 46, 47, 51, 53, 57, 60, 62, 65, 68, 71, 75, 77
3	0.5592	5, 6, 10, 14, 17, 18, 23, 24, 27, 28, 33, 34, 38, 39, 44, 45, 52, 54, 55, 59, 63, 66, 69, 73, 74

As shown in Table 5.5, the distribution system at bus 4 of the RBTS transmission system has a peak load of 40 MW distributed along 7 primary feeders between 38 LPs. Similar to bus 3, the LPs are aggregates of multiple customers with similar service requirements. The loads are classified into five categories. Type 1 and type 2 are residential loads with peak consumption of 0.8869 MW and 0.8137 MW respectively, type 3 and type 4 are small industrial loads with peak consumption of 1.63 MW and 2.445 MW respectively, and type 5 are commercial loads with a peak consumption of 0.6714 MW. Table 5.6 lists the LPs and their classifi-

cation. The system is supplied by 3 distribution substations. As shown in the one-line diagram in Figure 5.3, the substations are connected by 33 kV lines and one of the substations is directly connected to the transmission system. The system's branch and detailed load data are provided in Table A.3-Table A.6 in Appendix A. The system has an open-loop topology. For the purpose of this research, the normally open switch between F1 and F7, the normally open switch between F3 and F4 and the normally open switches between F2, F5, and F6 are closed to form a meshed distribution system. A summary of the studies in this chapter and the systems used for each study in presented in Table 5.7.

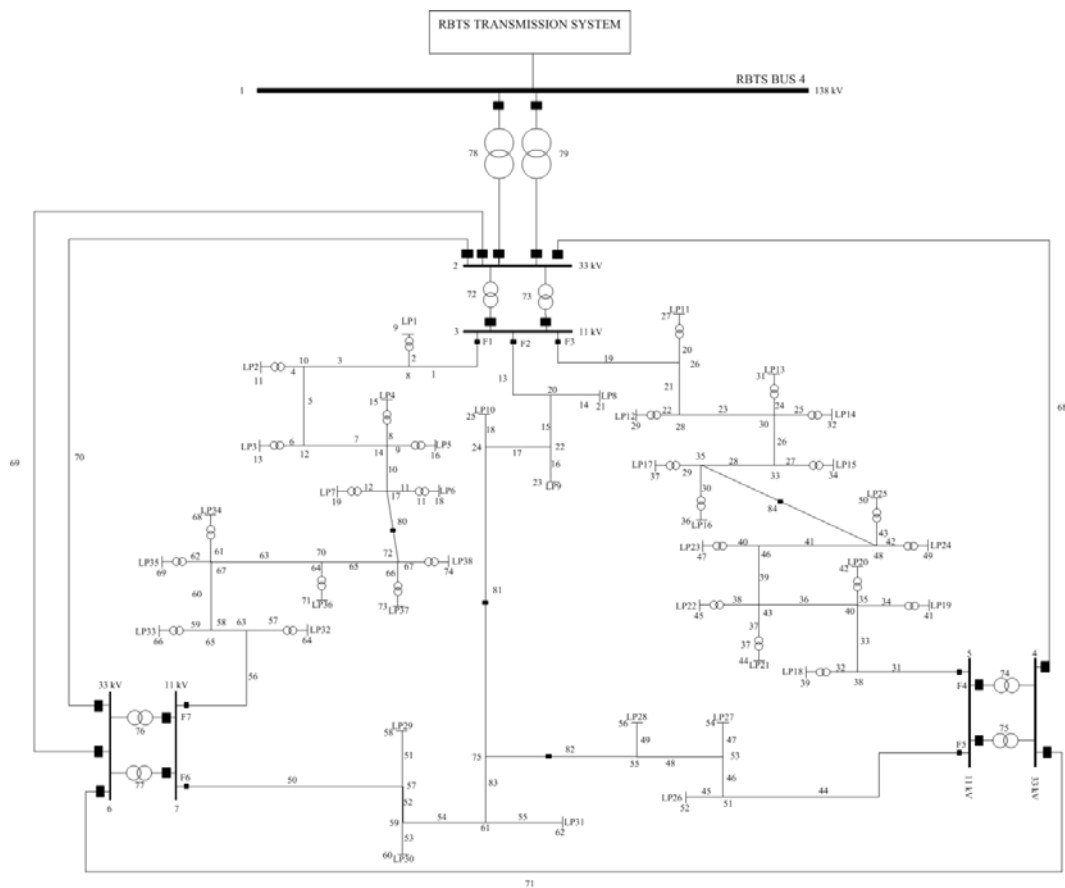


Figure 5.3. Distribution System at Bus 4 with a Meshed Topology

Table 5.5. Summary of Distribution System at Bus 4 of RBTS System

Number of Nodes	75
Number of Branches	84
Number of Distributed Generators	2
Number of Load Points	38
Total Peak Load	40 MW
Capacity of Distributed Generator	2.75 MW

Table 5.6. Bus 4 Distribution System Load Type Details

Load Type	Load Points
1	1-4, 11-13, 18-21, 32-35
2	5, 14, 15, 22, 23, 36, 37
3	8, 10, 26-30
4	9, 31
5	6, 7, 16, 17, 24, 25, 38

Table 5.7. Summary of Studies and Test Systems Used

Test Distribution System	Section	Characteristics	Study Objectives
Bus 3	5.2	<ul style="list-style-type: none"> - Radial topology - No congestion - No price sensitive resources 	<ul style="list-style-type: none"> - DLMP trends in a traditional distribution system - Cross-subsidy with average prices
	5.3	<ul style="list-style-type: none"> - Radial topology - No congestion - PRLs 	<ul style="list-style-type: none"> - Benefit of the DLMP to economic efficiency
	5.5	<ul style="list-style-type: none"> - Radial topology - No congestion - PRLs 	<ul style="list-style-type: none"> - Importance of iterative approach to calculating DLMPs
Bus 4	5.4	<ul style="list-style-type: none"> - Meshed topology - Congested - PRLs - DGs 	<ul style="list-style-type: none"> - DLMP in a congested distribution system

5.2 DLMP in a Traditional Distribution System

The test traditional distribution system is the distribution system at bus 3 of the RBTS system. The system is operated radially, the system lacks internal generation resources and all loads in the system are assumed to be perfectly inelastic. Hence, feeders and equipment in the system, as it is in traditional distribution sys-

tems, are oversized to avoid congestion. DLMPs in the system have no congestion component as a result. Price separation between nodes results from real power losses. This is reflected in Figure 5.4, the plots of the calculated DLMPs for the peak period of the test distribution system.

Figure 5.4 shows the computed DLMP at the LP nodes on each feeder. The LPs are numbered from the beginning to the end of each feeder (for example LP7 on F1 in Figure 5.2 is LP1 on F1 in the plot). The trend of the plots reflects the locational effect of real power losses. The farther a LP is from the beginning of a feeder, the higher the losses incurred in delivering energy to the LP; thus, the higher the DLMP at its node. This is true for any radial feeder with one injection point; losses incurred to deliver energy to a node will increase as the node gets farther from the source of injection. The notion of DLMPs increasing along a radial feeder is valid even for F1 where there is a decrease in the DLMP between consecutive LPs: the fourth and the fifth LPs. The decrease occurs because both LPs are connected to the same node on the primary feeder via laterals of different lengths. The lateral connecting the LP with the higher DLMP to the primary feeder node is longer than the length of the lateral connecting the LP with the lower DLMP to the primary feeder node. Both the fourth and fifth LPs are connected to node 4 (figure numbering) on F1. The lateral connecting the fifth LP to node 4 is of section type 1 and is 0.3728 miles long while the lateral connecting the fourth LP to node 4 is of section type 2 and is 0.4971 miles long.

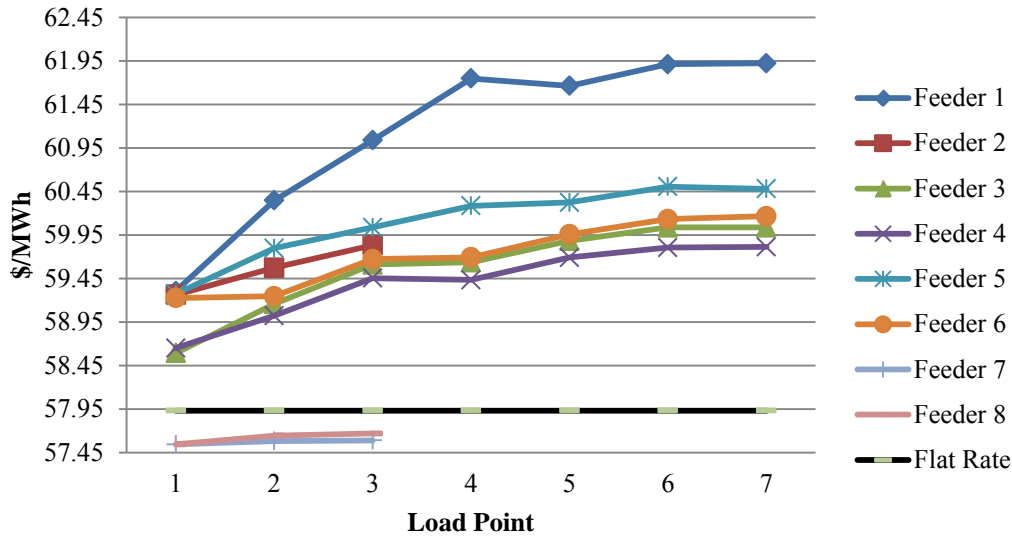


Figure 5.4. DLMP Across Feeders in the Test Distribution System (The LMP at the transmission proxy is indicated by the first point on the vertical axis)

The effect of losses is also apparent between feeders. From Figure 5.4, it can be deduced that the least amount of losses per MWh delivered are incurred on F7 and F8. Despite F7 and F8 having about 65 percent of the total system loading, this resulted because both feeders are directly connected to the sub-transmission bus. Hence, they are the closest feeders to the source of the system and are operated at 138 kV. F7 and F8 also have the shortest lengths in the system.

Effect of losses between feeders is also reflected in the trend of the DLMP at the first LP of F3 through F6. F3 and F4 are connected to the substation directly energized by the sub-transmission system while F1, F2, F5 and F6 are connected through 33 kV lines to the substation F3 and F4 are connected to. This resulted in the DLMP at the first LP on F3 and F4 being lower than the DLMP at the first LP on F1, F2, F5, and F6. The DLMP at the first LP on F1, F2, F5, and F6 are close because the 33 kV lines connecting each substation to the main substation are of equal lengths and the 33kV/11kV transformers have the same impedance. The

divergence of DLMPs further down F1 through F6 is a result of different feeder section lengths, loading, and impedance. The higher impedance of F1 dominates.

The total payment to the transmission system is used to calculate a flat rate (FR) that can be used to represent average rates from COS regulation. The rate, \$57.93/MWh, is the cost per MWh to recover the payment (energy and losses) to the transmission system. Cross-subsidization under the FR pricing scheme is apparent. Some LPs pay more than their DLMP while others pay less (DLMP is the accurate marginal cost that captures the individual contribution of each load to losses). Figure 5.4 shows that the loads on F7 and F8 will pay more than their true cost to consume under the FR scheme, i.e., the loads on F7 and F8 will subsidize the other loads in the system. The economic benefit of contributing less to losses will not be realized by the loads on F7 and F8 as a result. In the traditional distribution system where loads are assumed to be perfectly inelastic and there is limited price sensitive resources, operating with average rates may be acceptable. In the enhanced distribution system, however, cross-subsidies will distort prices and send incorrect economic signals to price sensitive resources and negatively affect economic efficiency. The locational information provided by the DLMP, which may not be readily predictable in congested systems, will also be lost with average prices. Note that contemporary RTPs also cause cross-subsidies. While contemporary RTPs capture and reflect conditions in the transmission system, they do not reflect conditions in the individual distribution system they are used in.

5.3 DLMP in an Enhanced Distribution System with Price Responsive Loads

One of the major advantages of the DLMP is its capability to improve economic efficiency by properly incentivizing price sensitive resources to behave optimally in a manner that benefits system operations. The actions incentivized by the DLMP are compared to the action incentivized by a FR to illustrate the capability of the DLMP to improve economic efficiency in this section. The price sensitive resources are flexible loads. The test distribution system is the distribution system at bus 3 of the RBTS system. Twenty percent of the peak load in the test system is considered elastic for the enhanced distribution system. The LPs selected as price responsive loads are listed in Table 5.8. Each PRL has a two-step bid. It is assumed that only part of the demand of each PRL is sensitive to the price range expected for the DLMPs. The first step of the demand bid represents the portion of the demand of each price responsive LP that is inflexible and the second step represents the flexible portion. The bid value of the inflexible portion is \$64.45/MWh for all the PRL. The flexible portion of a load has one of the 4 values in Table 5.8. The values represent different levels of flexibility with the lowest representing the highest flexibility and the highest representing the lowest flexibility. The details of the PRL are listed in Table A.2 in Appendix A.

Table 5.8. Bid Value of Flexible Portion of Demand

Bid Value (\$)	Load Point
55	3, 11, 27, 32
57.65	19, 21, 39, 40, 42, 43
58.95	2, 8, 9, 12, 14, 25, 26, 33, 35
61.45	1, 4, 13, 18, 20, 28, 34

The resulting DLMP at the nodes of the flexible LPs, the FR established in Section 5.2, and the bid value of the flexible part of the LPs are plotted in Figure 5.5. The action incentivized by the DLMP and the FR is shown in Table 5.9. Table 5.9 is obtained based on the intersection of a price with the bid value plot. Whenever a price is less than or equal to the value of the flexible portion of a load, the flexible portion of the load is consumed. Whenever a price is higher than the value of the flexible portion of a load, the flexible portion is not consumed. The behavior incentivized by the DLMP is the optimal behavior because the DLMP is an accurate economic signal. The behavior incentivized by the FR deviates from that of the DLMP; hence, it is sub-optimal. For example, the behavior of LPs 2, 19, 21, 39, 40, 42, and 43 deviates from the optimal behavior. LP2 is incentivized to consume the flexible portion of its demand even though the value it places on the flexible portion is less than the true cost to consume. LPs 19, 21, 39, 40, 42 and 43 are incentivized not to consume even though the value they place on consumption is higher than the true cost to consume. As discussed in Section 3.1, deviation from optimal behavior leads to a reduction in economic efficiency: deadweight loss. Hence, the FR pricing mechanism is inferior to the DLMP pricing mechanism. In an enhanced distribution system, the benefits of having distribution resources will be reduced as a result of wrong price signals. For example, a load whose consumption further exacerbates the cost of congestion may be incentivized to consume by a FR pricing mechanism during a period when the DLMP would otherwise discourage consumption by sending a higher pricing signal.

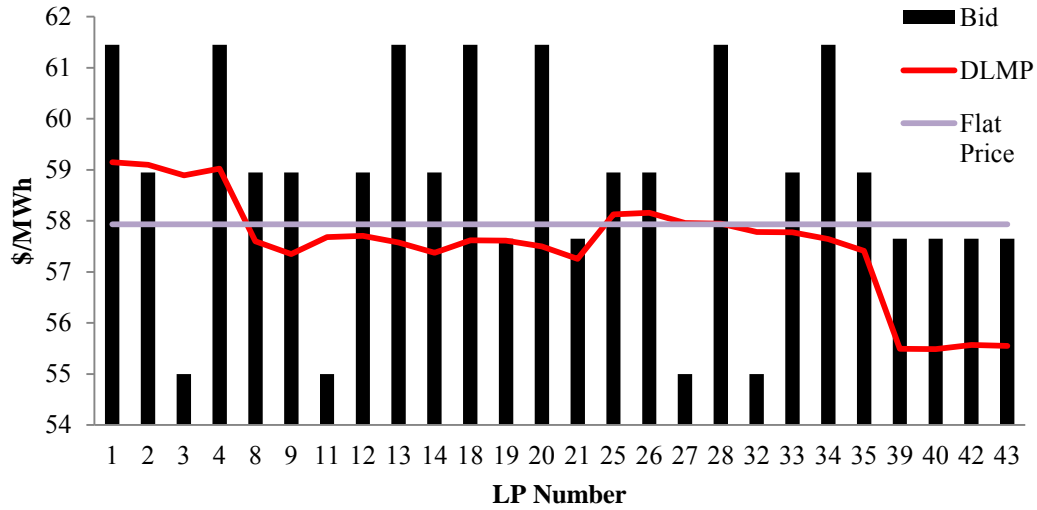


Figure 5.5. Flexible Portion of Demand, DLMP, and Flat Price

Table 5.9. Action Incentivized by DLMP and Flat Price (Black – Consumption both prices, White – No consumption both prices, Red – Consumption one price, No Consumption one price)

LP #	1	2	3	4	8	9	11	12	13	14	18	19	20	21	25	
DLMP	Black	White	White	Black	Black	Black	White	Black	Black	Black	Black	Black	Red	Black	Red	Black
FP	Black	Red	White	Black	Black	Black	White	Black	Black	Black	Black	White	Black	White	Black	Black

LP #	26	27	28	32	33	34	35	39	40	42	43
DLMP	Black	White	Black	White	Black	Black	Black	Red	Red	Red	Red
FP	Black	White	Black	White	Black	Black	Black	White	White	White	White

5.4 DLMP in a Meshed Distribution System with Congestion

Today, there are distribution systems that are meshed; however, they are primarily found in large metropolitan cities. If the existence of meshed distribution systems increases in the future, congestion can cause higher nodal price separation than losses could. Price separation as a result of congestion reflects the ability of the DLMP to internalize congestion management. The distribution system at bus 4 of the RBTS system is used to illustrate DLMPs in a meshed and congested

distribution system. To create congestion, the capacity limit for line section 17, between nodes 22 and 24 on F2, is set to 1.9 MW. A 750 kW DG with a marginal cost of \$18/MWh is placed at node 22. A 2 MW DG, with a marginal cost of \$40/MWh, is placed at bus 4. The DGs are in addition to the transmission system, which is an infinite generator with a marginal cost of \$54.63/MWh. Type 1 loads are modeled as perfectly inelastic loads while type 2 through type 5 are elastic loads with the demand bids in Figure 5.6. The development of the demand bids is discussed in details in Chapter 6.

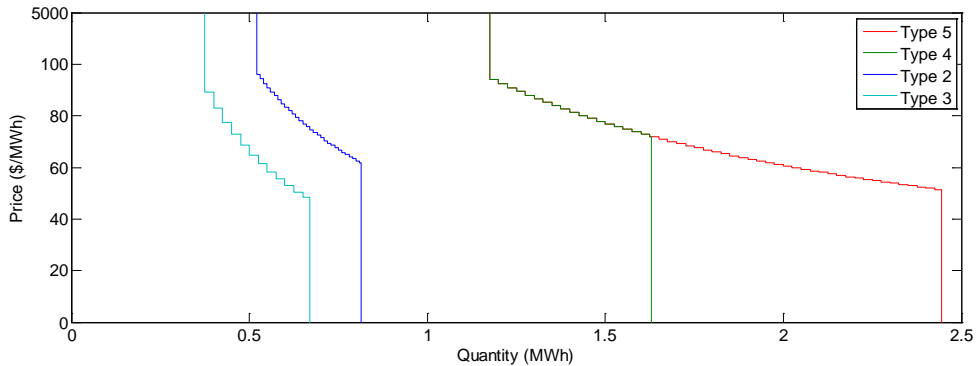


Figure 5.6. Elastic Load Bids

Several DLMP trends that results for the congested system, as shown by Figure 5.7, are different from the trends in the uncongested system, which can be seen by Figure 5.8. The highest DLMP in the congested system (\$92.54) is much higher than the highest DLMP in the uncongested system (\$60.26) and occurs at different locations: LP3 on F1 and LP8 of F4 in the congested and uncongested system respectively. The lowest DLMP in the congested system is also lower than the lowest DLMP in the uncongested system and occur at different locations. Of note are the DLMPs on F2, which has the congested segment, and the DLMPs on

F5 and F6. While the DLMP on F2 increased between its first and second LPs and decreased between its second and third LPs for the uncongested system, it does the opposite in the congested system. The values of the DLMPs at the first and the second LPs on F2 are also lower in the congested system than in the uncongested system and higher for the third LP in the congested system than in the uncongested system. The lower DLMPs incentivized a 15 percent increase in the consumption at the second LP on F2 and the higher DLMP incentivized a 26 percent decrease in the consumption at the third LP. The DLMPs on F5 and F6 are noticeably affected because both feeders are directly connected to F2. The DLMPs on the feeders are higher in the congested system. The higher DLMPs resulted in a consumption decrease of 9.5 percent at the third LP on F6.

DLMP separation as a result of congestion is a tool for system operation and provides valuable information for system upgrades and resource location. The change in consumption between the congested and the uncongested system aided with respecting the line flow limit of segment 17. For example, the change in the consumption of the second and the third LPs on F2 have the effect of reducing power flow on the segment. Increasing the consumption at the second LP reduces the power flow to segment 17 because the LP is before the congested segment and reducing the consumption at the third LP reduces the power flow because the LP is after the congested segment: the net power flow on the feeder is from the beginning of the feeder to the end. The trend of the DLMPs on F2 also signifies that the nodes on the feeder have the greatest impact on congestion and it will be more effective to locate the DG at node 22, at node 24, or at node 25 to relieve congest-

tion on segment 17. The inversion of the DLMP trend on F2 in the congested test system, as compared with the uncongested system, signifies that the DLMP trend in a congested system may be different from the DLMP trend in a radial system; this also communicates that the trend of the DLMP in a congested system may not be readily predictable.

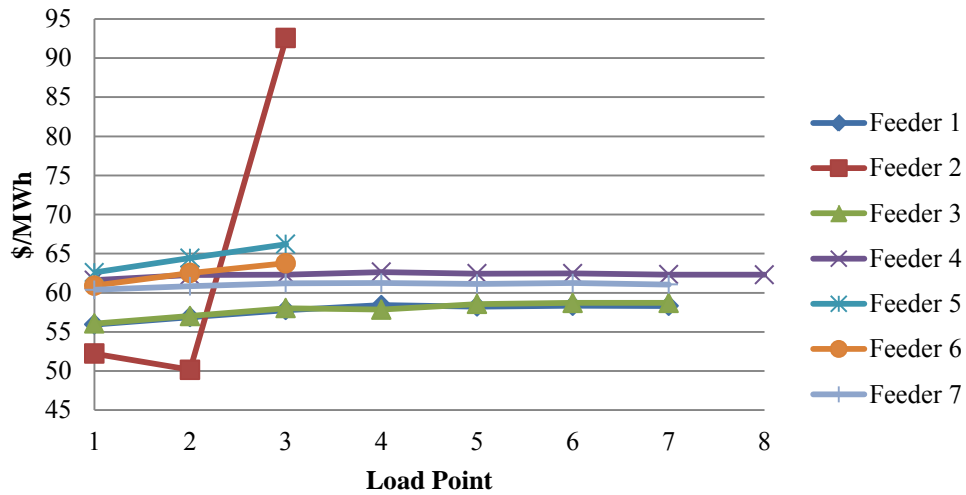


Figure 5.7. DLMPs in Enhanced Distribution System with Congestion

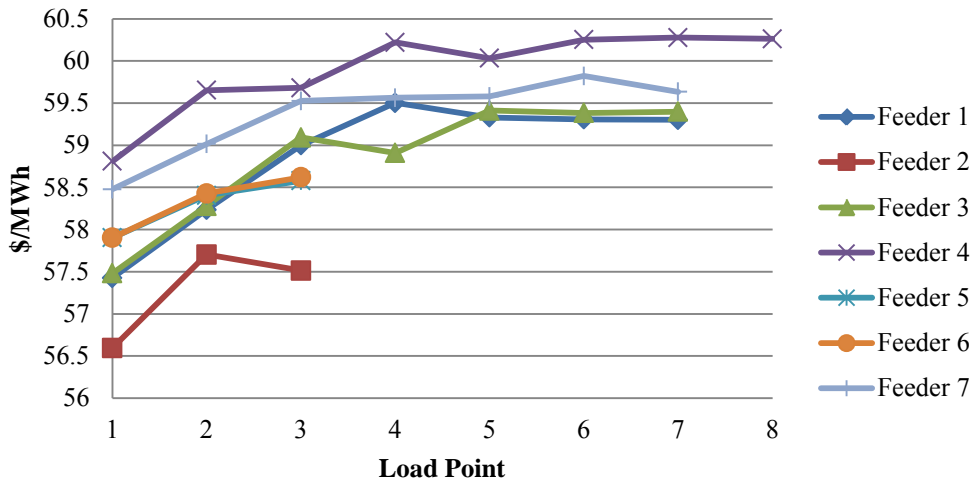


Figure 5.8. DLMPs in Enhanced Distribution System without Congestion

5.5 Optimal Coupling of the Transmission and the Distribution System

If the benefits of the expected DSRs are to be effectively propagated throughout the whole power system, the transmission and the distribution systems must be optimally coupled. This is the reason behind the iterative framework discussed in Section 3.2. Optimal coupling of the transmission and distribution system is illustrated using the test distribution system in Section 5.3 and the RBTS transmission system. The iterative process for the study converged in 3 iterations. The resulting LMPs in the transmission system from the first and the second iterations are shown in Figure 5.9. There is a difference between the LMPs in both iterations because the solutions of the first iteration (single-shot approach) are sub-optimal while the solutions for the second iteration (iterative approach) are optimal. The sub-optimal solutions of the single-shot approach resulted because of an inaccurate representation of the distribution system. The peak load, 85 MW, was the initial load forecast. It resulted in generator 4, with a marginal cost of \$55/MWh, being the marginal generator. The resulting LMP at the distribution proxy bus caused the price sensitive distribution loads to deviate from their forecasted peak, resulting in an aggregate distribution consumption of 79.10 MW. The new model of the distribution system resulted in generator 1, with a marginal cost of \$53/MWh, becoming the new marginal generator in the second iteration. Generator 1 remained the marginal generator in the third iteration and LMPs remained the same between the second and the third iterations. Since it is not possible to perfectly approximate the flexible resources in the distribution system at the distribution proxy when solving the transmission system, such an iterative frame-

work is preferred in order to achieve an integrated framework between the two systems. Note that in a congested transmission system, LMPs can change between iterations even if the marginal generator remains the same.

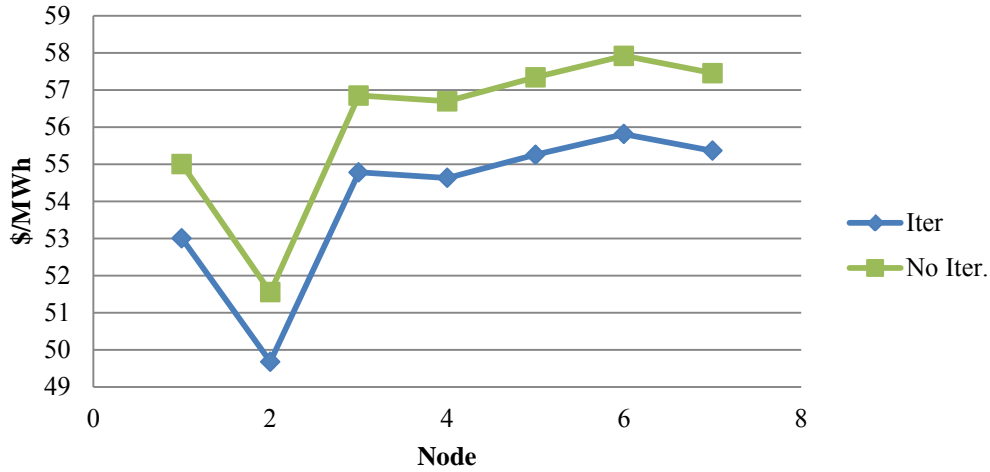


Figure 5.9. Transmission LMP for 1st and 2nd Iterations

The solutions from the single-shot approach are confirmed to be sub-optimal and the results from the iterative approach are confirmed to be optimal by comparing the resulting LMPs and DLMPs from both approaches to that obtained by using a single model of the transmission and the distribution systems. The single model is the true problem and its solution is the global optimal solution. Figure 5.10 shows that the results from the iterative framework converges to the same solution as the single model while the results of the single-shot approach deviates from the results of the combined system.

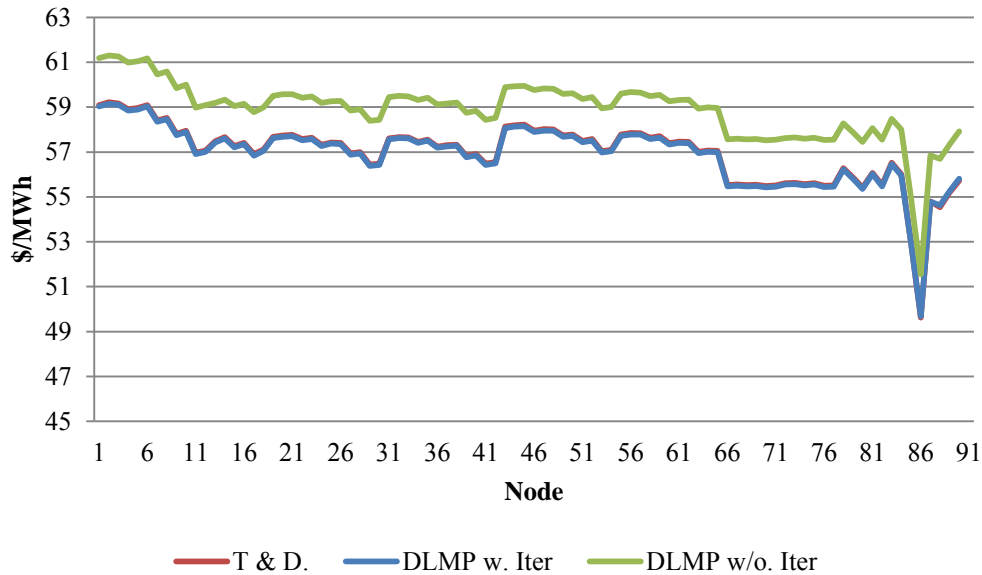


Figure 5.10. Comparison of the Iterative and Single-shot Solutions to the Solutions from a Single Model of the Transmission and the Distribution System

The effect of sub-optimal solutions includes loss of economic efficiency. The sub-optimal prices of the single-shot approach incentivized sub-optimal behavior of the PRL in the distribution system and it would also incentivize sub-optimal behavior of DGs and ESSs. This is illustrated in Figure 5.11 and Table 5.10. Figure 5.11 shows the value of the flexible portion of price responsive loads in the test distribution system and the DLMP at the price responsive LP nodes for the iterative and the single-shot approach. Table 5.10 shows the action incentivized by both approaches. The consumption incentivized by the single-shot approach deviates from the consumption incentivized by the DLMP for several LPs. The deviation results in efficiency loss as shown in Table 5.11

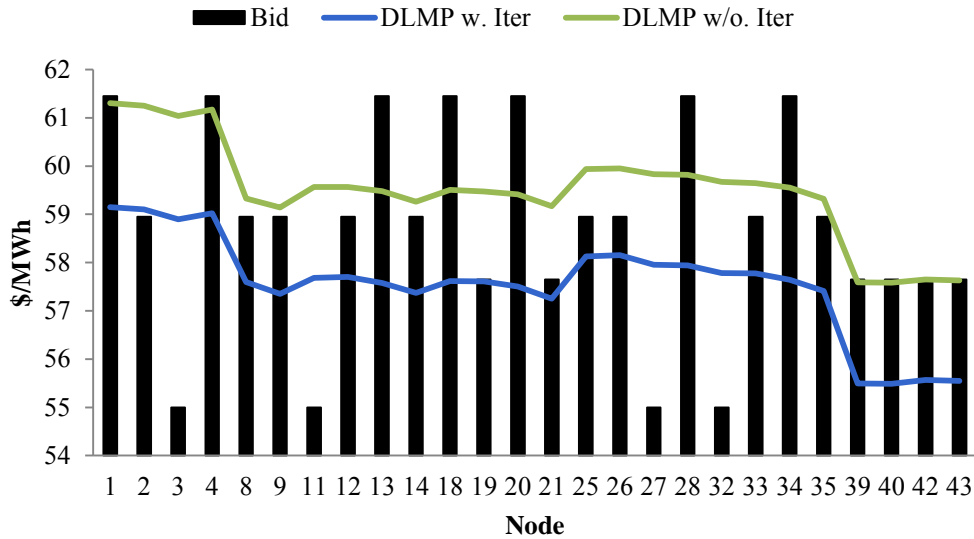


Figure 5.11. Flexible Portion of Demand and DLMP for Iterations 1 and 2

Table 5.10. Action Incentivized by DLMP for Iterations 1 and 2 (Black – Consumption both prices, White – No consumption both prices, Red – Consumption one price, No Consumption one price, Gray – Partial Consumption)

LP #	1	2	3	4	8	9	11	12	13	14	18	19	20	21
DLMP w. Iter.	Black	White	White	Black	Red	Red	White	Red	Black	Red	Black	Red	Black	Red
DLMP Single-shot	Black	White	White	Black	White	White	White	White	Black	White	Black	White	Black	White

LP #	25	26	27	28	32	33	34	35	39	40	42	43
DLMP w. Iter.	Red	Red	White	Black	White	Red	Black	Red	Black	Black	Black	Black
DLMP Single-shot	White	White	White	Black	White	White	Black	White	Black	Black	Gray	Black

Table 5.11. Comparison of Resulting Market Surplus for Iterative and Single-shot Approach

Approach	Total Demand Value (\$)	Elastic Demand Value (\$)	Gen. Cost (\$)	Market Surplus (\$)
Iterative	5296.68	912.89	4668.04	628.64
Single-shot	5030.01	646.22	4575.00	455.00

While the DLMPs for the single-shot approach are higher than the DLMPs of the iterative process for this study, this trend cannot be guaranteed to always occur. If the study had been started with a low aggregate distribution demand for the first iteration, the DLMPs in the first iteration may have been lower than the DLMPs in the second iteration. What can be guaranteed is the demonstrated im-

provement in economic efficiency. Optimally coupling the transmission and distribution systems will reduce operational costs and improve reliability. For example, if DSRs are used for ancillary services, it will be important that the control signal, such DSRs act upon, be accurate for both transmission and distribution system operations.

5.6 Conclusion

Several studies have been used to numerically illustrate the DLMP in this chapter. The studies showed that in the traditional distribution system, where there is no congestion and the network is operated radially, DLMPs increase from the point of generation injection to feeder ends as only losses cause DLMP separation. The study on an enhanced system with price responsive load showed that contemporary prices in the distribution system will reduce economic efficiency in the enhanced distribution system partly because of the cross subsidies that distort prices and wrongly incentivize distribution resources. A study in the chapter shows that in a congested system, the DLMP trend is not as predictable as in an uncongested system as a result of the DLMP internalizing congestion management. The trend of DLMPs in a congested system can provide valuable information for locating resources in an enhanced system. The chapter also illustrated the need to optimally couple the transmission system and the enhanced distribution system. The coupling, which can be achieved through a mechanism, such as the iterative DLMP calculation approach, allows for the proper modeling of the price sensitive resources in both systems in the decomposed OPF problem.

Chapter 6. Comparison of the DLMP to Contemporary Prices in the Distribution System

Simulation results that compare the impact of the DLMP to the impact of a RTP, a TOU rate, and a FR are reported in this chapter. Multi-period studies are conducted on enhanced distribution systems with PRLs and a meshed topology with and without congestion. The test system is described in Section 6.1 and the modeling approach for the PRLs in Section 6.2. The iterative framework discussed in Section 3.2 may fail to converge. The convergence issue is discussed in Section 6.3. An alternative framework, used to calculate DLMPs for the studies in this chapter, and the framework for calculating other tested pricing indices is described in Section 6.4. The results in Section 6.5 through Section 6.8 cover various studies involving different demand elasticity as well as networks with and without congestion. A concluding paragraph is presented in Section 6.9.

6.1 Test System

The test systems reported in this chapter are the IEEE 30 bus system and the distribution system at bus 4 of the RBTS system. The IEEE 30 bus system represents the transmission system; its one line diagram is shown in Figure 6.1 and a summary of its characteristics are presented in Table 6.1. The branch and the load details of the system are listed in Table A.7 and Table A.8 in Appendix A. The data for the IEEE 30 bus system was obtained from test case case30pwl in MATPOWER [34]. The system in case30pwl was modified from the original IEEE test system using data from [35]. Data obtained from [35] include branch

limits. For this research, the test distribution system is placed at bus 5. The generator data in case30pwl were replaced with the generator data in Table 6.2. The generator data were obtained from the reliability test system (RTS) [36], [37]. For the studies in this chapter, all transmission loads, except for the load at bus 5, are perfectly inelastic. The perfectly inelastic loads have a 24 hour load profile as shown by Figure 6.2. The load profile is a spring weekday load profile from the RTS system. The hourly load details for the test transmission system are in Table A.8 in Appendix A.

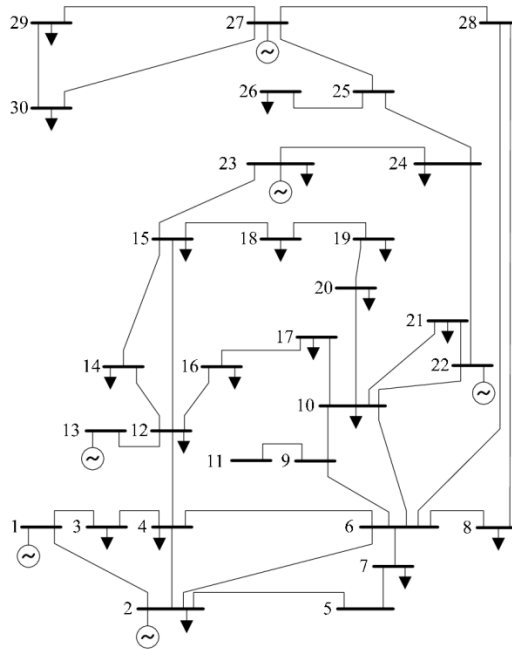


Figure 6.1. One-line Diagram of IEEE 30-Bus System [38] (Test Distribution system at bus 5 not shown)

Table 6.1. Summary of IEEE 30-Bus System

Number of Buses	30
Number of Branches	41
Number of Generators	6
Number of Load Points	21
Total Peak Load (incl. distribution system peak load)	229.20 MW
Total Generation Capacity	360.00 MW

Table 6.2. Generator Data for the Test Transmission System

Gen No.	Bus No.	Min. Output (MW)	Max Output (MW)	Marginal Cost (\$/MWh)	Gen. Type
1	1	0.00	76.00	19.64	Fossil Steam Coal
2	2	0.00	20.00	163.02	Comb Turbine Oil
3	22	0.00	12.00	94.74	Fossil Steam Oil
4	27	0.00	76.00	19.64	Fossil Steam Coal
5	23	0.00	76.00	19.64	Fossil Steam Coal
6	13	0.00	100.00	75.64	Fossil Steam Oil

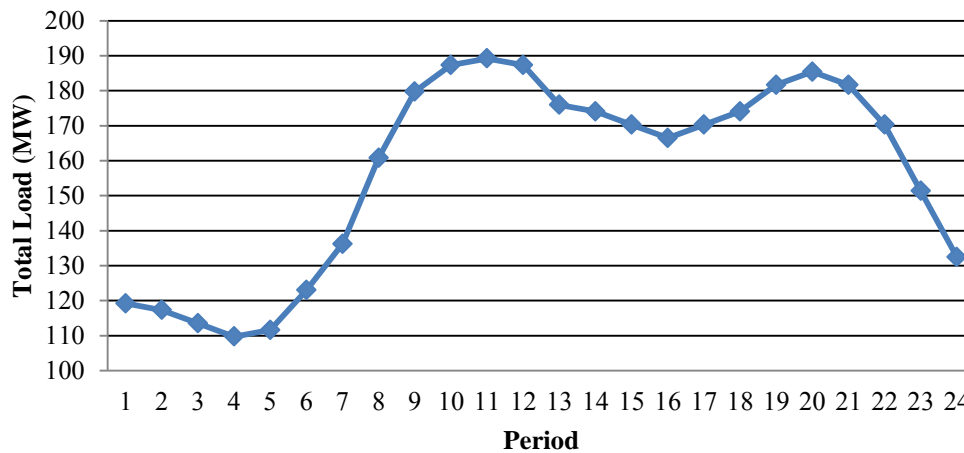


Figure 6.2. Hourly Profile of the Total Inelastic Load in the Test Transmission System

The test distribution system is the distribution system at bus 4 of the RBTS system. It is the same system used for the study in Section 5.4. For Case Study 1 – 3 in this chapter, the test distribution system feeders are sized so that the distribution system is not congested and there are no DGs in the system. Similar to Section 5.4, congestion is created for Case Study 4 and DGs are added to the system. The load data for the simulation is created from the peak load information of the test system, which is provided in Table A.9 in Appendix A. A subset of the loads has demands that do not respond to prices, i.e., perfectly inelastic demand, and a subset has price responsive demands. Load type 1 is classified as perfectly inelas-

tic and load types 2, 3, 4, and 5 are classified as price responsive loads. Table 5.6 presents the details of the LPs. The perfectly inelastic loads have the load profile shown by Figure 6.3. The load profile is obtained from the AEP Ohio Columbus Southern Power Company [39]. It is the load profile for the residential customer class for spring 2012. The peak of 13.30 MW occurs at 8 PM and it is just 33.25 percent of the total possible peak of 40 MW in the test system. The details of the type 1 loads are listed in Table A.10 in Appendix A.

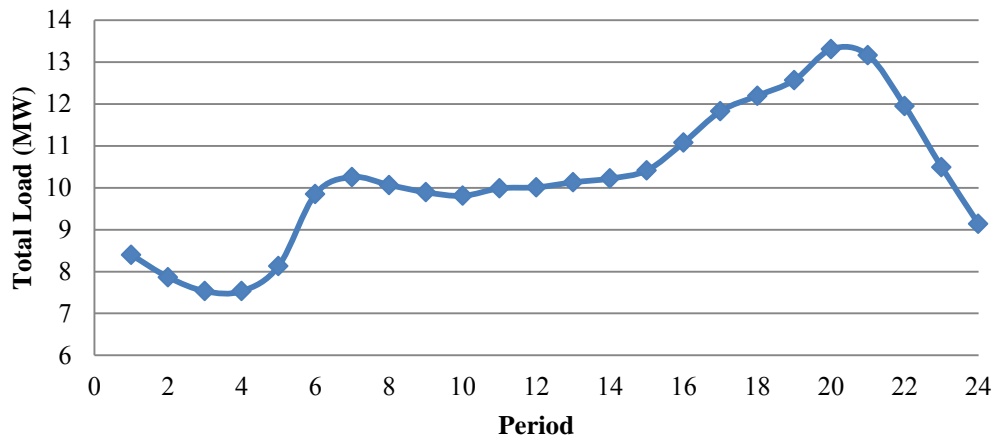


Figure 6.3. Hourly Profile of the Total Perfectly Inelastic Load in the Test Distribution System

6.2 Economic Modeling of Distribution Loads

The assumption of demand response necessitates the modeling of the sensitivity of demand to prices. In the current electricity market environment, some ISOs and Regional Transmission Operators (RTOs) allow loads to submit monotonically non-increasing step bids to purchase electricity. The bids represent the quantity that a load is willing to purchase or consume at a specified price. Price sensitive loads are modeled in the lossy DCOPF using the same approach. The

problem of determining the bid curve of a load is complex and several papers have attempted and proposed different solutions to the problem [72]-[74]. The crux of developing a bid function is to determine the consumption level that maximizes the benefit a load receives from consuming at different prices. This is achieved, in this research, with a demand curve. The demand curve is the plot of the price of a good and the quantity of the good that a consumer is willing to consume at each price. Load demand curves are approximated by step functions to form bid curves. Approximating a demand curve by a step function is a simple approach to the problem of determining a bid curve. While a demand curve is developed based on consumer preferences [77], other factors, such as the fact that electricity markets are two-settlement markets, the bids of other loads, and the offer of generators, could affect the consumption level that maximizes the economic benefit a load obtains from consuming at a certain price.

There are several functional forms to the demand curve. These functional forms include linear, exponential, log, and quadratic forms [1]. Each functional form has its own properties. The power form is selected for this research because of its constant elasticity property [1], [75]. Equation (6.1) is a generic form of the power model of a demand curve. P_o and Q_o in the equation represent a reference price and quantity that can be used to scale the demand curve. ϵ in the equation is the coefficient of price elasticity of demand. In economics, the price elasticity of a good represents the sensitivity of the good to prices. It is quantified by the coefficient of price elasticity ϵ , which is described by (6.2). The coefficient of elasticity is defined as the percent change in quantity demanded of a good for a percent

change in the price of the good. As represented by the negative slope of a demand curve, there is usually an inverse relationship between the price and the quantity of a good demanded. Hence, the coefficient of price elasticity of demand is usually a negative value. The more negative the coefficient of elasticity of a good, the more price sensitive the good is. A coefficient of price elasticity of zero indicates a perfectly inelastic demand, i.e., demand that does not respond to prices. A coefficient of price elasticity greater than -1 (absolute value less than 1 but greater than 0) represents inelastic demand, i.e., a change in price results in a smaller percentage change in demand. A coefficient of price elasticity of -1 represents unit elasticity, i.e., a percent change in price results in a percent change in quantity demanded. A coefficient of price elasticity less than -1 (absolute value greater than 1) represents elastic demand, i.e., a small change in price leads to a greater percentage change in quantity demanded.

$$Q = Q_o \left(\frac{P}{P_o} \right)^\varepsilon \quad (6.1)$$

$$\frac{P dQ}{Q dP} \quad (6.2)$$

Determining the coefficient of price elasticity of a good is complex. It is estimated by fitting observations from empirical econometric experiments by a demand curve. Over the years researchers have produced several works estimating the coefficient of elasticity of electricity consumption. The numbers from the studies show a wide degree of variation. According to a summary in [76], the short-run coefficient of price elasticity from different studies range from -0.01 to -0.9. The study in [78] estimates the short-run coefficient to be as high as -2.57

(2.57% change in consumption for a 1% change in price). Several factors are responsible for the variation in estimated coefficient of electricity. The factors include the prices observed data are obtained for, the approach for fitting the observed data, and the environment under which the loads are observed. For example, loads exposed to a RTP may have a different elasticity than loads exposed to a FR. Similarly, smart loads making autonomous decision may have different elasticity from loads controlled by human beings, as a result of the ease that technology provides [70]. It is likely that loads exposed to the DLMP and the smart grid environment will be more elastic than loads in the contemporary distribution system. As a result, studies are conducted in this chapter for elasticity ranging from -0.2 to -4.2. The demand curves, for the elastic load types at the elasticity used in the simulations, are shown in Figure 6.4 – Figure 6.7.

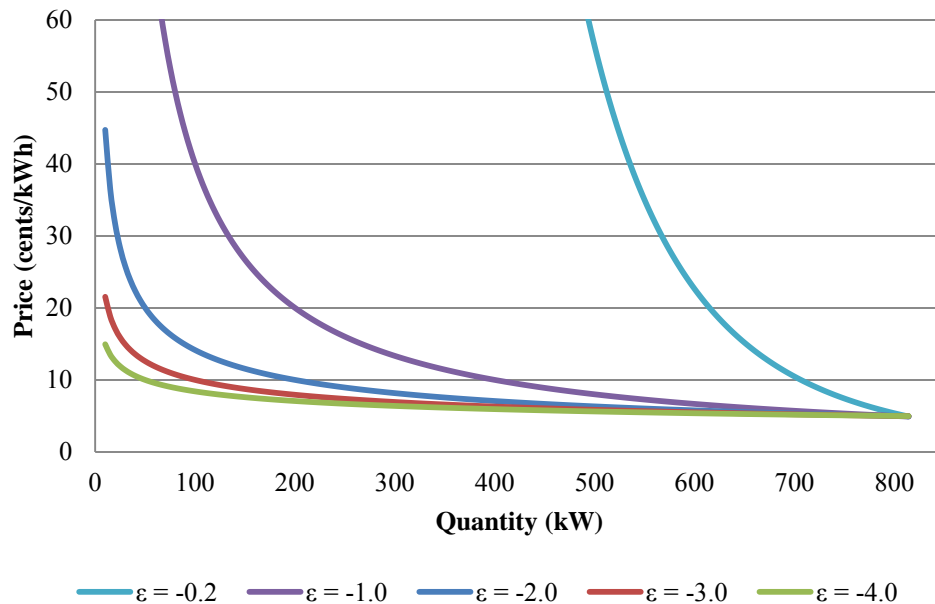


Figure 6.4. Type 2 Demand Curves with Different Coefficient of Elasticity

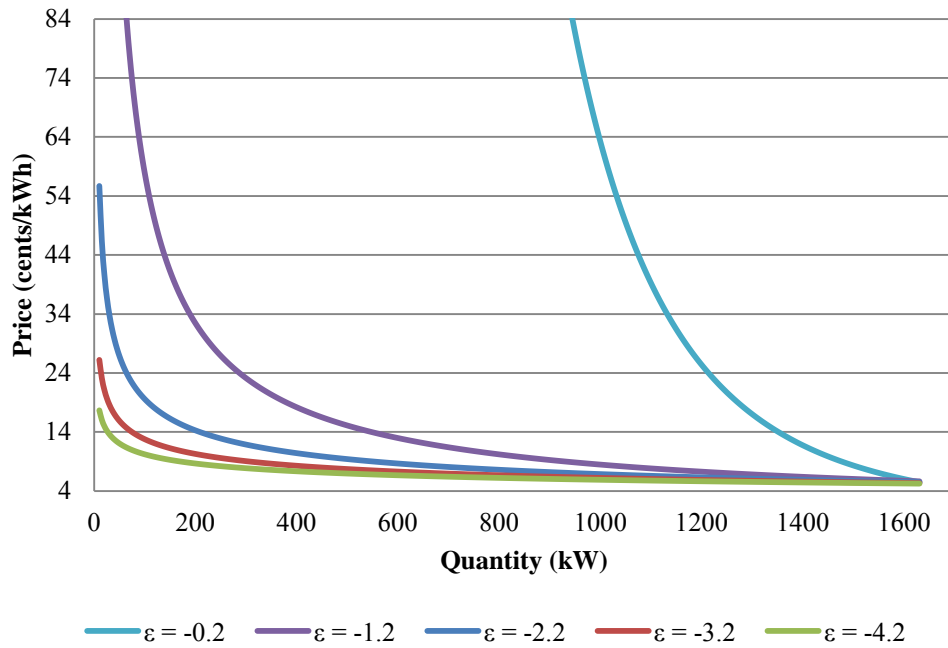


Figure 6.5. Type 3 Demand Curves with Different Coefficient of Elasticity

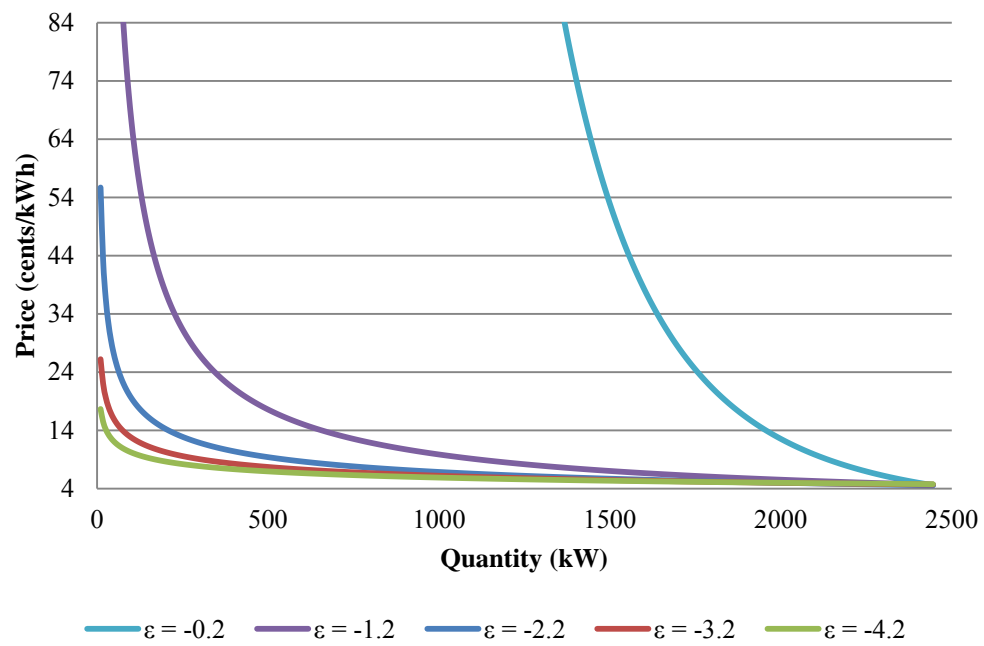


Figure 6.6. Type 4 Demand Curves with Different Coefficient of Elasticity

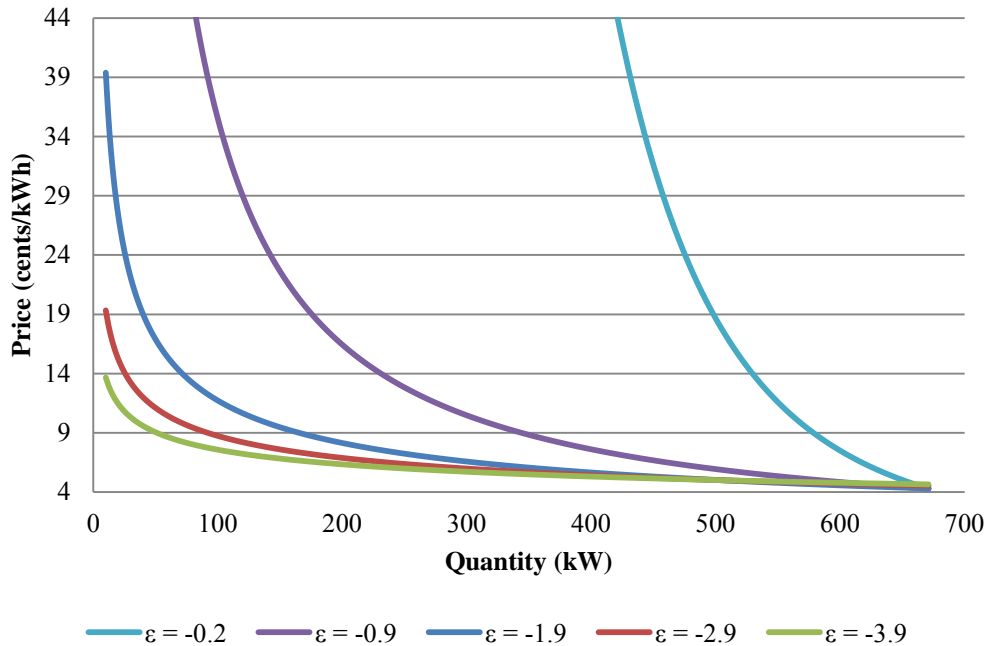


Figure 6.7. Type 5 Demand Curves with Different Coefficient of Elasticity

Note that the price elasticity of demand can be affected by time. Consequently, there is short and long-run elasticity. In economics, short-run signifies a period in which certain parameters are held constant. For example, it can be assumed that the number of generators in a system is fixed in the short-run. Long-run signifies that the parameters held constant in the short-run are variable. Time provides the opportunity to seek out substitutes or alternative; hence, the price elasticity of demand in the long-run is usually higher than in the short-run. The short-run elasticity of demand is used to develop the demand curves in this research.

6.3 Convergence Problems with Iterative Framework

While the iterative framework for calculating the DLMP provides a way to accurately model the price sensitivity of distribution resources for the transmission system OPF and vice versa, there is no guarantee of convergence to a solu-

tion or convergence to the correct or optimal solution. One of the major factors that can lead to non-convergence of the iterative framework includes the non-continuity of generator offer curves and load bids. A load or a generator could set the clearing price as a result of the step curves of generator offers and load bids. A generator setting the clearing price is illustrated in Figure 6.8 and a load setting the clearing price is illustrated in Figure 6.9. If a load sets the clearing price in the distribution system OPF, the approximation of the distribution system by a perfectly inelastic curve for the transmission system OPF may be inadequate. A perfectly inelastic demand model of the distribution system sends the signal that distribution loads will consume regardless of proxy LMP. This is inaccurate for a distribution system with price sensitive resources and the inaccuracy matters in the situation where a distribution load sets the clearing price. As shown in Figure 6.10, the inelastic representation results in a non-unique clearing price in the transmission OPF. While the clearing price in the distribution system is a specific price between P_A and P_B , any price between P_A and P_B could be the clearing price in the transmission system OPF: the inelastic representation sends the signal that a load is willing to consume the fixed demand at any price between P_A and P_B . If the solution algorithm selects any price other than the distribution system clearing price, the distribution system consumption incentivized by the selected price will deviate from the optimal consumption.

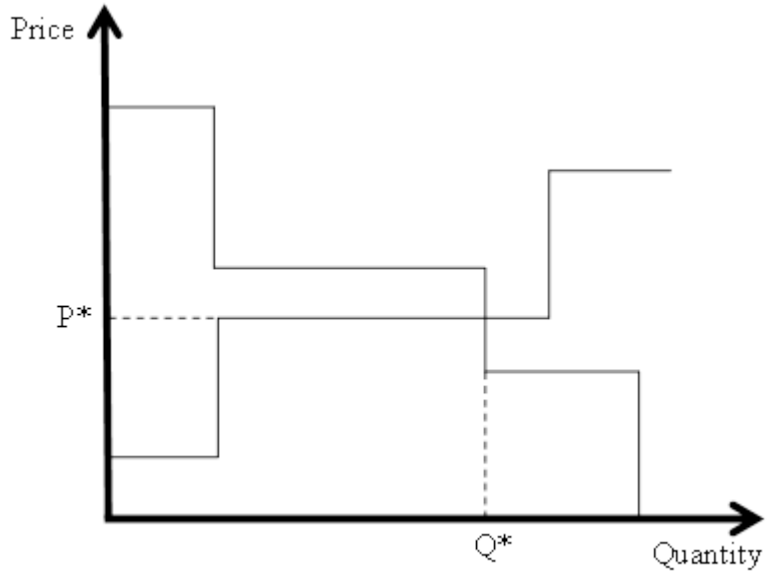


Figure 6.8. Generator Sets Clearing Price

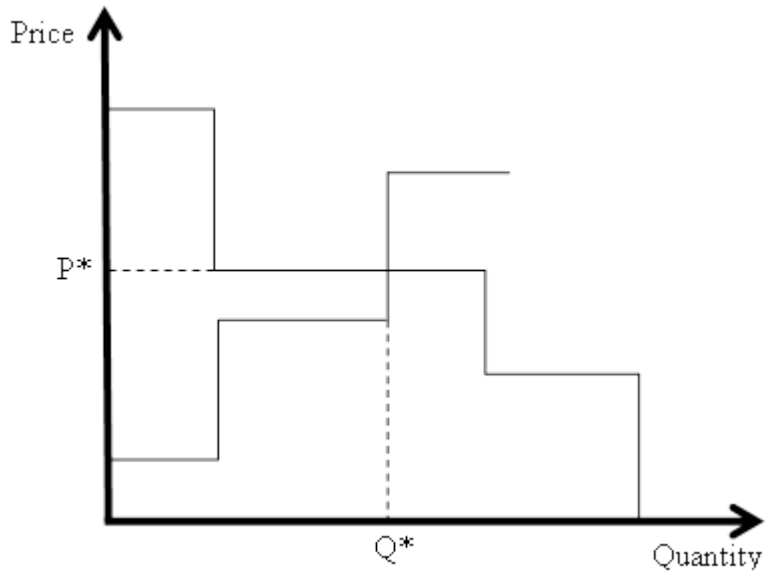


Figure 6.9. Load Sets Clearing Price

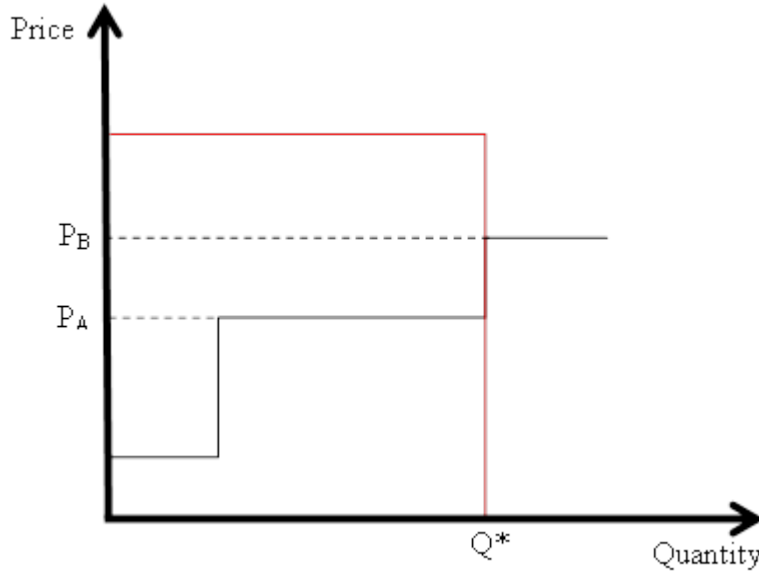


Figure 6.10. Inelastic Distribution Load Sets Clearing Price in Transmission

OPF

The situation described in the preceding paragraph occurred in the simulations conducted for this research, Figure 6.11 and Figure 6.12. In Figure 6.11, the proxy LMPs for five iterations and the optimal proxy LMPs are shown. The figure show the proxy LMP jumping between the prices in iterations 1, 3, and 5 and the prices in iterations 2 and 4 for some of the periods, e.g., 3, 5, 13, 17, and 22. The proxy LMPs in the periods could not converge to the optimal price. The prices in Figure 6.11 incentivized the consumption in Figure 6.12, which does not settle to the optimal solution. A representation, more accurate than the inelastic demand curve, is required to solve this convergence problem of the iterative framework. Simply using a step bid rather than an inelastic demand curve may not resolve the problem as the vertical portion of the step demand bid curve can overlap with the vertical portion of the supply curve and cause the same problem.

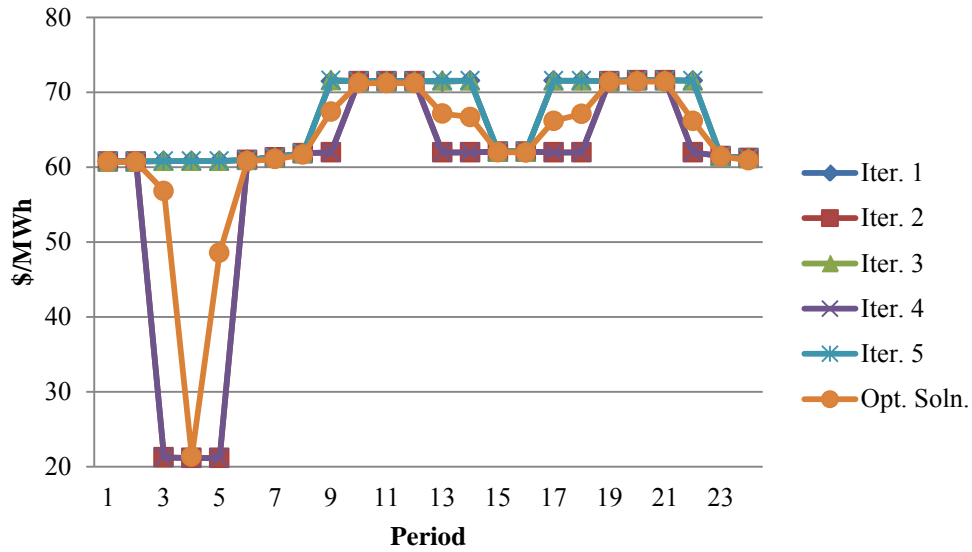


Figure 6.11. Proxy LMP Changing from one Iteration to the other and the Optimal Proxy LMP

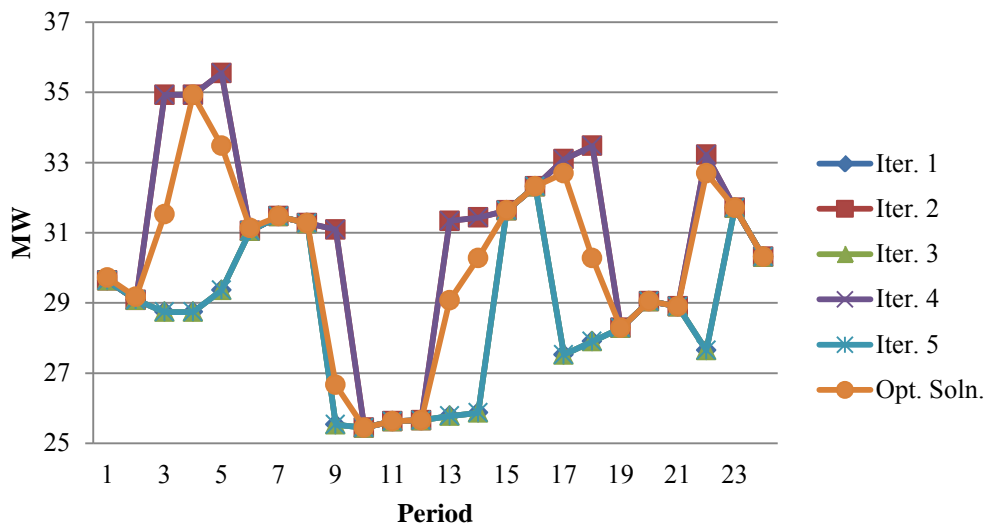


Figure 6.12. Infinite Generator Output Changing from one Iteration to the other and the Optimal Infinite Generator Output

A similar problem could result even when a generator sets the price in the transmission system OPF. The infinite generator model of the transmission system sends the signal that the cost to consume is the fixed marginal cost, distribution proxy LMP, regardless of the consumption level in the distribution system.

Hence, the optimization algorithm could select any consumption between Q_A and Q_B as the clearing consumption as shown in Figure 6.13. A consumption level other than the optimal consumption that cleared in the transmission system OPF can cause a change to the proxy LMP. Non-convergence as a result of the infinite generator model can be handled by adding additional constraints to the OPF and a small cost to the objective that penalizes deviation from the optimal consumption.

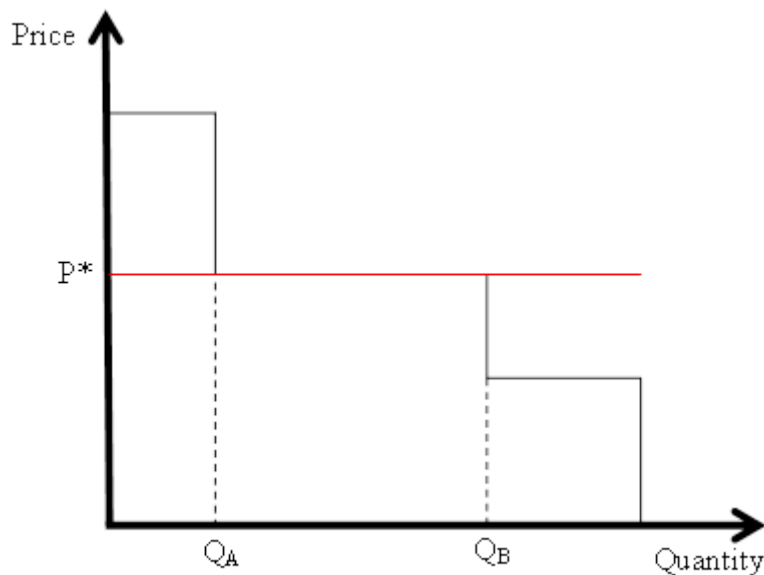


Figure 6.13. Infinite Generator Sets Clearing Price in Distribution OPF

Convergence may also be dependent on the amount of flexibility in the decomposed problem, occurrence of congestion and the initial solution. The iterative framework may have convergence problems if a distribution system has multiple connections to the transmission system, i.e., multiple infinite generators. The dispatch of the infinite generators may change from iteration to iteration as a result of the MC of the generators changing such that it may be cheaper to purchase losses from different generators at different iterations. A similar situation may arise if the transmission system has multiple distribution systems connected. Con-

gestion and changes in the consumption of other distribution systems may cause the proxy LMP at a distribution system to change from iteration to iteration. Congestion may also cause non-monotonicity of LMPs. For example, congestion can cause an LMP to decrease even with increased consumption. Non-monotonicity of LMPs can also cause non-convergence. As will be discussed in the future work section in Chapter 7, the convergence problem of the iterative framework needs to be further investigated.

6.4 Sampling Approach for Calculating Prices

In order to overcome the convergence problem of the iterative framework, for the purpose of conducting the studies in this chapter, a sampling approach [79] was employed for calculating DLMPs. The approach is illustrated in Figure 6.14. An aggregate demand curve is developed by determining the resulting aggregate demand in the distribution system at different sample marginal costs for the infinite generator. The aggregate demand at each sample marginal cost is the infinite generator output obtained by solving the lossy DCOPF for the distribution system. The aggregate demand curve fully represents the price elasticity of distribution system loads, the local generation resources in the distribution system, and the network condition, e.g., congestion, of the distribution system. The process mimics a scenario where information is available to accurately model the prices sensitive resources and the network conditions of a distribution system.

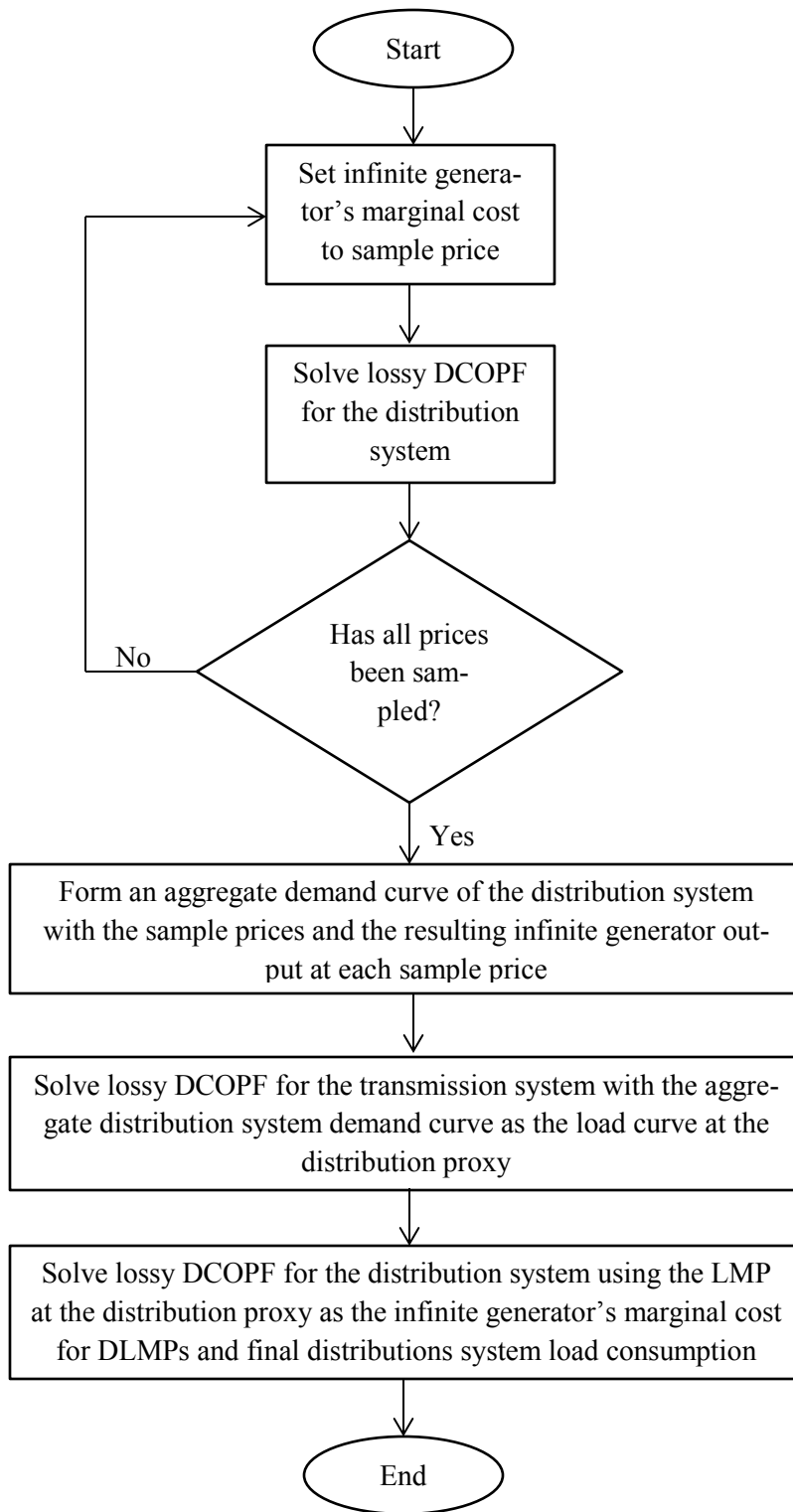


Figure 6.14. Sampling Approach for Calculating DLMP

A similar technique is employed for the RTP, TOU, and FR simulations. The process for the RTP simulations is depicted in Figure 6.15. In the RTP process, the aggregate demand at each sample price does not properly capture losses and network conditions in the distribution system. A sample RTP is simply propagated throughout the distribution system without a marginal loss or congestion component. The same is done in the process that determines the final consumption in the distribution system. The prices in the final process are, however, the LMP at the distribution proxy bus. The difference between the DLMP and the RTP processes for the sampling approach represents the difference in the application of the DLMP and the contemporary RTP. While the DLMP is calculated from a distribution system OPF, the RTP is calculated without proper consideration of the distribution network. The RTP could simply be the proxy LMP. Hence, the DLMP reflects both the transmission system and the distribution system network and generation conditions and the price sensitivity of loads and other resources, the RTP reflects the transmission system network and generation conditions. The RTP inaccurately represents the price sensitive resources in the distribution system as it does not reflect the response of the resources to losses and other distribution network conditions.

The TOUs and FRs in these studies are determined based on the total distribution system load payment to the transmission system resulting from the DLMP simulations. The FR is the load weighted average of the load payment to the transmission system. This includes the cost of losses, which is socialized based on MW consumption. Two periods types are used for the TOU. The peak period runs

from 7 a.m. to 9 p.m. and the off-peak period is every period not included in the peak period.

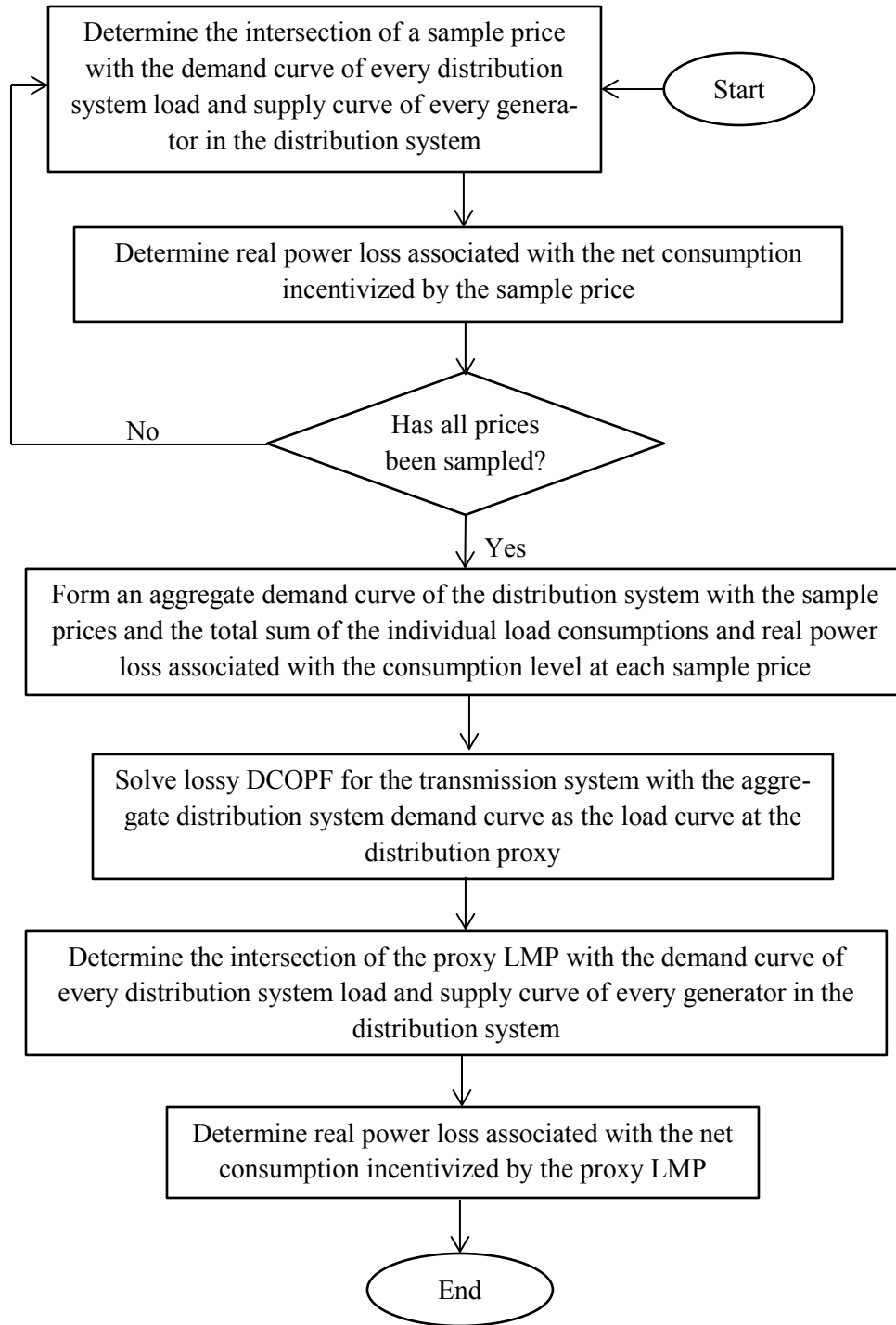


Figure 6.15. Sampling Approach for Calculating RTP

6.5 Case Study 1: ϵ of -0.2 and No Congestion

As discussed in Section 6.2, a load with a coefficient of elasticity of -0.2 is inelastic. Hence, small changes in consumption are expected for large changes in prices. This is reflected in the results of simulations with ϵ of -0.2. The prices in the simulations are shown in Figure 6.16 and the aggregate consumption incentivized by the prices in Figure 6.17. Note that the DLMP in Figure 6.16 is for a node, 49, that demonstrates a consistently high deviation from the RTP. The deviation of each price from the DLMP in each hour represents the inaccuracy of the price. Despite the significant inaccuracy shown by Figure 6.17, Figure 6.18 shows that the aggregate consumption incentivized for each period, by all the prices, is largely the same. As shown in Figure 6.18, the absolute percentage deviation from the optimal DLMP aggregate consumption is less than 1.7 percent for the FR for all time periods except for H4, less than 1.5 percent for the TOU rate for all time periods except for H4 and H22, and approximately 1 percent or less for all time periods for the RTP. It takes a very high price differential in H4 to obtain a 4.89 percent deviation in H4 for the FR and 3.32 and 3.01 percent in H4 and H22 for the TOU rate. The inaccuracy of the FR, TOU, and RTP has limited impact on consumption as a result of highly inelastic loads.

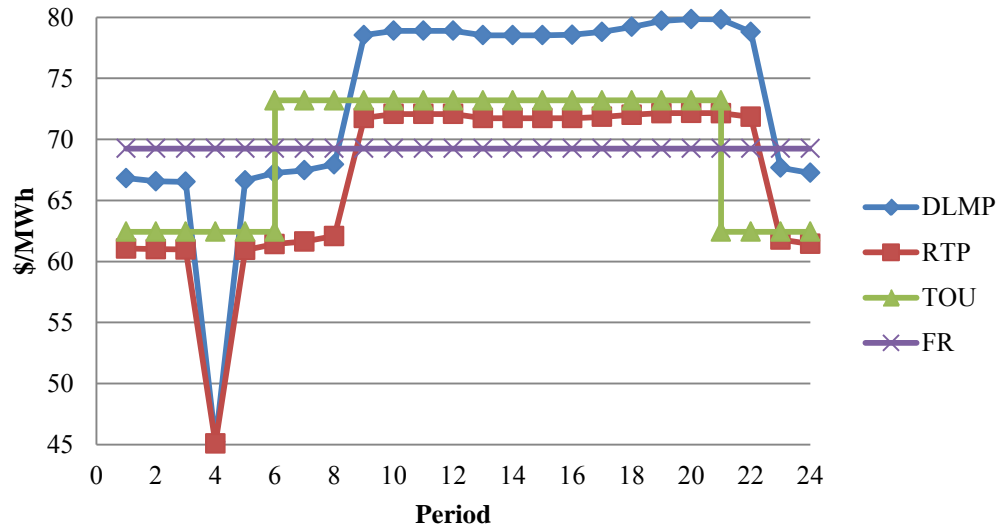


Figure 6.16. Prices at ϵ of -0.2

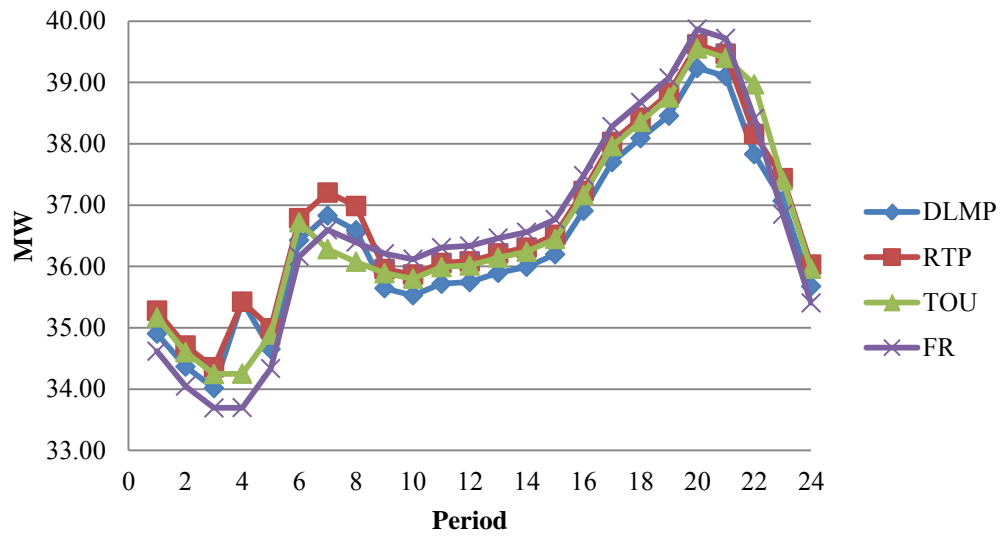


Figure 6.17. 24 Hour Aggregate Load Consumption at ϵ of -0.2

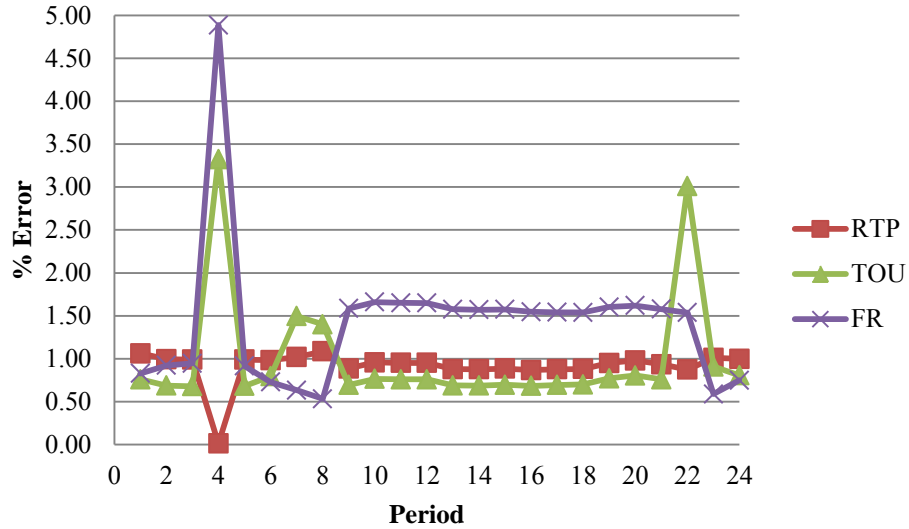


Figure 6.18. Absolute Percentage Deviation from Optimal Aggregate Consumption at ϵ of -0.2

6.6 Case Study 2: ϵ around -1.0 and No Congestion

The impact of the inaccuracy of the FR, TOU, and the RTP on consumption are masked in case study 1 because the distribution system loads are highly inelastic. At higher elasticity, the deviation is more pronounced. For price differentials similar to or less than those obtained for ϵ of -0.2, Figure 6.19, the incentivized aggregate consumption for ϵ around -1.0, Figure 6.20, show higher deviation from each other. The consumption incentivized by the FR and the TOU show different trends from the optimal consumption incentivized by the DLMP. For example, the consumption incentivized by the DLMP increases from H2 to H4 and decreases from H4 to H6 while the consumption incentivized by the FR and the TOU decrease from H2 to H4 and increase from H4 to H6. In H7 to H22, the FR and the TOU rate are unable to capture the details of the trend of the optimal consumption. While the optimal DLMP consumption increased and decreased several times, the FR and the TOU rate consumption simply increased. Figure 6.21 shows

that the aggregate consumption incentivized by the FR deviates by higher than 8 percent for half the periods and by 18.98 percent in H4. For the TOU, the deviation is approximately 6 percent or higher for over half of the periods and 11.19 percent and 10.58 percent in H4 and H22.

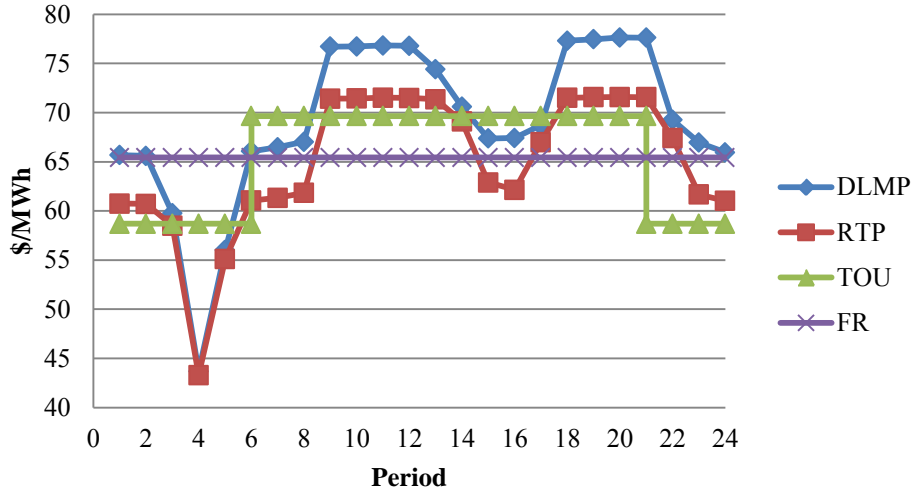


Figure 6.19. Prices at ϵ around -1.0

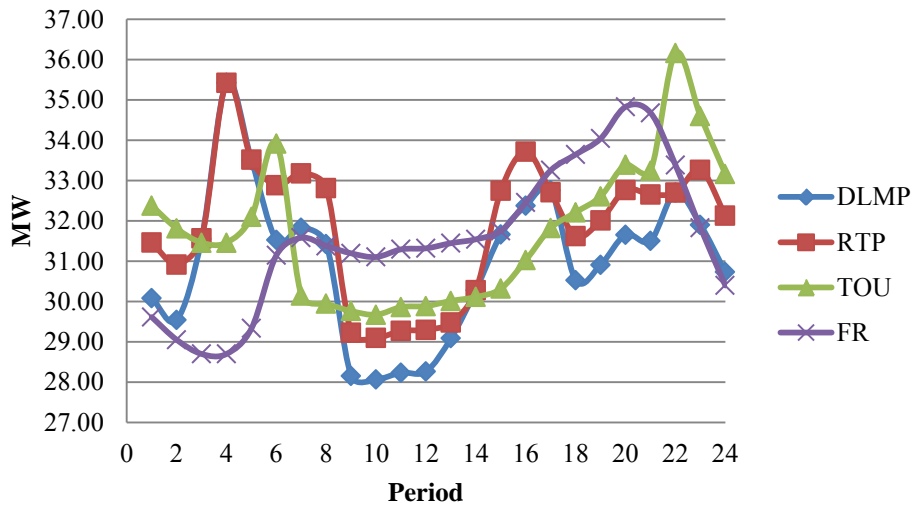


Figure 6.20. 24 Hour Aggregate Load Consumption at ϵ around -1.0

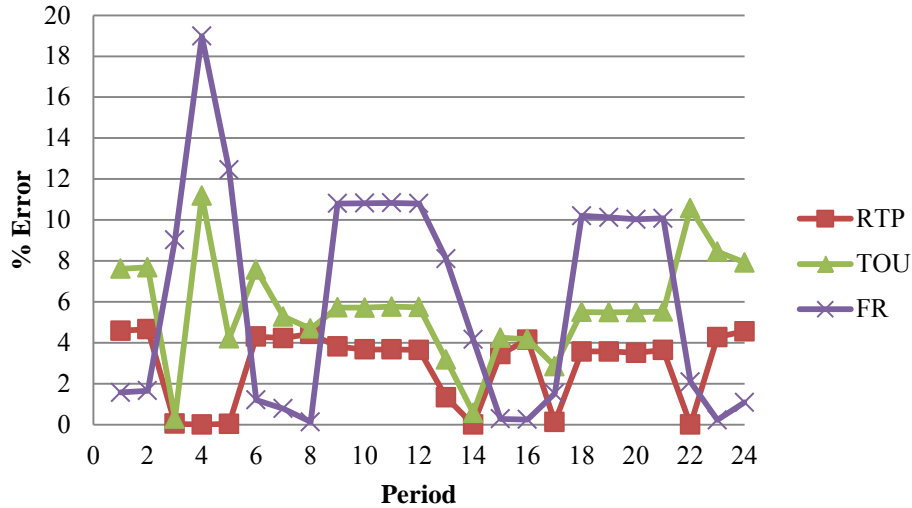


Figure 6.21. Absolute Percentage Deviation from Optimal Aggregate Consumption at ϵ around -1.0

While the RTP incentivizes consumption with the same trend as the DLMP, the level of consumption for two-thirds of the periods is different from the level of consumption incentivized by the DLMP. The deviation is about 4 percent in most of the periods. Inspecting the real power consumption deviation at the aggregate level somewhat obfuscates the impact of the inaccuracy of the RTP on incentivized consumption. There are inelastic loads in the test system whose deviation from the optimal consumption, including the losses associated with the inelastic consumption, is zero. At the individual load level, the inaccuracy of the RTP is more pronounced. This is reflected in Figure 6.22 – Figure 6.25, the plot of the absolute percentage deviation of the individual load consumption incentivized by the RTP from the individual optimal DLMP consumption. While the maximum deviation at the aggregate level is about 4 percent, the individual deviations are as high as about 8. All of the elastic loads demonstrate individual deviations of about 4 percent or higher in about two-thirds of the periods.

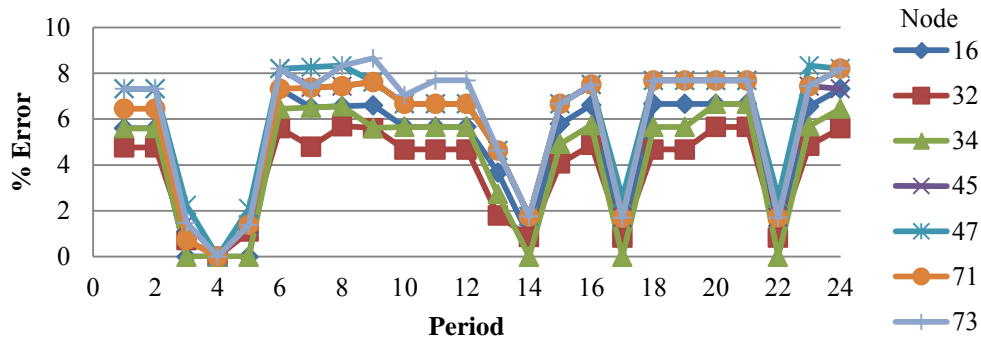


Figure 6.22. Type 2 Loads Absolute Percentage Deviation from Optimal Consumption at ϵ around -1.0

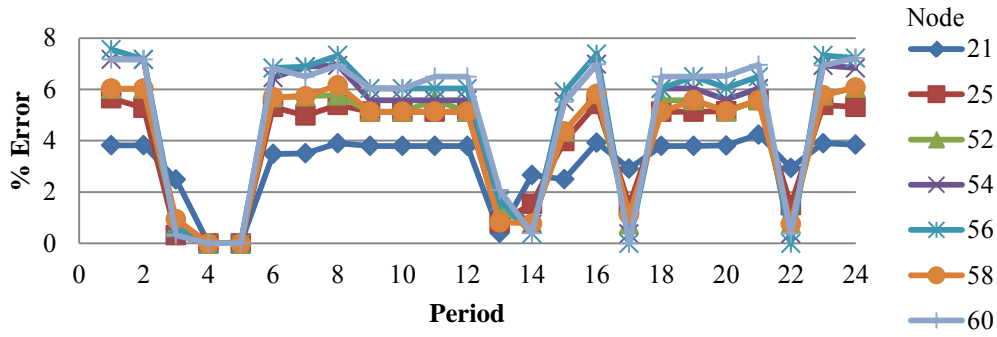


Figure 6.23. Type 3 Loads Absolute Percentage Deviation from Optimal Consumption at ϵ around -1.0

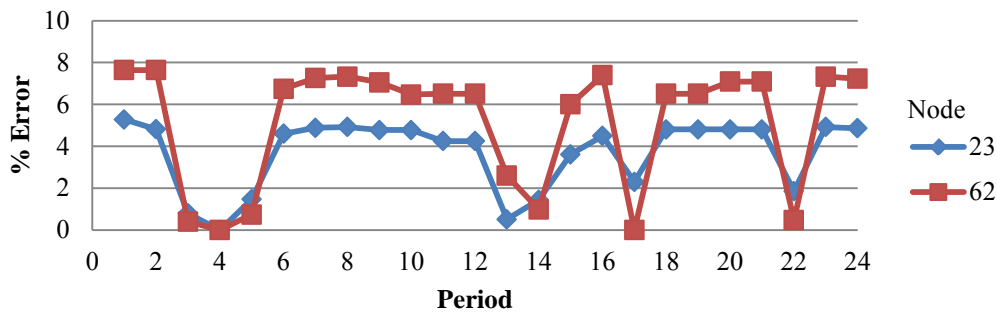


Figure 6.24. Type 4 Loads Absolute Percentage Deviation from Optimal Consumption at ϵ around -1.0

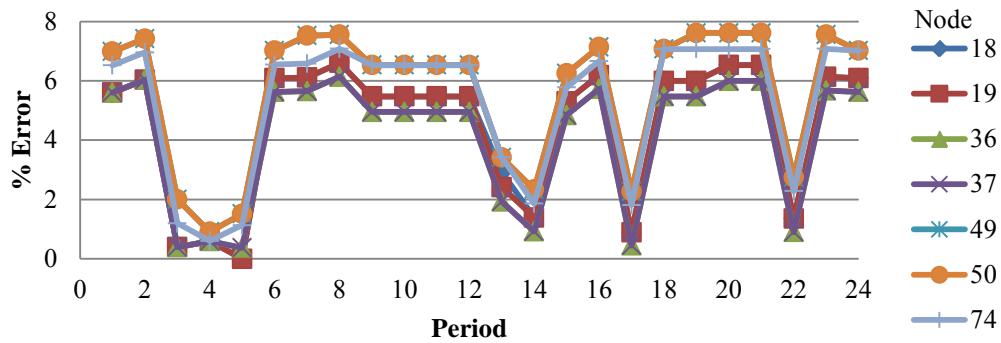


Figure 6.25. Type 5 Loads Absolute Percentage Deviation from Optimal Consumption at ϵ around -1.0

6.7 Case Study 3: ϵ from around -2.0 to around -4.0 and No Congestion

The DLMP is best for a distribution system with substantial amount of flexible resources. With increased load flexibility, results of Case Study 3 show that the disadvantage of contemporary prices, in terms of deviation from optimal consumption, also increases. As shown in Figure 6.26, the minimum deviation of the consumption incentivized by the FR for ϵ around -4.0 is 10.92 percent. Periods in between H7 and H24 for ϵ around -4.0 have deviations approximately between 15 and 20 percent. In the off-peak period, the deviation is as high as 38.54 percent. For ϵ around -3.0, the deviation is as high as 34.02 percent and more than two-thirds of the periods have deviations greater than 10 percent. H11 and H20 (for ϵ around -3.0) and H10 to H12 and H19 to H21 (for ϵ around -2.0) show higher deviations than for ϵ around -4.0 as a result of congestion in the transmission system. The increased elasticity, for ϵ around -4.0, helps relieve the congestion. Hence, only a small spike in H20 when ϵ is around -4.0.

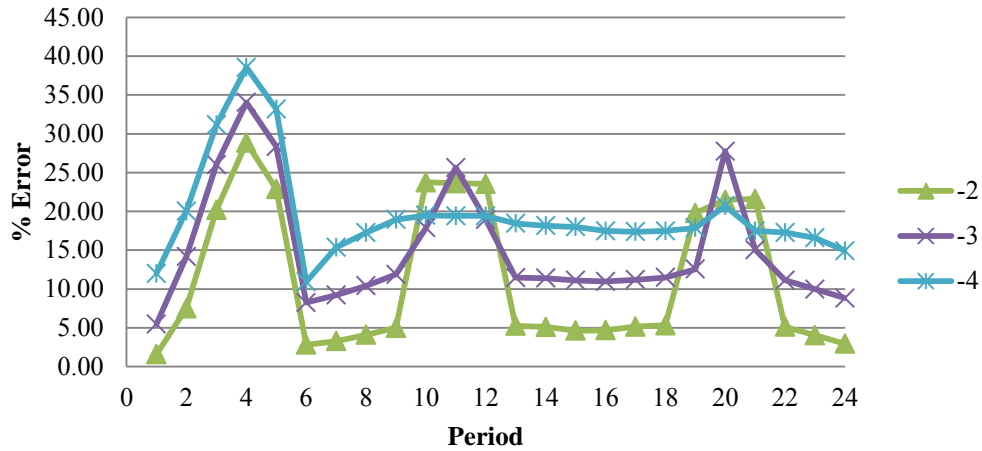


Figure 6.26. FR Absolute Percentage Deviation from Optimal Consumption at Higher ϵ

In the off-peak period, Figure 6.27 shows that a significant deviation from the optimal consumption is incentivized by the TOU rate. The deviations are as high as about 46 percent, 32 percent, and 20 percent for an ϵ around -4.0, -3.0, and -2.0 respectively. During the peak period, the results show an interesting trend. Except for H10 – H12 and H19 – H21 (for ϵ around -2.0), H11 and H20 (for ϵ around -3.0), and H20 (for ϵ around -4.0), the deviation in the peak period is less than or approximately 5 percent. This results because of the increased elasticity of the distribution loads, which helps relieve the congestion in the transmission system. The profile of the resulting DLMPs, during the peak periods, became flatter as elasticity increased. Since the TOU rate is determined based on the DLMP and the consumption resulting from the DLMP, the peak TOU rate becomes more accurate than what may be obtained in actual practice. In practice, TOU rates are determined based on consumption and costs over a very large time horizon.

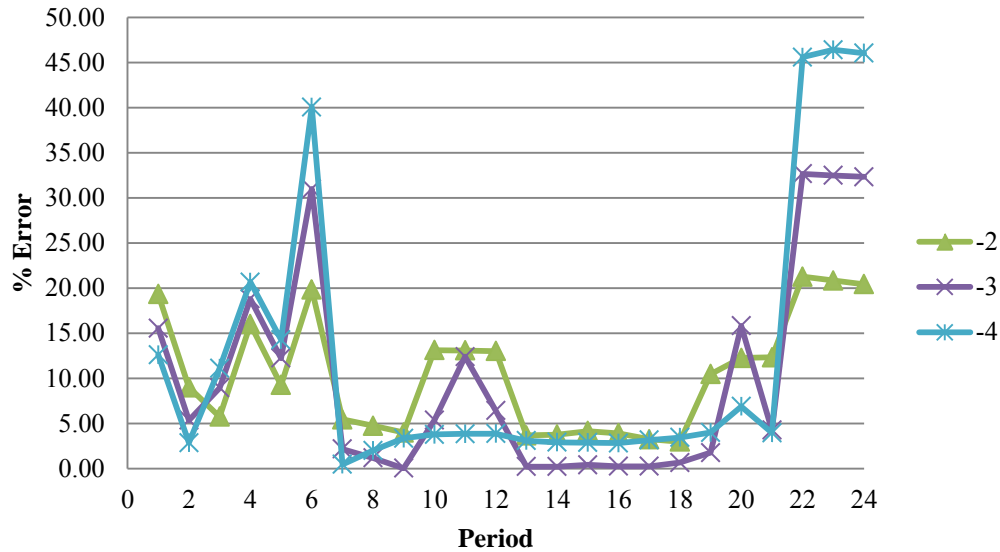


Figure 6.27. TOU Absolute Percentage Deviation from Optimal Consumption at Higher ϵ

As elasticity increases, the difference between DLMPs and the RTP reduces. In spite of the reduction, the deviation of the consumption incentivized by the RTP from the optimal DLMP consumption increases as a result of increased load flexibility. This is seen both at the aggregate consumption level, Figure 6.28, and at the individual consumption level Figure 6.29 – Figure 6.40. At the aggregate level, the deviation is approximately between 5 and 7 percent for sixteen periods (for ϵ around -2.0), approximately between 6.5 and 7.5 percent for thirteen periods (for ϵ around -3.0), and between 7 and 9 percent for sixteen periods (for ϵ around -4.0). At the individual consumption level, all type 2 loads exhibit deviations of approximately between 8 and 15 percent for about two-third of the periods (for ϵ around -2.0), approximately between 10 and 20 percent (for ϵ around -3.0) for over half of the periods, and approximately between 15 and 29 percent for about two-thirds of the periods (for ϵ around -4.0). All but one type 3 loads exhibit deviations of approximately between 8 and 12 percent for about two-third of the

periods (for ϵ around -2.0), approximately between 10 and 15 percent (for ϵ around -3.0) for over half of the periods, and approximately between 15 and 20 percent for about two-thirds of the periods (for ϵ around -4.0). Similar significant deviations are reflected for the type 4 loads with deviations of approximately between 15 and 19 percent for about 16 periods for one of the loads and deviation between 10 and 15 percent for the other load at ϵ around -4.0. All type 5 loads exhibit deviations approximately between 8 and 16 percent for about two-third of the periods (for ϵ around -2.0), approximately between 13 and 20 percent (for ϵ around -3.0) for over half of the periods, and approximately between 15 and 27 percent for about two-thirds of the periods (for ϵ around -4.0).

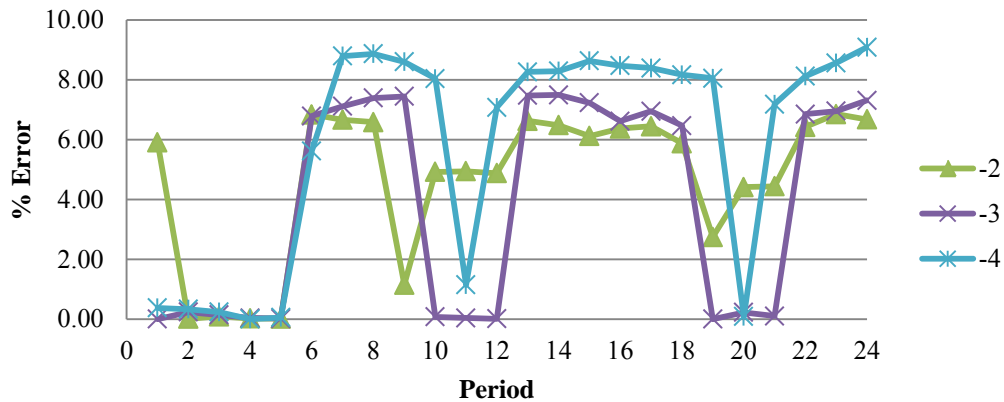


Figure 6.28. RTP Absolute Percentage Deviation from Optimal Consumption at Higher ϵ

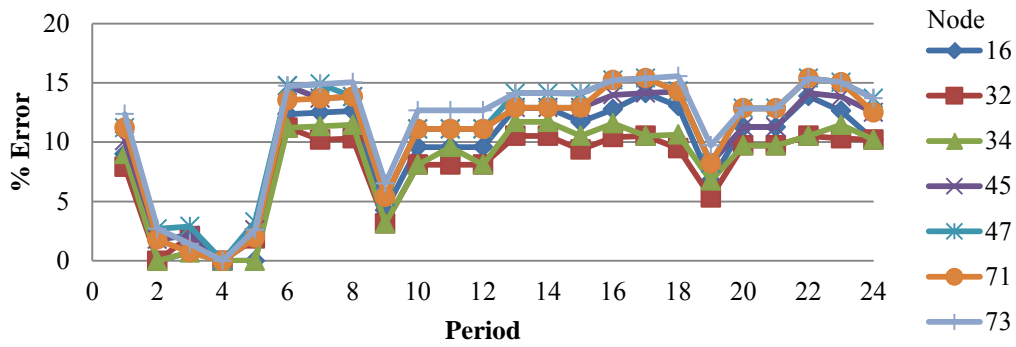


Figure 6.29. Type 2 Loads Absolute Percentage Deviation from Optimal Consumption at ϵ around -2.0

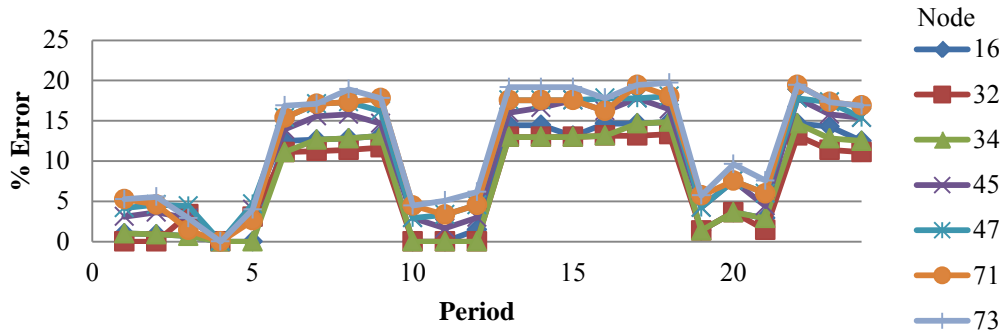


Figure 6.30. Type 2 Loads Absolute Percentage Deviation from Optimal Consumption at ϵ around -3.0

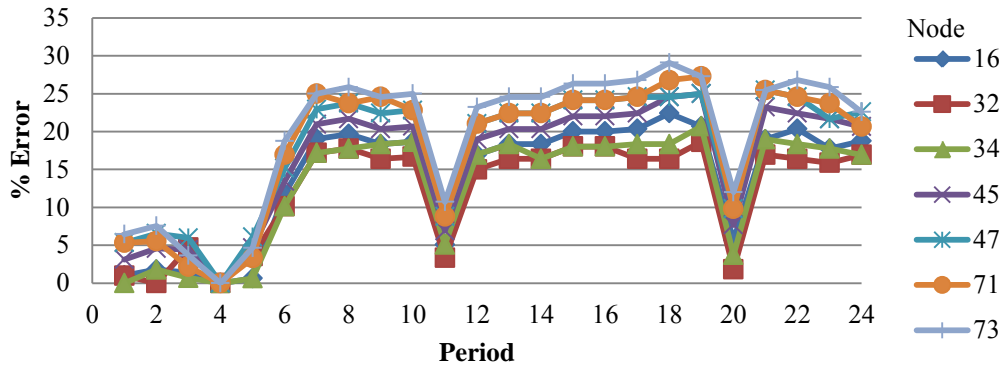


Figure 6.31. Type 2 Loads Absolute Percentage Deviation from Optimal Consumption at ϵ around -4.0

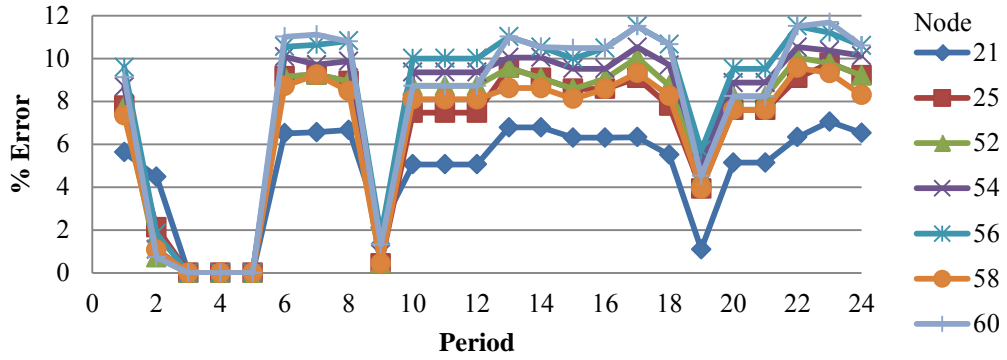


Figure 6.32. Type 3 Loads Absolute Percentage Deviation from Optimal Consumption at ϵ around -2.0

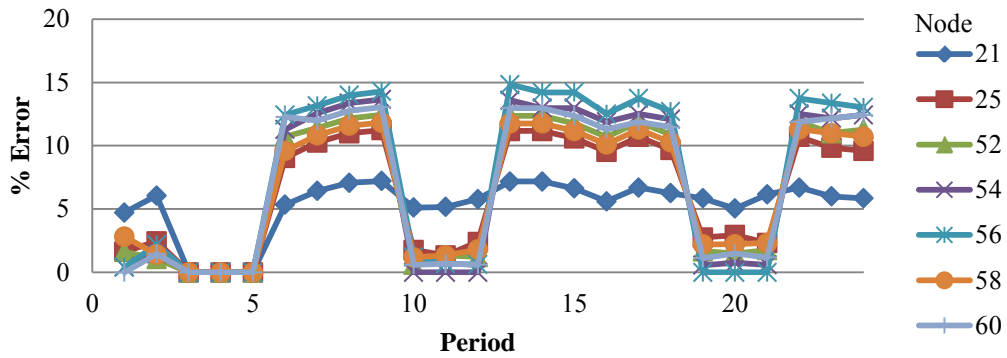


Figure 6.33. Type 3 Loads Absolute Percentage Deviation from Optimal Consumption at ϵ around -3.0

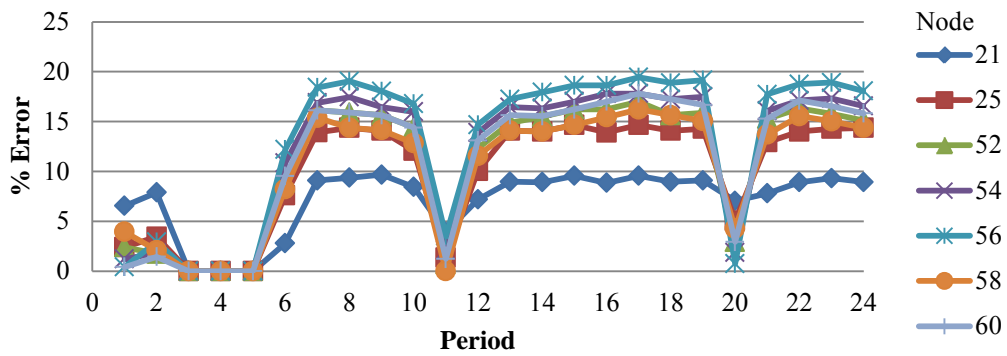


Figure 6.34. Type 3 Loads Absolute Percentage Deviation from Optimal Consumption at ϵ around -4.0

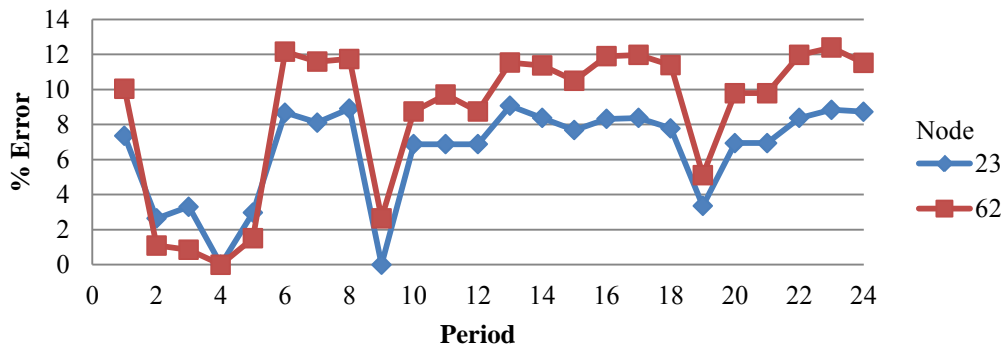


Figure 6.35. Type 4 Loads Absolute Percentage Deviation from Optimal Consumption at ϵ around -2.0

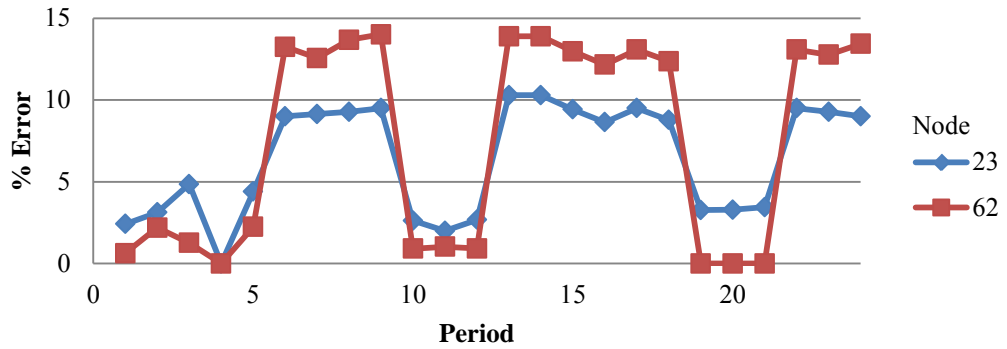


Figure 6.36. Type 4 Loads Absolute Percentage Deviation from Optimal Consumption at ϵ around -3.0

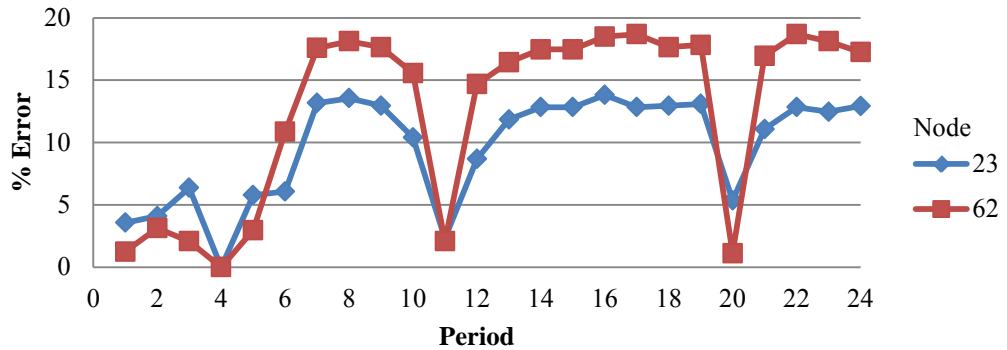


Figure 6.37. Type 4 Loads Absolute Percentage Deviation from Optimal Consumption at ϵ around -4.0

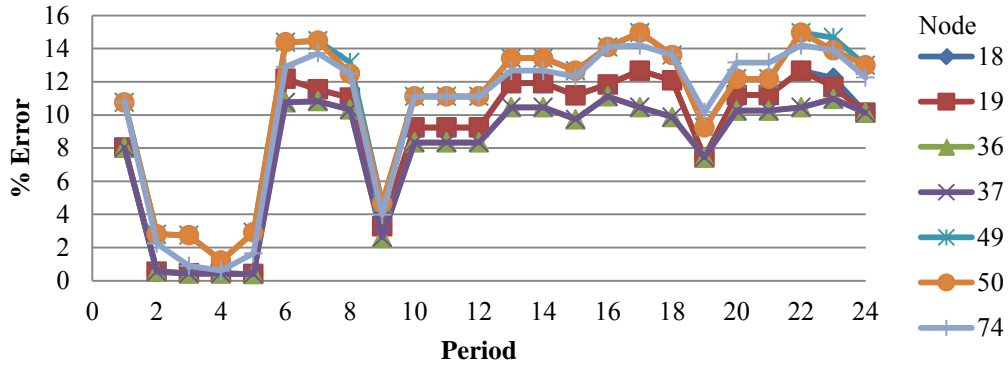


Figure 6.38. Type 5 Loads Absolute Percentage Deviation from Optimal Consumption at ϵ around -2.0

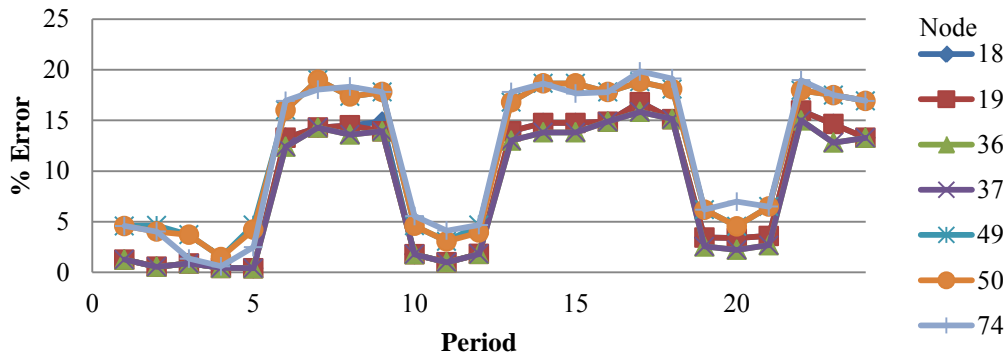


Figure 6.39. Type 5 Loads Absolute Percentage Deviation from Optimal Consumption at ϵ around -3.0

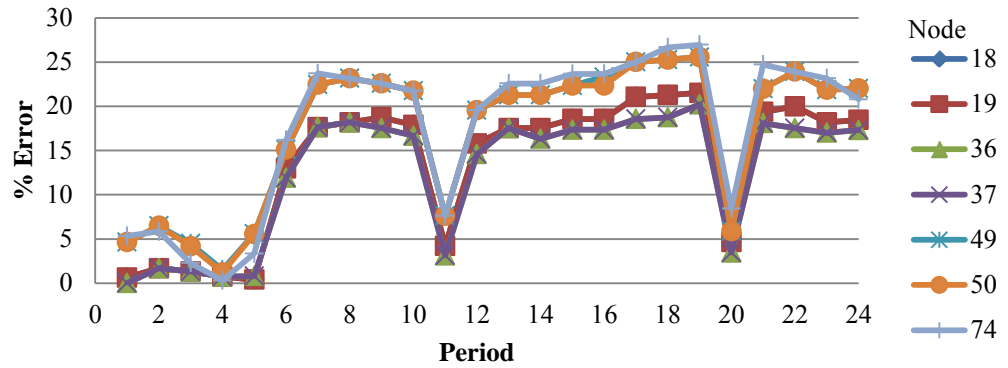


Figure 6.40. Type 5 Loads Absolute Percentage Deviation from Optimal Consumption at ϵ around -4.0

6.8 Case Study 4: Congested Distribution Network

While inaccurate, the RTPs in case studies 1 – 3 have the same trend as the DLMP and incentivized aggregate consumptions with similar trend as the DLMP's aggregate consumptions. The RTP is able to reflect a similar trend as the DLMP because there is no congestion in the distribution system. The DLMPs take the shape of the LMP at the proxy bus, the RTP, as a result. The inaccuracy of the RTP in case studies 1 – 3 results because the RTP does not properly reflect distribution losses. Congestion in the distribution network could cause the DLMP to take a different trend than the proxy LMP. Hence, the inaccuracy of the RTP could be much more significant in a congested system and the inaccuracy could have significant reliability impacts. In a distribution system with congestion, only the DLMP internalizes congestion. The RTP will result in a need for load curtailment, which may be sub-optimal, to maintain reliability. This is illustrated by conducting studies on the same test system in case studies 1 – 3 but with the rating of segment 17 reduced to 1.6 MW to cause congestion. The test system also has DGs as described in Section 5.4 and the loads have ϵ around -2.0.

Figure 6.41 shows the plot of the resulting RTP and the DLMPs at one of the nodes significantly impacted by the congestion. The figure shows that the price differential between the DLMP and the RTP in H1 to H5 is significantly high: as high as \$52.20 in H3. The consumption incentivized by both the DLMP and the RTP at node 25 is shown in Figure 6.42 and the difference between the DLMP and the RTP consumption, as a percentage of the optimal consumption, is shown in Figure 6.43. The figures show that the RTP consumption deviates by more than

15 percent from the DLMP consumption for two-thirds of the periods. The deviation in H1 – H5 is especially high. This results from the severity of the congestion in those periods and the significant load curtailment that may be required to rectify the overload on branch 17 as a result of the consumption incentivized by the RTP. This is illustrated in Figure 6.44, which shows the flow on branch 17 in the DLMP study and in the RTP study. The internalization of congestion by the DLMP results in a situation where branch 17 flow is never more than 1.6 MW while the RTP results in a situation where the line flow is more than the line limit in several periods. The periods where the line flow, as a result of the consumption incentivized by the RTP, is much higher than the limit correspond to the periods with the highest deviations, as shown by Figure 6.43. The RTP solution will require an operator to take steps to curtail load to mitigate the overload on branch 17. The operator intervention would be sub-optimal and would not be required for this example when using the DLMP. The deviation of the consumption incentivized by the RTP in the congested system is compared to the deviation incentivized in case study 3, an uncongested system, in Figure 6.45.

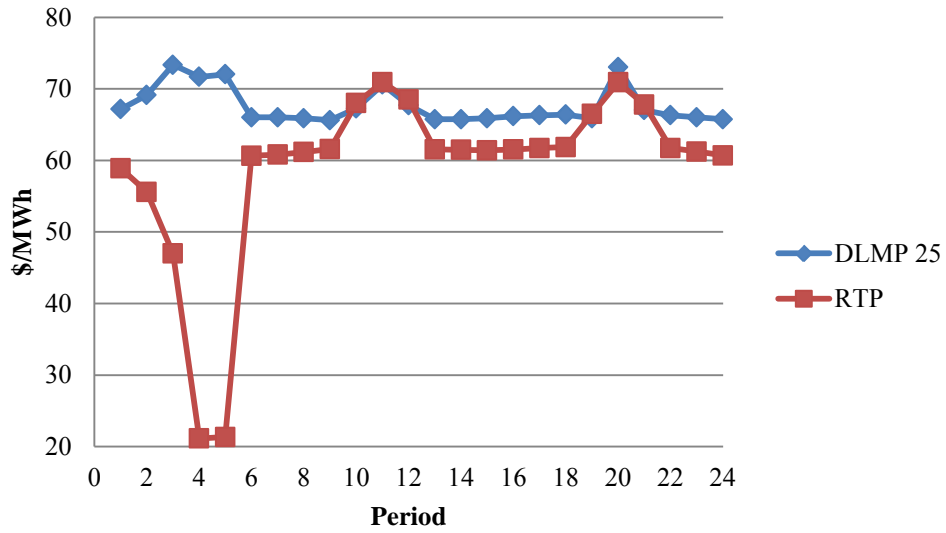


Figure 6.41. DLMP at Node 25 and RTP in Congested Network

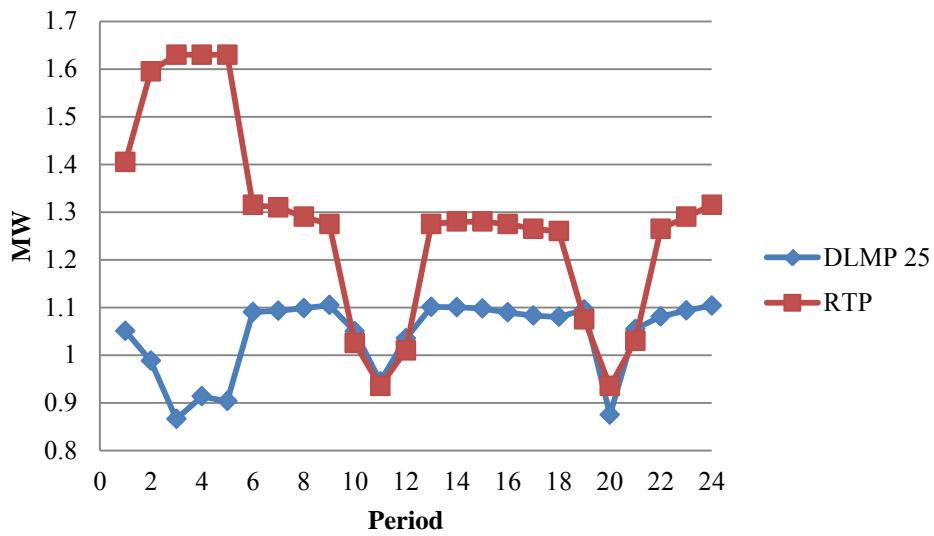


Figure 6.42. Real Power Consumption Incentivized by the DLMP and the RTP at Node 25 in the Congested Network

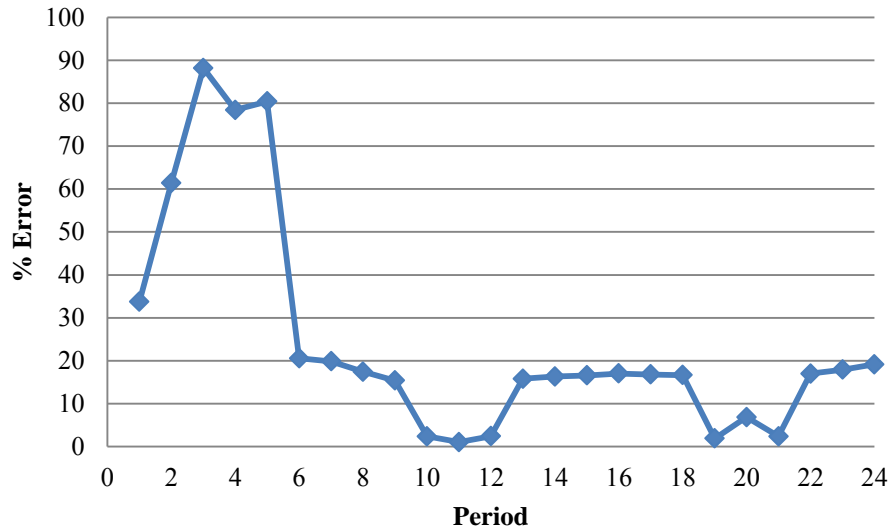


Figure 6.43. Absolute Percentage Deviation of the Consumption the RTP Incentivized at Node 25 from the Consumption Incentivized by the DLMP in the Congested Network

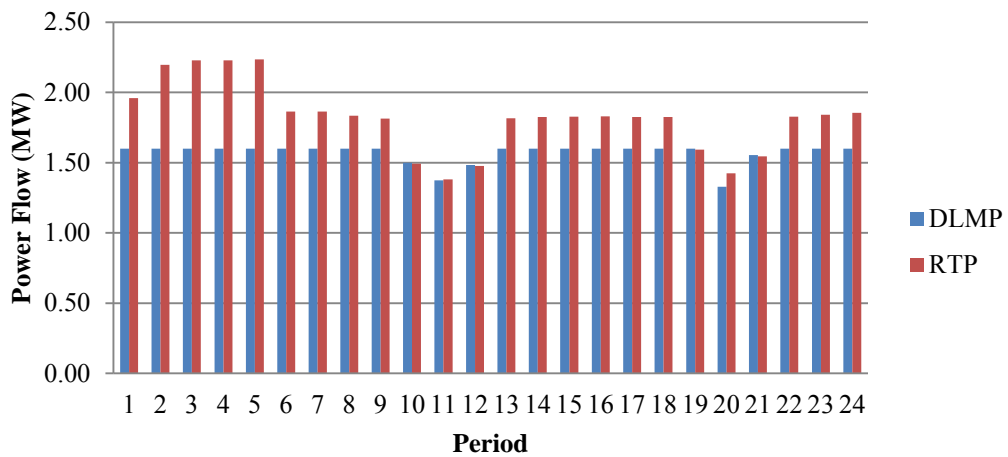


Figure 6.44. Power Flow on Branch 17 as a result of the Consumption Incentivized by the DLMP and RTP in the Congested Network

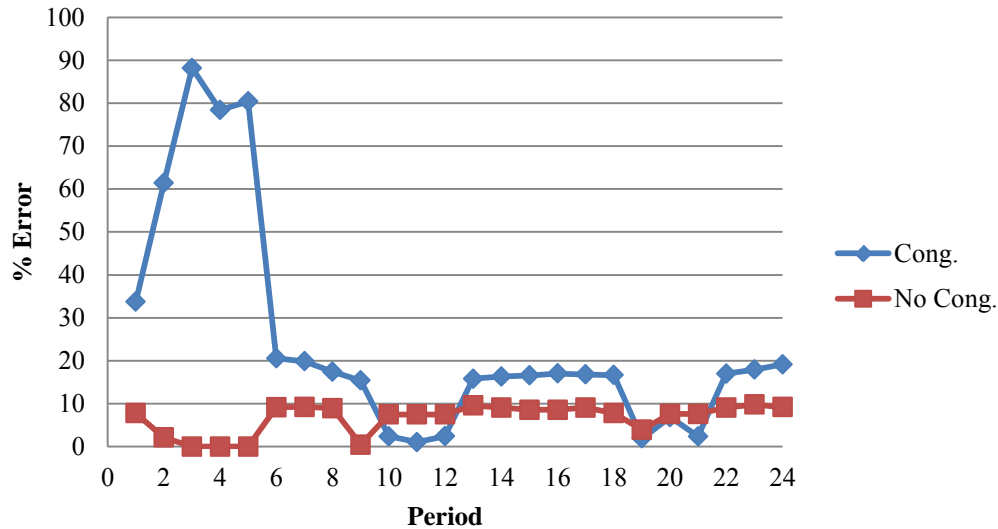


Figure 6.45. Comparison of the Absolute Percentage Deviation of the Consumption Incentivized by the RTP at Node 25 for Congested and Uncongested Network

6.9 Conclusion

The advantage of the DLMP over contemporary prices is tested numerically in this chapter. The DLMP pricing mechanism is tested on enhanced distribution systems with price responsive loads. The simulations are conducted with and without congestion in the enhanced distribution systems. Results of the simulations show that despite the inaccuracy of the FR, TOU, and the RTP, the contemporary prices perform well when the price sensitive loads are highly inelastic. As elasticity increases, the inaccuracy of the prices leads to deviation between the consumption incentivized by the contemporary prices and the optimal consumption incentivized by the DLMP. The deviation becomes significant as elasticity increases and it is more pronounced at individual load levels than at the aggregate level since the inelastic loads averaged out some of the effects. In the case where there are important network characteristics, such as congestion, in the distribution system, the RTP could incentivize significantly inaccurate consumption. The RTP

in the congested system also resulted in line overloads, i.e., the inaccuracy of the RTP not only affected economic efficiency negatively, it also affected reliability negatively.

Chapter 7. Conclusions and Future Work

7.1 Conclusions

The use of the DLMP in enhanced distribution systems is proposed in this thesis. The proposed DLMP is an extension of the LMP concept to the distribution system and the DLMP has similar properties to the LMP. This thesis defined the DLMP and discussed its properties. The properties provide the DLMP the capability to incentive DSRs to behave optimally in a manner that benefits economic efficiency and reliability.

As part of the calculation approach for the DLMP, this thesis also discussed a lossy DCOPF formulation that endogenously captures real power losses. The lossy DCOPF formulation uses piecewise linear functions to approximate losses. The approximation technique could break down and lead to incorrect solutions under the scenario that negative DLMPs/LMPs occur. The breakdown was theoretically proven in this work. A MILP formulation for correcting the breakdown is also discussed.

Computational limitations necessitates that the OPF problem for calculating DLMPs be decomposed into a transmission and a distribution system OPF. The decomposition requires iteration between both problems to ensure adequate modeling of the distribution system, including its DSRs, for the transmission system OPF and an adequate representation of the transmission system for the distribution system OPF. The iterative process optimally couples the transmission and the distribution systems. Previous work calculated nodal distribution prices using de-

composed OPF problems but such approaches did not provide a mechanism that optimally couples the transmission and the distribution systems together. Due to non-convexities resulting from the staircase bid and offer curves as well as non-monotonicity of LMPs, there is no guarantee that the iterative process will converge or converge to a correct or globally optimal solution.

The iterative framework and a sampling approach, which does not suffer from the convergence problems of the iterative framework, are used to demonstrate the superiority of the DLMP over contemporary pricing schemes in the distribution system. The DLMP and the contemporary pricing schemes are compared through the incentivized behavior of PRLs. Simulations show that, as the flexibility of loads increase, the contemporary prices incentivized significant sub-optimal behavior of PRLs. The superiority of the DLMP results from its calculation by the interaction of the demand and supply curves, its property as a nodal price, and the capability of the DLMP to adequately reflect the time dependence of energy prices. As such, the DLMP can reflect the network conditions of both the transmission and the distribution system and it can reflect the generation condition in both systems. The contemporary RTP, while reflecting the transmission system state, does not reflect the distribution system state (network and demand and supply conditions). The FR and the TOU do not reflect any system state, do not reflect time dependence of energy prices in the case of FR, and inadequately reflect time dependence of energy prices in the TOU case. Cross-subsidies, which distort prices, also result with the use of the contemporary prices. As a result, contemporary prices are inadequate for operating under the enhanced distribution system envi-

ronment. The demonstrated superiority of the DLMP is expected to carry through in an enhanced distribution system with other price sensitive resources such as DGs and ESSs.

7.2 Future Work

While this thesis demonstrated and discussed the potential benefits and the need for the DLMP, additional work is required to fully develop the calculation and the application framework of the DLMP. In the area of the DLMP's calculation framework, the iterative approach of calculating the DLMP must be further investigated to develop solutions to its convergence issues. The solution may include a better representation of the distribution system in the transmission system OPF and the transmission system in distribution OPF model. Further work is also necessary to determine the suitability of the DCOPF for calculating DLMPs and for improving the OPF formulation. As discussed in this work, the assumptions in the DCOPF, while accurate for the transmission system, may be inaccurate for the distribution system. Hence, there may be a need to explore a better OPF model for the distribution system. In the area of the application framework of the DLMP, there is a need to explore the communication architecture between DSR and the market.

While PRLs are studied in this work, there is a need to also study ESSs and DGs with the iterative approach. Part of the benefit of the DLMP is also the benefits to the transmission system; these benefits should also be studied and benefits to congestion management and ancillary services demonstrated.

REFERENCES

- [1] F.C. Schweppe *et al.*, *Spot Pricing of Electricity*, Boston, MA: Kluwer Academic Publishers, 1988.
- [2] S. Stoft, *Power System Economics*, Piscataway, NJ: IEEE Press, 2002.
- [3] T. Orfanogianni, G. Gross, "A general formulation for LMP evaluation," *IEEE Trans. Power Syst.*, vol. 22, no. 3, pp. 1163-1173, Aug. 2007.
- [4] D. Kirschen, G. Strbac, *Fundamentals of Power System Economics*, New York: John Wiley & Sons, 2010.
- [5] H. Liu, L. Tesfatsion, A.A. Chowdhury, "Locational marginal pricing basics for restructured wholesale power markets," in *Proc. 2009 IEEE Power & Energy Society General Meeting*, pp. 1-8, July 2009.
- [6] P.R. Gribik, W.W. Hogan, S.L. Pope, Market-Clearing Electricity Prices and Energy Uplift, Tech. Rep. 2007. [Online]. Available: <http://www.whogan.com/>
- [7] E. Litvinov *et al.*, "Marginal loss modeling in LMP calculation," *IEEE Trans. Power Syst.*, vol. 19, pp. 880-888, May 2004.
- [8] E. Litvinov, "Design and operation of the locational marginal prices-based electricity markets," *Generation, Transmission & Distribution, IET*, vol. 4, no. 2, pp. 315-323, Feb. 2010.
- [9] W.W. Hogan, Financial Transmission Right Formulations, Tech. Rep., 2002. [Online]. Available: <http://www.whogan.com/>
- [10] W.W. Hogan, Contract Networks for Electric Power Transmission: Technical Reference, Tech. Rep., 1992. [Online]. Available: <http://www.whogan.com/>
- [11] California ISO. (2012, Nov.). California Independent System Operator Corporation Fifth Replacement FERC Electric Tariff Section 27: CAISO Mar-

- kets and Processes. [Online]. Available: http://www.caiso.com/Documents/TableOfContents_Nov5_2012.pdf
- [12] ISO New England. (2013, Jan.). Manual M-11: ISO New England Manual for Market Operations. [Online]. Available: http://www.iso-ne.com/rules_proceeds/isone_mnls/index.html
- [13] Electric Reliability Council of Texas. (2013, Feb.). ERCOT Nodal Protocols Section 4: Day-Ahead Operations. [Online]. Available: <http://www.ercot.com/mktrules/nprotocols/current>
- [14] Midwest ISO. (2012, Jan.). Business Practices Manual: Energy and Operating Reserve Markets. [Online]. Available: <https://www.midwestiso.org/Library/Tariff/Pages/Tariff.aspx>
- [15] PJM Interconnection. (2010, Sept.). PJM Open Access Transmission Tariff Section 2: Calculation of Locational Marginal Prices: [Online]. Available: <http://www.pjm.com/~media/documents/agreements/tariff.ashx>
- [16] F. Li, R. Bo, "DCOPF-based LMP simulation: algorithm, comparison with ACOPF, and sensitivity," *IEEE Trans. Power Syst.*, vol. 22, no. 4, pp. 1475-1485, Nov. 2007.
- [17] T. Wu, Z. Alaywan, A. D. Papalexopoulos, "Locational marginal price calculations using the distributed-slack power-flow formulation," *IEEE Trans. Power Syst.*, vol. 20, no. 2, pp. 1188- 1190, May 2005.
- [18] J. Meisel, "System incremental cost calculations using the participation factor load-flow formulation," *IEEE Trans. Power Syst.*, vol. 8, no. 1, pp. 357-363, Feb 1993.
- [19] Z. Hu *et al.*, "An iterative LMP calculation method considering loss distributions," *IEEE Trans. Power Syst.*, vol. 25, no. 3, pp. 1469-1477, Aug. 2010.
- [20] A. L. Motto *et al.*, "Network-constrained multiperiod auction for a pool-based electricity market," *IEEE Trans. Power Syst.*, vol. 17, no. 3, pp. 646-653, Aug 2002.

- [21] N. Alguacil, A. L. Motto, A. J. Conejo, "Transmission expansion planning: a mixed-integer LP approach," *IEEE Trans. Power Syst.*, vol. 18, no. 3, pp. 1070- 1077, Aug. 2003.
- [22] H. Zhang *et al.*, "A mixed-integer linear programming approach for multi-stage security-constrained transmission expansion planning," *IEEE Trans. Power Syst.*, vol. 27, no. 2, pp. 1125-1133, May 2012.
- [23] B. F. Hobbs *et al.*, "Improved transmission representations in oligopolistic market models: quadratic losses, phase shifters, and DC Lines," *IEEE Trans. Power Syst.*, vol. 23, no. 3, pp. 1018-1029, Aug. 2008.
- [24] B. B. Chakrabarti *et al.*, "Alternative loss model for the New Zealand electricity market using SFT," in *Proc. 2011 IEEE Power and Energy Society General Meeting*, pp. 1-8, 24-29 July 2011.
- [25] P.S. Martin, "Mejoras en la eficacia computacional de medelos probabilistas de explotación generación/red a medio plazo," Ph.D. dissertation (in Spanish), Univ. Pontifical de Comillas, Madrid Spain, 1998.
- [26] R. Palma-Benhke *et al.*, "Modeling network constrained economic dispatch problems," Elect. Power Optimization Center, Auckland, Tech Rep., 2009.
- [27] P. S. Martin and A. Ramos, "Modeling Transmission Ohmic Losses in a Stochastic Bulk Production Cost Model," [Online]. Available: <http://www.iit.upcomillas.es/~aramos/papers/losses.pdf>
- [28] R. Billinton and S. Jonnavithula, "A test system for teaching overall power system reliability assessment," *IEEE Trans. Power Syst.*, vol. 11, no. 4, pp. 1670-1676, Nov 1996.
- [29] R. N. Allan *et al.*, "A reliability test system for educational purposes-basic distribution system data and results," *IEEE Trans. Power Syst.*, vol. 6, no. 2, pp. 813-820, May 1991.
- [30] R. Billinton *et al.*, "A reliability test system for educational purposes-basic results," *IEEE Trans. Power Syst.*, vol. 5, no. 1, pp. 319-325, Feb 1990.

- [31] R. Billinton *et al.*, "A reliability test system for educational purposes-basic data," *IEEE Trans. Power Syst.*, vol. 4, no. 3, pp. 1238-1244, Aug 1989.
- [32] D. A. Haughton, "State estimation for enhanced monitoring, reliability, restoration and control of smart distribution systems," Ph.D. dissertation, Arizona State Univ., Tempe U.S.A, 2012.
- [33] B. R. Sathyanarayana, "Sensitivity-based pricing and multiobjective control for energy management in power distribution system," Ph.D. dissertation, Arizona State Univ., Tempe U.S.A, 2012.
- [34] R. D. Zimmerman, C. E. Murillo-Sanchez, R. J. Thomas, "Matpower: steady-state operations, planning and analysis tools for power systems research and education," *IEEE Trans. Power Syst.*, vol. 26, no. 1, pp. 12-19, Feb. 2011.
- [35] O. Alsac, B. Stott, "Optimal load flow with steady state security," *IEEE Trans. on Power App. and Syst.*, vol. PAS 93, no. 3, pp. 745-751, 1974.
- [36] C. Grigg *et al.*, "The IEEE reliability test system-1996. A report prepared by the Reliability Test System Task Force of the Application of Probability Methods Subcommittee," *IEEE Trans. Power Syst.*, vol. 14, no. 3, pp. 1010-1020, Aug 1999.
- [37] K. W. Hedman *et al.*, "Co-optimization of generation unit commitment and transmission switching with N-1 reliability," *IEEE Trans. Power Syst.*, vol. 25, no. 2, pp. 1052-1063, May 2010.
- [38] F. Gonzalez-Longatt. *IEEE 30 bus test* [Online]. Available: http://www.fglongatt.org/Test_Case_IEEE_30.html
- [39] AEP Ohio. *Columbus Southern Power Company Class Load Profiles Jan-Dec 2012* [Online]. Available: <https://www.aepohio.com/service/choice/cres/LoadProfiles.aspx>
- [40] J. J. Burke, "Utility distribution design fundamentals and characteristics," in *Power Distribution Engineering Fundamentals and Applications*, New York: Dekker, 1994.

- [41] W. H. Kersting, "Introduction to distribution systems," in *Distribution System Modeling and Analysis*, 2nd ed. Boca Raton: CRC, 2007.
- [42] P. M. Sotkiewicz, J. M. Vignolo, "Nodal pricing for distribution networks: efficient pricing for efficiency enhancing DG," *IEEE Trans. Power Syst.*, vol. 21, no. 2, pp. 1013-1014, May 2006.
- [43] K. Shaloudegi *et al.*, "A novel policy for locational marginal price calculation in distribution systems based on loss reduction allocation using game theory," *IEEE Trans. Power Syst.*, vol. 27, no. 2, pp. 811-820, May 2012.
- [44] N. Steffan, G. T. Heydt, "Quadratic programming and related techniques for the calculation of locational marginal prices in distribution systems," in *Proc. North American Power Symposium (NAPS)*, 2012, pp.1-6, 9-11 Sept. 2012.
- [45] B. R. Sathyanarayana, G. T. Heydt, "Sensitivity-based pricing and optimal storage utilization in distribution systems," *IEEE Trans. Power Del.*, vol. 28, no. 2, pp. 1073-1082, April 2013.
- [46] G. T. Heydt, "The next generation of power distribution systems," *IEEE Trans. Smart Grid*, vol. 1, no. 3, pp. 225-235, Dec. 2010.
- [47] G. T. Heydt *et al.*, "Pricing and control in the next generation power distribution system," *IEEE Trans. Smart Grid*, vol. 3, no. 2, pp.907-914, June 2012.
- [48] 110th Congress of United States, "Smart Grid," Title XIII, Energy Independence and Security Act of 2007, Washington DC, December 2007.
- [49] Office of Electricity Delivery and Energy Reliability, United States Department of Energy. (2008). *The Smart Grid – An Introduction* [Online]. Available: http://energy.gov/sites/prod/files/oeprod/DocumentsandMedia/DOE_SG_Book_SinSin_Pages%281%29.pdf
- [50] Office of Electricity Delivery and Energy Reliability, United States Department of Energy. (2009). *What the Smart Grid Means to You (Utilities) and the People You Serve* [Online]. Available: <http://energy.gov/sites/prod/files/oeprod/DocumentsandMedia/Utilities.pdf>

- [51] Office of Electricity Delivery and Energy Reliability, United States Department of Energy. (2009). *What the Smart Grid Means to Americans (Consumer Advocates)* [Online]. Available: <http://energy.gov/sites/prod/files/oeprod/DocumentsandMedia/ConsumerAdvocates.pdf>
- [52] Office of Electricity Delivery and Energy Reliability, United States Department of Energy. (2009). *What the Smart Grid Means to American's Future (Technology Providers)* [Online]. Available: <http://energy.gov/sites/prod/files/oeprod/DocumentsandMedia/TechnologyProviders.pdf>
- [53] H. Farhangi, "The path of the smart grid," *IEEE Power and Energy Magazine*, vol. 8, no. 1, pp. 18-28, January-February 2010.
- [54] F. Xi *et al.*, "Smart Grid — The new and improved power grid: a survey," *IEEE Communications Surveys & Tutorials*, vol. 14, no. 4, pp. 944-980, Fourth Quarter 2012.
- [55] V. C. Gungor *et al.*, "Smart grid technologies: communication technologies and standards," *IEEE Trans. Ind. Informat.*, vol. 7, no. 4, pp. 529,539, Nov. 2011.
- [56] J. C. Bonbright, *Principle of Public Utility Rates*, New York, NY: Columbia Univ. Press, 1961.
- [57] M. H. Dworkin. (2003, Jan.). *The PSB process: the scope, the players, and the rules of practice before the public service board* [Online]. Available: <http://gmcboard.vermont.gov/sites/gmcboard/files/PBS041212.pdf>
- [58] H. S. Parmesano, C. S. Martin, "The evolution in U.S. electric utility rate design," *Annu. Rev. Energy*, vol. 8, pp. 45-94, Nov. 1983.
- [59] M. A. Jamison, "Rate of return: regulation," Public Utility Research Center, University of Florida, Tech. Rep. [Online]. Available: http://warrington.ufl.edu/centers/purc/purcdocs/papers/0528_jamison_rate_of_reurr.pdf

- [60] The Regulatory Assistance Project. (2011, Mar.). *Electricity regulation in the US: a guide* [Online]. Available: www.raponline.org/document/download/id/645
- [61] L. J. Vogt, *Electricity Pricing Engineering Principles and Methodologies*, Boca Raton, FL: CRC Press, 2009.
- [62] P. Q. Hanser, "Issues in cost allocation – Wisconsin Public Utility Institute," The Brattle Group, Tech. Presentation. [Online]. Available: <http://wpui.wisc.edu/wp-content/uploads/2012/07/Cost-Allocation-2012.pdf>
- [63] G. Barbose *et al.*, "A survey of utility experience with real time pricing" Ernest Orlando Lawrence Berkeley National Laboratory, Berkeley, CA, Tech Rep. DE-AC03-76SF00098, Dec. 2004. [Online]. Available: <http://eetd.lbl.gov/ea/ems/reports/54238.pdf>
- [64] S. Braithwait *et al.*, "Retail electricity pricing and rate design in evolving markets" Edison Electric Institute, Washington, D.C, Tech Rep. [Online]. Available: http://www.eei.org/ourissues/electricitydistribution/Documents/Retail_Electricity_PPricin.pdf
- [65] H. Averch, L. Johnson, "The behavior of the firm under regulatory constraint," *Amer. Econ. Rev.*, vol. 52, no. 5, pp. 1052-1069, Dec. 1962.
- [66] S. Borenstein "Time-varying retail electricity prices: theory and practice," in Griffin and Puller, eds., *Electricity Deregulation: Choices and Challenges*, Chicago, IL: Univ. of Chicago Press, 2005.
- [67] A. Faruqui *et al.*, "Time-varying and dynamic rate design" The Brattle Group, Tech Rep. [Online]. Available: <http://www.brattle.com/Experts/ExpertDetail.asp?ExpertID=164>
- [68] O. W. Akinbode, K. W. Hedman, "Fictitious losses in the DCOPF with a piecewise linear approximation of losses," to be published in *Proc. 2013 IEEE Power and Energy Society General Meeting*.
- [69] D. N. Jones, P. C. Mann, "The fairness criterion in public utility regulation: does fairness still matter?" *J. of Econ. Issues*, vol. 35, no. 1, pp. 153-172, Mar. 2001.

- [70] M. D. Ilic, J. Donadee, "Distribution pricing and tariff structure: the ongoing US reforms," in *Proc. 2011 IEEE Power and Energy Society General Meeting*, pp. 1-2.
- [71] Pacific Gas and Electric Company, "Voltage tolerance boundary," Pacific Gas and Electric Company, [Online]. Available: http://www.pge.com/includes/docs/pdfs/mybusiness/customerservice/energy_status/powerquality/voltage_tolerance.pdf
- [72] H. Oh, R. J. Thomas, "Demand-side bidding agents: modeling and simulation," *IEEE Trans. on Power Syst.*, vol. 23, no. 3, pp. 1050-1056, Aug. 2008.
- [73] Y. Liu, X. Guan, "Purchase allocation and demand bidding in electric power markets," *IEEE Trans. on Power Syst.*, vol. 18, no. 1, pp. 106-112, Feb. 2003.
- [74] G. B. Sheble, "DSM economic marginal demand bidding," in *Proc. 2010 IEEE Power and Energy Society General Meeting*, pp. 1-7.
- [75] P. R. Thimmapuram *et al.*, "Modeling and simulation of price elasticity of demand using an agent-based model," in *Proc. 2010 Innovative Smart Grid Technologies (ISGT)*, pp. 1-8.
- [76] M. A. Bernstein, J. Griffin, "Regional differences in the price-elasticity of demand for energy," the RAND Corporation, Tech. Rep. [Online]. Available: http://www.rand.org/content/dam/rand/pubs/technical_reports/2005/RAND_TR292.pdf
- [77] H. R. Varian, *Intermediate Microeconomics a modern approach*, 8th ed. New York: W. W. Norton, 2010.
- [78] M. Filippini, "Electricity demand by time of use: An application of the household AIDS model," *Energy Economics*, vol. 17, no. 3, pp. 197-204, Jul. 1995.
- [79] N. Singhal, K. W. Hedman, "An integrated transmission and distribution systems model with distribution-based LMP (DLMP) pricing," submitted to *North American Power Symposium (NAPS)*, 2013.

APPENDIX A

SIMULATION DATA AND RESULTS DETAILS

Appendix A. Simulation Data and Results Details

Table A.1. RBTS Transmission System Branch Data

No.	From Bus	To Bus	Length (mi)	R p.u	X p.u.	B/2 p.u	Current Rating p.u.	MVA Rating (p.u.)
1	1	3	46.6028	0.0342	0.1800	0.0106	0.85	0.85
2	2	4	155.3428	0.1140	0.6000	0.0352	0.71	0.71
3	1	2	124.2742	0.0912	0.4800	0.0282	0.71	0.71
4	3	4	31.0686	0.0228	0.1200	0.0071	0.71	0.71
5	3	5	31.0686	0.0228	0.1200	0.0071	0.71	0.71
6	1	3	46.6028	0.0342	0.1800	0.0106	0.85	0.85
7	2	4	155.3428	0.1140	0.6000	0.0352	0.71	0.71
8	4	5	31.0686	0.0228	0.1200	0.0071	0.71	0.71
9	5	6	31.0686	0.0228	0.1200	0.0071	0.71	0.71
10	3	7	0.0000	0.0128	0.0640	0.0000	1.55	1.55
11	3	7	0.0000	0.0128	0.0640	0.0000	1.55	1.55
100 MVA Base								

Table A.2. Flexible Load Data for RBTS Bus 3 Distribution System

Feeder	Load Point	Peak Load (MW)	Flexible Part of Load (MW)	Inflexible Part of Base Load (MW)	% of Peak Load that is Flexible
F1	LP1	0.8367	0.2740	0.5627	32.75
	LP2	0.7750	0.2740	0.5010	35.36
	LP3	0.5222	0.2740	0.2482	52.48
	LP4	0.8367	0.2740	0.5627	32.75
F2	LP8	1.0167	0.3050	0.7117	30.00
	LP9	1.0167	0.3050	0.7117	30.00
F3	LP11	0.8500	0.2650	0.5850	31.14
	LP12	0.8500	0.2650	0.5850	31.14
	LP13	0.8500	0.2650	0.5850	31.14
	LP14	0.9250	0.2650	0.6600	28.62
F4	LP18	0.8500	0.2780	0.5720	32.68
	LP19	0.5222	0.2780	0.2442	53.20
	LP20	0.8367	0.2780	0.5587	33.20
	LP21	0.8367	0.2780	0.5587	33.20
F5	LP25	0.8500	0.2450	0.6050	28.77
	LP26	0.7750	0.2450	0.5300	31.56
	LP27	0.9250	0.2450	0.6800	26.44
	LP28	0.5222	0.2450	0.2772	46.84
F6	LP32	0.8367	0.2610	0.5757	31.24
	LP33	0.8367	0.2610	0.5757	31.24
	LP34	0.8367	0.2610	0.5757	31.24
	LP35	0.8367	0.2610	0.5757	31.24
F7	LP39	6.9167	2.5400	4.3767	36.75
	LP40	6.9167	2.5400	4.3767	36.75
F8	LP42	11.5833	3.0000	8.5833	25.97
	LP43	11.5833	3.0000	8.5833	25.97

Table A.3. RBTS Bus 4 Distribution System 11 kV Feeder Loading and Impedance Summary

Feeder	Peak Loading (MW)	Conductor Rating (A)	Feeder Length (mi)	R (Ω /mi)	X (Ω /mi)
1	5.70	530.00	5.4370	0.307088	0.629576
2	5.71	530.00	2.7030		
3	5.63	530.00	5.3127		
4	6.52	530.00	5.8098		
5	4.89	530.00	2.6719		
6	5.71	530.00	2.6719		
7	5.85	530.00	5.3438		

Table A.4. RBTS Bus 4 Distribution System Feeder Section Summary

Section Type	Length (mi)	Section Number
1	0.3728	2, 6, 10, 14, 17, 21, 25, 28, 30, 34, 38, 41, 43, 46, 49, 51, 55, 58, 61, 64, 67
2	0.4660	1, 4, 7, 9, 12, 16, 19, 22, 24, 27, 29, 32, 35, 37, 40, 42, 45, 48, 50, 53, 56, 60, 63, 65
3	0.4971	3, 5, 8, 11, 13, 15, 18, 20, 23, 26, 31, 33, 36, 39, 44, 47, 52, 54, 57, 59, 62, 66

Table A.5. RBTS Bus 4 Distribution System 11 kV Network Feeders Impedance Summary

Section #	Length (mi)	R (Ω /mi)	X (Ω /mi)
80	9.32057	0.30709	0.629576
81	3.10686	0.30709	0.629576
82	3.10686	0.30709	0.629576
83	6.21371	0.30709	0.629576
84	6.21371	0.30709	0.629576

Table A.6. RBTS Bus 4 Distribution System 33 kV Feeders Impedance Summary

Branch No.	Peak Loading (MW)	Conductor Rating (A)	Feeder Length (mi)	R (Ω /mi)	X (Ω /mi)
68	5.70	730.00	6.2137	0.187726	0.600135
69	5.71	730.00	9.3206		
70	5.63	730.00	9.3206		
71	6.52	730.00	6.2137		

Table A.7. IEEE 30-Bus System Branch Data

No.	From bus	To bus	kV Base	MVA Base	R (p.u.)	X (p.u.)	G (p.u.)	B (p.u.)	Branch Limit (p.u.)
1	1	2	135	100	0.0200	0.0600	5.0000	-15.0000	1.3
2	1	3	135	100	0.0500	0.1900	1.2953	-4.9223	1.3
3	2	4	135	100	0.0600	0.1700	1.8462	-5.2308	0.65
4	3	4	135	100	0.0100	0.0400	5.8824	-23.5294	1.3
5	2	5	135	100	0.0500	0.2000	1.1765	-4.7059	1.3
6	2	6	135	100	0.0600	0.1800	1.6667	-5.0000	0.65
7	4	6	135	100	0.0100	0.0400	5.8824	-23.5294	0.9
8	5	7	135	100	0.0500	0.1200	2.9586	-7.1006	0.7
9	6	7	135	100	0.0300	0.0800	4.1096	-10.9589	1.3
10	6	8	135	100	0.0100	0.0400	5.8824	-23.5294	0.32
11	6	9	135	100	0.0000	0.2100	0.0000	-4.7619	0.65
12	6	10	135	100	0.0000	0.5600	0.0000	-1.7857	0.32
13	9	11	135	100	0.0000	0.2100	0.0000	-4.7619	0.65
14	9	10	135	100	0.0000	0.1100	0.0000	-9.0909	0.65
15	4	12	135	100	0.0000	0.2600	0.0000	-3.8462	0.65
16	12	13	135	100	0.0000	0.1400	0.0000	-7.1429	0.65
17	12	14	135	100	0.1200	0.2600	1.4634	-3.1707	0.32
18	12	15	135	100	0.0700	0.1300	3.2110	-5.9633	0.32
19	12	16	135	100	0.0900	0.2000	1.8711	-4.1580	0.32
20	14	15	135	100	0.2200	0.2000	2.4887	-2.2624	0.16
21	16	17	135	100	0.0800	0.1900	1.8824	-4.4706	0.16
22	15	18	135	100	0.1100	0.2200	1.8182	-3.6364	0.16
23	18	19	135	100	0.0600	0.1300	2.9268	-6.3415	0.16
24	19	20	135	100	0.0300	0.0700	5.1724	-12.0690	0.32
25	10	20	135	100	0.0900	0.2100	1.7241	-4.0230	0.32
26	10	17	135	100	0.0300	0.0800	4.1096	-10.9589	0.32
27	10	21	135	100	0.0300	0.0700	5.1724	-12.0690	0.32
28	10	22	135	100	0.0700	0.1500	2.5547	-5.4745	0.32
29	21	22	135	100	0.0100	0.0200	20.0000	-40.0000	0.32
30	15	23	135	100	0.1000	0.2000	2.0000	-4.0000	0.16

No.	From bus	To bus	kV Base	MVA Base	R (p.u.)	X (p.u.)	G (p.u.)	B (p.u.)	Branch Limit (p.u.)
31	22	24	135	100	0.1200	0.1800	2.5641	-3.8462	0.16
32	23	24	135	100	0.1300	0.2700	1.4477	-3.0067	0.16
33	24	25	135	100	0.1900	0.3300	1.3103	-2.2759	0.16
34	25	26	135	100	0.2500	0.3800	1.2083	-1.8366	0.16
35	25	27	135	100	0.1100	0.2100	1.9573	-3.7367	0.16
36	28	27	135	100	0.0000	0.4000	0.0000	-2.5000	0.65
37	27	29	135	100	0.2200	0.4200	0.9786	-1.8683	0.16
38	27	30	135	100	0.3200	0.6000	0.6920	-1.2976	0.16
39	29	30	135	100	0.2400	0.4500	0.9227	-1.7301	0.16
40	8	28	135	100	0.0600	0.2000	1.3761	-4.5872	0.32
41	6	28	135	100	0.0200	0.0600	5.0000	-15.0000	0.32

Table A.8. 24 Hour Load Data for the Inelastic Loads in the Test Transmission System

Bus No.	H1	H2	H3	H4	H5	H6	H7	H8
1	0.00	0.00	0.00	0.00	0.00	0.00	0.00	0.00
2	13.67	13.45	13.02	12.59	12.80	14.11	15.62	18.45
3	1.51	1.49	1.44	1.39	1.42	1.56	1.73	2.04
4	4.79	4.71	4.56	4.41	4.48	4.94	5.47	6.46
5	0.00	0.00	0.00	0.00	0.00	0.00	0.00	0.00
6	0.00	0.00	0.00	0.00	0.00	0.00	0.00	0.00
7	14.36	14.14	13.68	13.22	13.45	14.82	16.42	19.38
8	18.90	18.60	18.00	17.40	17.70	19.50	21.60	25.50
9	0.00	0.00	0.00	0.00	0.00	0.00	0.00	0.00
10	3.65	3.60	3.48	3.36	3.42	3.77	4.18	4.93
11	0.00	0.00	0.00	0.00	0.00	0.00	0.00	0.00
12	7.06	6.94	6.72	6.50	6.61	7.28	8.06	9.52
13	0.00	0.00	0.00	0.00	0.00	0.00	0.00	0.00
14	3.91	3.84	3.72	3.60	3.66	4.03	4.46	5.27
15	5.17	5.08	4.92	4.76	4.84	5.33	5.90	6.97
16	2.21	2.17	2.10	2.03	2.07	2.28	2.52	2.98
17	5.67	5.58	5.40	5.22	5.31	5.85	6.48	7.65
18	2.02	1.98	1.92	1.86	1.89	2.08	2.30	2.72
19	5.99	5.89	5.70	5.51	5.61	6.18	6.84	8.08
20	1.39	1.36	1.32	1.28	1.30	1.43	1.58	1.87
21	11.03	10.85	10.50	10.15	10.33	11.38	12.60	14.88
22	0.00	0.00	0.00	0.00	0.00	0.00	0.00	0.00
23	2.02	1.98	1.92	1.86	1.89	2.08	2.30	2.72
24	5.48	5.39	5.22	5.05	5.13	5.66	6.26	7.40
25	0.00	0.00	0.00	0.00	0.00	0.00	0.00	0.00
26	2.21	2.17	2.10	2.03	2.07	2.28	2.52	2.98
27	0.00	0.00	0.00	0.00	0.00	0.00	0.00	0.00
28	0.00	0.00	0.00	0.00	0.00	0.00	0.00	0.00
29	1.51	1.49	1.44	1.39	1.42	1.56	1.73	2.04
30	6.68	6.57	6.36	6.15	6.25	6.89	7.63	9.01
Total	119.20	117.30	113.52	109.74	111.63	122.98	136.22	160.82

Bus No.	H9	H10	H11	H12	H13	H14	H15	H16
1	0.00	0.00	0.00	0.00	0.00	0.00	0.00	0.00
2	20.62	21.48	21.70	21.48	20.18	19.96	19.53	19.10
3	2.28	2.38	2.40	2.38	2.23	2.21	2.16	2.11
4	7.22	7.52	7.60	7.52	7.07	6.99	6.84	6.69
5	0.00	0.00	0.00	0.00	0.00	0.00	0.00	0.00
6	0.00	0.00	0.00	0.00	0.00	0.00	0.00	0.00
7	21.66	22.57	22.80	22.57	21.20	20.98	20.52	20.06
8	28.50	29.70	30.00	29.70	27.90	27.60	27.00	26.40
9	0.00	0.00	0.00	0.00	0.00	0.00	0.00	0.00
10	5.51	5.74	5.80	5.74	5.39	5.34	5.22	5.10
11	0.00	0.00	0.00	0.00	0.00	0.00	0.00	0.00
12	10.64	11.09	11.20	11.09	10.42	10.30	10.08	9.86
13	0.00	0.00	0.00	0.00	0.00	0.00	0.00	0.00
14	5.89	6.14	6.20	6.14	5.77	5.70	5.58	5.46
15	7.79	8.12	8.20	8.12	7.63	7.54	7.38	7.22
16	3.33	3.47	3.50	3.47	3.26	3.22	3.15	3.08
17	8.55	8.91	9.00	8.91	8.37	8.28	8.10	7.92
18	3.04	3.17	3.20	3.17	2.98	2.94	2.88	2.82
19	9.03	9.41	9.50	9.41	8.84	8.74	8.55	8.36
20	2.09	2.18	2.20	2.18	2.05	2.02	1.98	1.94
21	16.63	17.33	17.50	17.33	16.28	16.10	15.75	15.40
22	0.00	0.00	0.00	0.00	0.00	0.00	0.00	0.00
23	3.04	3.17	3.20	3.17	2.98	2.94	2.88	2.82
24	8.27	8.61	8.70	8.61	8.09	8.00	7.83	7.66
25	0.00	0.00	0.00	0.00	0.00	0.00	0.00	0.00
26	3.33	3.47	3.50	3.47	3.26	3.22	3.15	3.08
27	0.00	0.00	0.00	0.00	0.00	0.00	0.00	0.00
28	0.00	0.00	0.00	0.00	0.00	0.00	0.00	0.00
29	2.28	2.38	2.40	2.38	2.23	2.21	2.16	2.11
30	10.07	10.49	10.60	10.49	9.86	9.75	9.54	9.33
Total	179.74	187.31	189.20	187.31	175.96	174.06	170.28	166.50

Bus No.	H17	H18	H19	H20	H21	H22	H23	H24
1	0.00	0.00	0.00	0.00	0.00	0.00	0.00	0.00
2	19.53	19.96	20.83	21.27	20.83	19.53	17.36	15.19
3	2.16	2.21	2.30	2.35	2.30	2.16	1.92	1.68
4	6.84	6.99	7.30	7.45	7.30	6.84	6.08	5.32
5	0.00	0.00	0.00	0.00	0.00	0.00	0.00	0.00
6	0.00	0.00	0.00	0.00	0.00	0.00	0.00	0.00
7	20.52	20.98	21.89	22.34	21.89	20.52	18.24	15.96
8	27.00	27.60	28.80	29.40	28.80	27.00	24.00	21.00
9	0.00	0.00	0.00	0.00	0.00	0.00	0.00	0.00
10	5.22	5.34	5.57	5.68	5.57	5.22	4.64	4.06
11	0.00	0.00	0.00	0.00	0.00	0.00	0.00	0.00
12	10.08	10.30	10.75	10.98	10.75	10.08	8.96	7.84
13	0.00	0.00	0.00	0.00	0.00	0.00	0.00	0.00
14	5.58	5.70	5.95	6.08	5.95	5.58	4.96	4.34
15	7.38	7.54	7.87	8.04	7.87	7.38	6.56	5.74
16	3.15	3.22	3.36	3.43	3.36	3.15	2.80	2.45
17	8.10	8.28	8.64	8.82	8.64	8.10	7.20	6.30
18	2.88	2.94	3.07	3.14	3.07	2.88	2.56	2.24
19	8.55	8.74	9.12	9.31	9.12	8.55	7.60	6.65
20	1.98	2.02	2.11	2.16	2.11	1.98	1.76	1.54
21	15.75	16.10	16.80	17.15	16.80	15.75	14.00	12.25
22	0.00	0.00	0.00	0.00	0.00	0.00	0.00	0.00
23	2.88	2.94	3.07	3.14	3.07	2.88	2.56	2.24
24	7.83	8.00	8.35	8.53	8.35	7.83	6.96	6.09
25	0.00	0.00	0.00	0.00	0.00	0.00	0.00	0.00
26	3.15	3.22	3.36	3.43	3.36	3.15	2.80	2.45
27	0.00	0.00	0.00	0.00	0.00	0.00	0.00	0.00
28	0.00	0.00	0.00	0.00	0.00	0.00	0.00	0.00
29	2.16	2.21	2.30	2.35	2.30	2.16	1.92	1.68
30	9.54	9.75	10.18	10.39	10.18	9.54	8.48	7.42
Total	170.28	174.06	181.63	185.42	181.63	170.28	151.36	132.44

Table A.9. RBTS Bus 4 Distribution System Bus and Load Details

Bus No.	Type	Peak Load kW	Bus No.	Type	Peak Load kW	Bus No.	Type	Peak Load kW
1	1	0	26	1	0	51	1	0
2	1	0	27	1	886.9	52	3	1630
3	1	0	28	1	0	53	1	0
4	1	0	29	1	886.9	54	3	1630
5	1	0	30	1	0	55	1	0
6	1	0	31	1	886.9	56	3	1630
7	1	0	32	2	813.7	57	1	0
8	1	0	33	1	0	58	3	1630
9	1	886.9	34	2	813.7	59	1	0
10	1	0	35	1	0	60	3	1630
11	1	886.9	36	5	671.4	61	1	0
12	1	0	37	5	671.4	62	4	2445
13	1	886.9	38	1	0	63	1	0
14	1	0	39	1	886.9	64	1	886.9
15	1	886.9	40	1	0	65	1	0
16	2	813.7	41	1	886.9	66	1	886.9
17	1	0	42	1	886.9	67	1	0
18	5	671.4	43	1	0	68	1	886.9
19	5	671.4	44	1	886.9	69	1	886.9
20	1	0	45	2	813.7	70	1	0
21	3	1630	46	1	0	71	2	813.7
22	1	0	47	2	813.7	72	1	0
23	4	2445	48	1	0	73	2	813.7
24	1	0	49	5	671.4	74	5	671.4
25	3	1630	50	5	671.4	75	1	0

Table A.10. Hourly Inelastic Loads in the RBTS Bus 4 Distribution System

Period	kW	Per Unit based on Peak kW
1	559.90	0.63
2	524.34	0.59
3	502.09	0.57
4	502.17	0.57
5	542.23	0.61
6	656.69	0.74
7	683.66	0.77
8	671.01	0.76
9	659.45	0.74
10	653.78	0.74
11	665.70	0.75
12	667.30	0.75
13	675.30	0.76
14	681.34	0.77
15	694.35	0.78
16	738.63	0.83
17	788.44	0.89
18	813.02	0.92
19	837.74	0.94
20	886.90	1.00
21	877.59	0.99
22	796.59	0.90
23	699.37	0.79
24	609.35	0.69